IDENTIFICATION, AND CHARACTERIZATION OF NOVEL INHIBITORS OF THE PRESYNAPTIC, HEMICHOLINIUM-3-SENSITIVE CHOLINE TRANSPORTER

By
Elizabeth Ann Ennis

Dissertation
Submitted to the Faculty of the
Graduate School of Vanderbilt University
in partial fulfillment of the requirements
for the degree of
DOCTOR OF PHILOSOPHY
in
Pharmacology

May, 2016
Nashville, Tennessee

Randy Blakely, Ph.D.

Craig Lindsley, Ph.D.

Kevin Currie, Ph.D.

Eric Delpire, Ph.D.

David Robertson, M.D.

For those who told me I could do anything I think I can

ACKNOWLEDGEMENTS

I am greatly humbled by the contributions of the many whom have aided me in my completion of my doctor of philosophy in pharmacology. I was given a great privilege by the Interdisciplinary Graduate Program when I was accepted as a Graduate Student at Vanderbilt University. I am extremely grateful for the support that I received from all of the teachers at this great University, particularly to Dr. Sebastian Joyce whose guidance led me to my mentor, Dr. Randy Blakely. Dr. Randy Blakely is a brilliant scientist and an inspiring mentor. The experience of working in his lab will be unparalleled for the rest of my professional life. He has provided me with immeasurable support through constructive criticism, funding, intellectual and scientific freedoms, and a blatant confidence in me regardless of my quirks. Thank you Randy. Before I relinquish this text to more formal matters, there are a few personal acknowledgements I would be remiss to exclude. I would like to acknowledge Dr. Ken Cohen without whom I wouldn't have been here and wouldn't have had the inspiration to pursue such a career. I thank my parents, Chris and Cherie Ennis, who are pillars in my life, fought for me to have a chance at life, and supported me, without contest, on every endeavor I have pursued. Finally, I want to mention my gratitude to Kristen Ennis, Noah Green, Christine Petersen, Cassie Retzlaff, Jane Wright, and the rest of my family, and friends who have shown me love and support, for it is those people who I pursue scientific endeavors such as this one.

These scientific endeavors that lead to my dissertation began with a high-throughput screen (HTS) which was dreamt up and executed by a team including Dr. Alicia Ruggiero, Dr. Corey Hopkins, numerous colleagues at the Molecule Library Probe

Production Center Network (MLPCN), Dr. Randy Blakely, and Dr. Craig Lindsley. I cannot thank these researchers enough for all of their hard work and guidance. Of those that initiated the HTS, I would like to especially acknowledge Dr. Craig Lindsley who has provided me with invaluable support throughout my entire graduate school career. Also, I would like to thank Dr. David Robertson and his team for their generous contributions to the ongoing cardiovascular studies, and Dr. Maureen Hahn who spent precious time editing this document. Finally, thank you to my committee, Dr. Kevin Currie, Dr. Eric Delpire, Dr. David Robertson, Dr. Craig Lindsley, and Dr. Randy Blakely. The time you have dedicated to me has shaped my graduate education and made this experience a positive one. Additionally, none of this would have been possible without the research grants from the National Institutes of Health (MH086530, RDB), the Alzheimer's Association, the training grant that funded my education NIH T32 Award (GM007628), and the Dystonia Medical Research Foundation (DMRF) that funded this research.

TABLE OF CONTENTS

LIST OF FIGURES

LIST OF TABLES

LIST OF ABBREVIATIONS

5-HT	Serotonin
Acetyl-CoA	Acetyl coenzyme A
ACh	Acetylcholine
AChE	Acetylcholinesterase, EC 3.1.1.7
ADHD	Attention-deficit hyperactivity disorder
BAC	Bacterial artificial chromosome
B_{MAX}	Maximum amount of drug or radioligand bound
cDNA	Complementary DNA
Ch	Choline
ChAT	Choline acetyltransferase, EC 2.3.1.6
cho-1	CHT gene, *C. elegans*
CHT	Choline Transporter, *SLC5A7 (*human), *Slc5a7* (rat/mouse)
CHT BAC	CHT overexpression mouse line
CHT HET	CHT heterozygous knock out mouse line
CNS	Central nervous system
CT1	Creatine transporter, SLC6A8
DA	Dopamine
DAT	Dopamine transporter
FDSS	Functional Drug Screening System
GABA	γ-aminobutyric acid
GAT1	GABA transporter, *SLC6A1*
GPCR	G-protein coupled receptor
[^{3}H]	Tritium labeled compound
HACU	High-affinity choline uptake
Hb9	Motor neuron-specific promoter
HC-3	Hemicholinium-3

HEK	Human embryonic kidney
HTS	High-throughput screen
K_D	Dissociation constant
K_I	Inhibition constant
K_M	Michaelis-Menten constant for the substrate concentration that is required for the reaction (enzyme or transport) to occur at half Vmax
LACU	Low-affinity choline uptake
LVAA-CHT	Human choline transporter with a leucine to alanine substitution at amino acid 531 and a valine to alanine substitution at amino acid 532
MKC-231	(2-(2-oxopyrrolidin-1-yl)-N- (2,3-dimethyl-5,6,7,8-tetrahydrofuro[2,3-b]quinolin-4-yl) acetoamide
ML352	N-((3-isopropylisoxazol-5-yl)methyl)-4-methoxy-3-((1-methylpiperidin-4-yl)oxy)benzamide
MLSMR	Molecular Library Small Molecule Repository
NIH	National Institutes of Health
NE	Norepinephrine
NET	Antidepressant-sensitive NE transporter, *SLC6A2*
NIS	Sodium-iodide symporter (*SLC5A5*)
PKA	Protein kinase A
PKC	Protein kinase C
SAR	Structure-activity relationship
SGLT	Sodium-dependent glucose transporter (*SLC5A1, 2, 4, 9, 10, 11*)
SMCT	Sodium-dependent monocarboxylate transporter (*SLC5A8, 12*)
SMIT	Sodium-dependent myo-inositol transporter (*SLC5A3*)
SLC6	Solute carrier 6 gene family, neurotransmitter-sodium symporter family
SMVT	Sodium-dependent multivitamin transporter, *SLC5A6*
TMD	Transmembrane domain
VAChT	Vesicular acetylcholine transporter, *SLC18A3*
V_{MAX}	Michaelis-Menten value for the maximal rate achieved by the system

CHAPTER 1

CHOLINE ON THE MOVE: PERSPECTIVES ON THE MOLECULAR PHYSIOLOGY AND PHARMACOLOGY OF THE PRESYNAPTIC CHOLINE TRANSPORTER (CHT)

Introduction

The neurotransmitter acetylcholine (ACh), acting on both muscarinic and nicotinic receptors in the central and peripheral nervous systems, controls or modulates virtually every physiological process from the regulation of skeletal and smooth muscle contraction to the modulation of heart rate and the control of higher brain functions such as attention, learning and memory (Olshansky, Sabbah, Hauptman, & Colucci, 2008; Sellers & Chess-Williams, 2012). Not surprisingly, alterations in cholinergic signaling underlie or impact risk for a wide variety of disorders, ranging from myasthenias, cardiovascular disease, and gastrointestinal disorders to addiction, attention-deficit/hyperactivity disorder (ADHD), and Alzheimer's disease (Alder, Chessell, & Bowen, 1995; Patane, 2014). In some cases, such as with Alzheimer's disease and its treatment with inhibitors of acetylcholinesterase (AChE) (Grutzendler & Morris, 2001), the understanding of cholinergic dysfunction has afforded opportunities for pharmacological intervention, though achieving specificity with such agents remains a challenge and the pervasive actions of ACh often limit therapeutic potential due to dose-limiting side effects (Alt et al., 2015). Thus, though the therapeutic potential of ACh-targeted medications is clear, much work remains to realize the potential of improving human health through cholinergic interventions that became apparent when Dale and Loewi first identified ACh and

established the principle of chemical signaling at cholinergic afferents to the heart, respectively (Dale, Laidlaw, & Symons, 1910; Karczmar, 1996; Zimmer, 2006).

The high-affinity choline transporter (CHT) is a protein essential to cholinergic signaling as it is the rate-limiting step in the synthesis of ACh (Figure 1). Though the characterization of CHT was considerably delayed, when compared to other cholinergic proteins and neurotransmitter transporters, studies on the mechanisms that control the localization of the transporter have revealed a unique opportunity to modulate cholinergic signaling. Until recently the only compound known to directly target CHT was hemicholinium-3 (HC-3) (Figure 2), a competitive inhibitor discovered over fifty years ago (Schueler, 1955). HC-3 was critical to defining high-affinity choline uptake (HACU), a process eventually attributed to CHT. Unfortunately, HC-3 displayed poor blood-brain barrier penetration and was extremely lethal, limiting its use as a therapeutic or an *in vivo* tool. Such an *in vivo* tool was the goal of high-throughput screening efforts that resulted in the discovery of ML352, as described in this thesis is a specific, and novel CHT inhibitor. CHT-directed modulators such as ML352 provide a path to a new era of cholinergic biology research with the potential to enhance the diagnosis of and/or treatment of cholinergic disorders.

In the introduction to this thesis, I have reflected upon how the major discoveries in cholinergic biology were shaped by the cholinergic compounds in each era and constructed them into a historical review to acknowledge the advancements in cholinergic biology that have led to the discoveries I have made during my graduate studies. The remainder of this dissertation describes my effort to develop compounds through high-

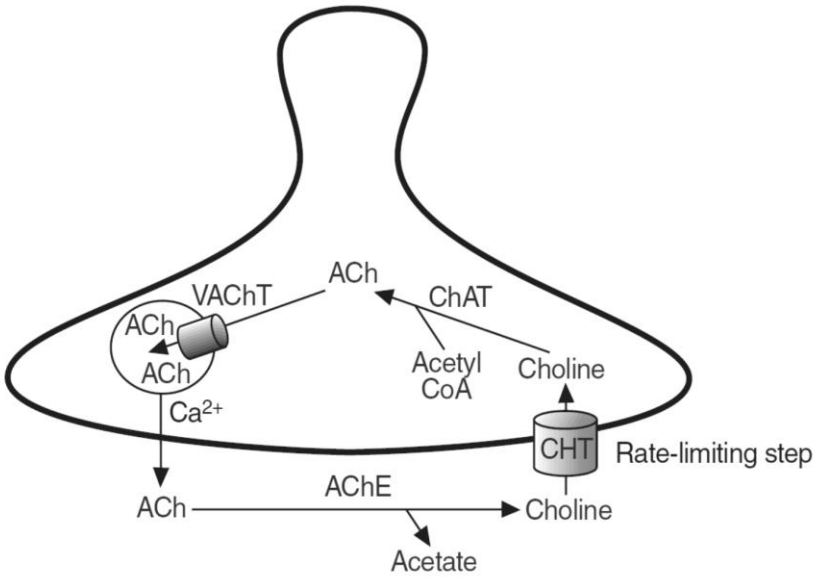

Figure 1. Support of acetylcholine (ACh) synthesis sustained by high affinity choline transporter (CHT)-mediated choline uptake. A) Choline acetyltransferase (ChAT) synthesizes acetylcholine (ACh) from choline (Ch) and acetyl coenzyme A which is then packaged into synaptic vesicles by the vesicular acetylcholine transporter (VAChT). Synaptic vesicles fuse with the plasma membrane on the presynaptic terminal in response to increased cytoplasmic [Ca^{2+}] releasing ACh which is then degraded by acetylcholinesterase (AChE). The high affinity choline transporter transports choline into the presynaptic terminal for the synthesis of ACh. Figure utilized with permission from the American Society of Pharmacology and Experimental Therapeutics. (Ferguson & Blakely, 2004)

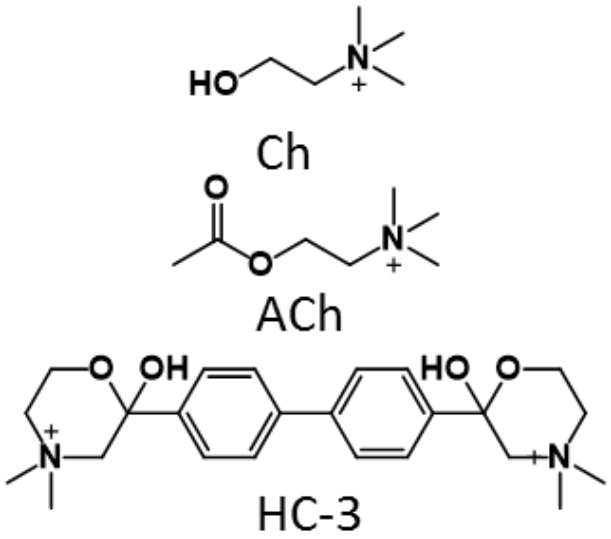

Figure 2. Structures of choline (Ch), acetylcholine (ACh), and hemicholinium-3 (HC-3).

throughput screening approaches, moving from initial hits to characterized compounds with novel mechanisms of action. The agent identified in this effort, ML352, and its analogs represents the first small molecule CHT inhibitors in fifty years.

The Scientific Scenery that Cholinergic Pharmacology in Context

Before Acetylcholine (ACh) was a Neurotransmitter

Before neuroscientists developed a conceptual understanding of neurotransmitters and neurons, cholinergic drugs, such as atropine, curare, nicotine and physostigmine had been in use for tribal medicines and rituals, as well as chemicals to facilitate ancient hunting techniques (Karczmar, 1993). These natural products, originating from mosses, beans, and whole plants, made their way into research laboratories in the late 19th century where their constituents were chemically extracted and tested on mammalian tissues. Consumption of the Calabar bean, for example, which contains physostigmine, was described to cause miosis, respiratory depression, muscle paralysis, and giddiness (Karczmar, 1993). Application of muscarine was found to induce a decrease in heart rate whereas curare blocked muscle contraction. Both muscarine and curare influenced neuronal stimulation at their respective tissues, leading to deinnervation studies that determined the site of their action. Degeneration of the nervous inputs revealed that muscarine and curare retained their ability to block the effects of tissue extracts and interacted with a receptive substance on the organ itself. Early experimentation with cholinergic compounds eventually led to the recognition of the

acetylcholine signal at the neuromuscular junction, and propelled the discovery of chemical neurotransmission.

Discovery of ACh and the Fundamentals of Chemical Neurotransmission

The application of exogenous chemicals and their actions supported the prediction by Cajal of an interface between neurons and their effector organs, which was followed by historic work to identify endogenous chemicals, such as norepinephrine (NE) and ACh, derived from tissue extracts. The actions of these agents led John Newport Langley and Paul Ehrlich to develop receptor theories to explain the communication seen between neurons and organs, which proposed the existence of a substance that interacted with a target molecule to transmit the message and a structure to receive the message. Evidence to support receptor theory was provided by Thomas Renton Elliott, who compared the effects of extracts containing epinephrine when applied to a particular tissue to that of neuronal excitation, and observed that they produced the same results. Being the first to present chemical transmission in writing to the scientific community, Elliott suggested that his observations may be the result of more than one type of “junction” or chemical signal, thus foreshadowing the discovery of ACh. Although, Elliott’s theory was presented in 1904, ACh had already been synthesized by René de M. Taveau for Reid Hunt in 1897. Together, they presented evidence that a precursor or derivative of choline was a hypotensive agent. This pioneering research by Langley, Ehrlich, Elliot, Hunt, and Taveau directed Sir Henry Hallett Dale and Otto Loewi to conduct more detailed studies on the actions of ACh (Dudley, 1929). Dale and Loewi went on to receive the Noble Prize in Physiology and Medicine in 1936 for their “discoveries relating to chemical transmission of nerve impulses".

With the recognition of ACh as a chemical messenger, cholinergic biology was ripe for discovery. Dale along with several other collaborators went on to investigate the effects of ACh at several different organs ranging from muscle to sweat glands (Clark, 1926b; Davis, 1931). During this era, direct injection of ACh into the limbs, heart, veins, and other regions of cats, dogs, and humans was found to trigger numerous biological consequences such as a change in blood pressure, the stimulation of peristalsis, and spontaneous convulsion at high doses. Lower doses of ACh injected in the lateral ventricle of a man caused nausea, vomiting, increased intestinal movements, and sweating without effecting respiration or circulation. To better understand the mechanism of ACh effects, the same drugs that suggested the existence of neurotransmission were used to modulate the actions of ACh. Atropine, previously shown to antagonize the effects of pilocarpine, also inhibited the ability of ACh to decrease the isometric contraction of an isolated ventricular strip from a frog heart (Clark, 1926a). Due to interactions between ACh and cholinergic drugs, such as atropine, it was hypothesized that they acted at the same site. These findings laid a conceptual foundation for the structure-activity relationship (SAR) studies that ultimately lead to the synthesis of HC-3, as noted below, a high-affinity inhibitor of high-affinity choline uptake (HACU) and ACh synthesis.

ACh, High-Affinity Choline Uptake (HACU) and the Birth of CHT

An Overview of the Mechanics of ACh Synapses

To delineate the actions of ACh, many have probed and elucidated the microscopic machinery that controls cholinergic signaling. The *in vitro* synthesis of ACh had been

described nearly fifty years before choline acetyltransferase (ChAT, EC 2.3.1.6, Figure 1), the enzyme responsible for the synthesis of ACh, was identified (Okuda & Haga, 2003; Prado et al., 2002). ChAT synthesizes ACh by transferring the acetyl group from acetyl coenzyme A (Acetyl-CoA) to cytosolic choline. The distribution of ChAT activity in vertebrates mirrored the distribution of ACh macroscopically (Feldberg & Mann, 1946) and antibody studies revealed the enzyme to be localized to neuronal processes that support ACh release (Kobayashi et al., 2002; Kus et al., 2003). Although a small fraction of ChAT was membrane-associated, the bulk of protein and enzymatic activity fractionates with the cytosol (Benishin & Carroll, 1983; Rylett, 1989; Tucek, 1967). Genetic elimination of ChAT is lethal in mice (Brandon et al., 2003) and loss of function mutations produce potentially fatal myasthenic disorders associated with episodic apnea in humans (Ohno et al., 2001).

After synthesis, cytosolic ACh is packaged into synaptic vesicles by the vesicular ACh transporter (VAChT, SLC18A3), a H^+/ACh antiporter embedded in the vesicle membrane. Intracellular acidification of cholinergic (and all) synaptic vesicles is accomplished through ATP hydrolysis by a H^+ pumping, vacuolar-type ATPase (Breer, Morris, & Whittaker, 1977). Upon vesicular fusion, ACh that is released into the extracellular space is rapidly hydrolyzed by acetylcholinesterase (AChE, EC 3.1.1.7), producing acetate and choline. Choline produced through this mechanism can rapidly diffuse from the synapse or, as noted below, be recaptured and recycled for subsequent ACh synthesis.

From ACh to HACU

ChAT is not generally thought to be saturated with choline in neurons (Haga & Noda, 1973), making the provision of choline rate-limiting in the production of ACh. However, whereas acetyl-CoA is an abundant contributor to cell metabolism and is at high levels intracellularly in many cells, the quaternary nitrogen of choline, which is obtained largely through dietary sources (Cohen & Wurtman, 1976; Jope & Jenden, 1979), precludes transfer of choline across the plasma membrane of cells via diffusion, necessitating support of ACh synthesis by an efficient choline transport process (Bligh, 1952) (Figure 2). The functional importance of choline uptake became apparent in studies documenting the decline of ACh release by cholinergic terminals in sympathetic ganglion after continual stimulation bathed in solutions lacking the precursor (Mulder, Yamamura, Kuhar, & Snyder, 1974; Perry, 1953). In Perry's studies, ganglia were treated with the AChE inhibitor, eserine, and perfused with choline-free medium, thereby depriving synapses of a supply of extracellular choline. These conditions were suspected to limit synthesis of ACh if endogenous pools of choline could not sustain ACh synthesis to keep pace with release. The comparison of a stimulated ganglion to an unstimulated ganglion revealed equal amounts of ACh in spite of the time-dependent decline in ACh release observed. These observations were explained by the hypotheses that exogenous choline is critical for ACh synthesis and that ACh resided in two compartments, a readily releasable pool and a reserve pool that supports the need for rapid versus sustained ACh release, respectively (Mulder et al., 1974; Perry, 1953). Birks, and reported a similar decline in ACh after repeated stimulation of cat cervical ganglion that could be rescued by the perfusion of blood containing choline (Macintosh, Birks, & Sastry, 1958). A choline transport system that supported ACh synthesis here had its origins and later was

demonstrated to be saturable by normal dietary sources of choline (Brunello, Cheney, & Costa, 1982). As the concentration of choline in the extracellular fluid was estimated to be approximately 10^{-5} M (Garguilo & Michael, 1996), a HACU process appeared responsible (compared to the amino acid and sugar transporters that work at mM substrate concentrations) for providing the precursor needed to sustain ACh synthesis (Mulder et al., 1974; Perry, 1953).

With the critical nature of choline uptake in ACh synthesis and release established, the investigation to determine the nature of choline influx into tissues was pursued through radiotracer methods. Brain slices and other tissues incubated with [^{14}C]choline demonstrated their ability to elevate choline levels to concentrations higher than that of the incubation medium, which was suggestive of an energy-dependent transport system (Hodgkin & Martin, 1965; Martin, 1968). Incubations with high (5 µM) and low (0.1 µM) concentrations of choline resulted in data that was better described by two separate Michealis-Menten constants, implying two separate transport systems. These initial uptake studies with [^{14}C]choline revealed the existence of a low affinity choline uptake (LACU) system but were unable to assert the existence of HACU due to limitations inherent in the high concentrations of [^{14}C]choline used at the time. The introduction of higher specific activity [^{3}H]choline allowed studies to be conducted at low enough concentrations to demonstrate HACU in preparations containing cholinergic terminals (Marchbanks, 1968, 1969). A number of other organic cation transporters and ion channels are known to provide for choline movement across cells, though with 1-2 orders of magnitude lower affinity (LACU) and the systems provide choline for other needs not specifically linked to ACh synthesis (e.g. phosphatidylcholine synthesis) (Tayebati &

Amenta, 2013). The high capacity of these LACU systems however means that care must be taken when working at or above concentrations of choline needed to saturate HACU, if the latter process is to be queried for its selective contributions. An additional source of choline for HACU is ACh hydrolysis, since AChE regenerates choline in the process of synaptic ACh inactivation (Okuda et al., 2003). As noted well below, presynaptic membrane deposition of CHT proteins occurs as a result of ACh vesicle fusion, which we speculated may have arisen as a mechanism to insure localization of the transporter proximal to release sites, thereby facilitating recapture of AChE-derived choline before the precursor can diffuse away from the synapse.

Studies with synaptosomes enabled researchers to make significant progress in the characterization of HACU (Diamond & Kennedy, 1969; Simon & Kuhar, 1976; Yamamura & Snyder, 1973). In 1966, Whittaker's curiosity about the localization of ACh in tissues led to extensive fractionation studies where he described the "characterization of acetylcholine-containing particle as pinched-off nerve endings (synaptosomes)" (Whittaker, 1965). With this preparation, Whittaker and Marchbanks noted a rapid uptake of choline that could then be recovered after lysing the synaptosomes in a hypotonic solution, supporting a transmembrane choline uptake process. The choline transport across the synaptosomal membrane was shown to be specifically dependent on the concentration of Na^+, providing a potential mechanism to drive uptake via coupling to a transmembrane Na^+ gradient, established by Na^+/K^+ ATPase. When monitored as a function of time and extra-synaptosomal choline concentration, the rate of choline "flux" was determined to have two components, a nonlinear one that was sensitive to choline concentration, and a linear component that was nonsaturable, with an estimated K_M of

232 μM (Marchbanks, 1968). By incubating synaptosomes in a solution containing radiolabeled [^{14}C]choline, an accumulation of [^{14}C]ACh could be detected (Potter, Glover, & Saelens, 1968). The synthesis of [^{14}C]ACh in synaptosomes, like choline transport, was also found to be dependent on the presence of Na^+ and Cl^- and unaffected by the addition of oxotremorine or ouabain (Marchbanks, 1969). As an aside, the Cl^- sensitivity of HACU initially led the Blakely lab to use homology-based cloning strategies to search (erroneously) for the gene encoding CHT in the family of transporters responsible for NE, dopamine (DA) and serotonin (5-HT) uptake, since these transporters, unlike glutamate and many other solute transporters, exhibit Cl^- dependence (Amara, 1992). Importantly, ACh that was synthesized from radiolabeled choline was found not only in the cytoplasm but also in the synaptic vesicle fraction, suggesting it can enter into a releasable neurotransmitter pool. As synaptosomes were shown to take up choline to support ACh synthesis, the synaptosomal uptake of choline was tested against the previous conditions known to distinguish HACU and that tracked with cholinergic regions in tissues. Two kinetically distinct choline uptake process were identified in synaptosomes, a low affinity and a high affinity, the latter associated with ACh synthesis (Yamamura & Snyder, 1972). The HACU process in synaptosomes was reported by numerous researchers to be saturable, and dependent on Na^+ (Diamond et al., 1969; Simon et al., 1976; Yamamura et al., 1973). Manipulations of the experimental conditions also determined that synaptosomal HACU was sensitive to temperature, pH and ion dependency and optimal at a temperature of 37^{o}C, a pH of 8.6, and in the presence of both Na^+ and Cl^- (Diamond et al., 1969). The compiled data on HACU led researchers to postulate that a “macro molecule with a high binding capacity for choline” could support the sodium-dependent

high-affinity choline uptake though, ironically, in their conclusions, they were hesitant to assert the existence of such macromolecules (Marchbanks, 1968).

Hemicholinium-3: Key Reagent in the Definition of HACU

Key to the evaluation of HACU in synaptosomes was the discovery of HC-3 (Birks, Macintosh, & Sastry, 1956; Diamond et al., 1969; Schueler, 1955). Long and Schuler synthesized and described the hemicholiniums, a collection of aromatic compounds containing a bis-quartenary ammonium (Figure 2). The *bis*-quartenary ammonium compounds became of interest when they, like curare, displayed anticholinergic effects in *ex vivo* nerve-tissue preparations from rat (Barlow & Ing, 1948), and a lethal toxicity that could be reversed by artificial respiration. The commonality in structure gave rise to a structure activity relationship (SAR) study around the core structure of hemicholinium. These studies noted that the third in the series of agents described, HC-3, was the most toxic, and this molecule became the focus of further study. HC-3 displayed a toxicity that was consistent across different animals, though the dose varied by species. Administration of HC-3 caused respiratory depression, and tonic and/or clonic convulsions followed by death. Schueler demonstrated that the convulsions were due to anoxia, as they could be prevented by artificial respiration, suggesting that their toxic actions might be largely peripherally-mediated. HC-3 came to be explored more deeply for effects on the cholinergic system due to the similarity of toxic effects to other agents that interfere with cholinergic signaling, as well as the presence in the HC-3 structure of two, ring-embedded, choline-like moieties. Over a thousand studies have been published

referencing HC-3 since its synthesis, attesting to the key role played by this agent in the study of cholinergic physiology in general, and HACU in particular.

In one of the earliest studies, Birks, and colleagues observed HC-3 applied to minced brains inhibited ACh synthesis and could be antagonized by the presence of choline. In their conclusions, they postulated that HC-3 might target HACU as opposed to ChAT, the ACh synthesizing enzyme (Birks et al., 1956), noting…

> "An alternative explanation would be that HC3, and other hemicholiniums, may compete with choline transport by a specific carrier system into interneuronal sites of acylation."

HC-3 Radioligand Binding: HACU enters the Molecular Era

Studies by Simpson and Smart of radiolabeled choline binding to hippocampal synaptosomes had detected Na^+-dependent binding sites that were sensitive to low concentrations of HC-3 (Simpson & Smart, 1982). Coyle's group (Sandberg & Coyle, 1985) capitalized on the availability of [^{3}H]HC-3 to identify molecular sites supporting HACU, using the same radioligand binding methods that Pert and Snyder had used to reveal the existence of endogenous receptors for opiate drugs (Pert & Snyder, 1973). Ironically, the opiate receptor identification was achieved in a fortuitous departure by this group from studies of choline uptake in the myenteric plexus, and their HACU work was published subsequently (Pert & Snyder, 1974). In 1985, Sandberg and Coyle, published their characterization of [^{3}H]HC-3 binding sites in rat brain membranes (Sandberg et al., 1985). Rainbow and Yamamura's groups first capitalized on the availability of [^{3}H]HC-3

to identify anatomically defined binding sites in brain preparations (Figure 3) (Rainbow, Parsons, & Wieczorek, 1984; Vickroy, Fibiger, Roeske, & Yamamura, 1984; Vickroy, Roeske, Gehlert, Wamsley, & Yamamura, 1985; Vickroy, Roeske, & Yamamura, 1984). In the Coyle studies (see also (Manaker, Wieczorek, & Rainbow, 1986; Vickroy, Roeske, et al., 1984), HC-3 binding to rat forebrain synaptic membranes was found to be saturable, reversible, pH dependent, and of high-affinity, with a K_D of 35 nM and a B_{MAX} of 56 fmol/mg. Binding conditions were determined to be optimal with coincubation with 200 mM NaCl in keeping with the Na^+ and Cl^- dependence of HACU. The rank-order potency of HACU inhibitors was preserved in competition studies of [^{3}H]HC-3 binding. Choline competed for [^{3}H]HC-3 binding with a K_i of 40 µM and [^{3}H]HC-3 binding distribution followed the expected distribution of cholinergic terminals suggesting that the site labeled by HC-3 bound to the endogenous site of HACU. Moreover, transection of the fornix, severing the septo-hippocampal projection, produced a loss of hippocampal [^{3}H]HC-3 binding sites in parallel with a loss of ChAT activity. Though these studies, and those of others in the field with similar approaches, a molecular entity supporting HACU began to clearly emerge, though it would be another 15 years before the molecular nature of that entity, now known as CHT, would be revealed (Apparsundaram, Ferguson, & Blakely, 2001; Apparsundaram, Ferguson, George, & Blakely, 2000; Okuda et al., 2000).

With a radioligand probe for CHT in hand, Coyle's group would move on to make important contributions to our understanding of HACU regulation. Lowenstein and Coyle (Lowenstein & Coyle, 1986) demonstrated that brain membrane binding sites labeled by [^{3}H]HC-3 were sensitive to drugs administered to animals, paralleling effects obtained when HACU was assessed *ex vivo*, further validating [^{3}H]HC-3 as a probe useful to the

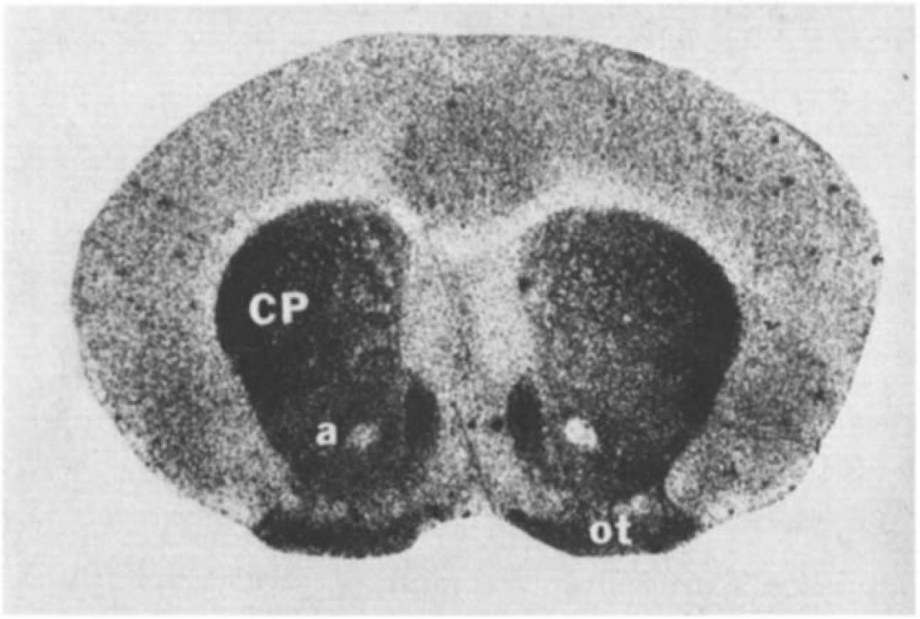

Figure 3. Rat brain autoradiogram of sodium-dependent [^{3}H]hemicholinium-3 (HC-3) binding sites. High levels of [^{3}H]HC-3 binding is seen in caudate-putamen (CP), nucleus accumbens (a), and olfactory tubercle (ot). Figure republished with permission from Elsevier (Rainbow et al,1984).

study of HACU/CHT and identifying changes in density that foreshadowed changes in surface expression of CHT proteins and exposure of choline uptake sites following depolarization (Ferguson et al., 2003a) (Figure 4). Saltarelli in Coyle's group (Saltarelli, Lowenstein, & Coyle, 1987) reported that an increase in the density of [^{3}H]HC-3 binding sites could be detected by treating membranes with elevated K^+ solutions, suggesting that either the binding site can move between open and closed states, or that tethered vesicles harboring CHT can fuse under these conditions, exposing CHT binding sites. Further studies denoted an ability of calcium-dependent mechanisms and phospholipases to modify HACU in brain slices as well as the membrane density of [^{3}H]HC-3 binding sites (Saltarelli, Lopez, Lowenstein, & Coyle, 1988; Saltarelli, Yamada, & Coyle, 1990; K. Yamada, Saltarelli, & Coyle, 1988a, 1989, 1991b), consistent with a highly dynamic state of CHT availability. That these changes were likely to be of physiological or pathophysiological relevance was supported by in findings of rapid and significant CHT elevations following seizures generated by pilocarpine (K. Yamada, Saltarelli, & Coyle, 1991a).

CHT Molecular Biology and Regulation

Early Efforts to Identify CHT Proteins

To our knowledge, Marchbanks was the first to report successful reconstitution of synaptic HACU from solubilized proteins (King & Marchbanks, 1982; Marchbanks, 1982), demonstrating HC-3 sensitive choline uptake in liposomes and providing prescient evidence for the trafficking of CHT on ACh filled vesicles. In these studies, the group

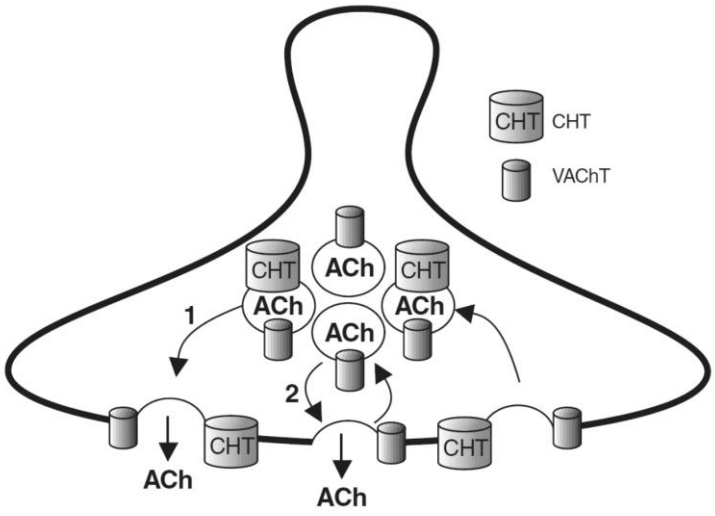

Figure 4. Diagram of the localization of CHT and its vesicular trafficking. CHT protein is largely localized at steady state to a subset of VAChT positive synaptic vesicles. Fusion of synaptic vesicles releases ACh and delivers CHT to the plasma membrane where the protein functions to take up choline released from ACh hydrolysis. Figure utilized with permission from the American Society of Pharmacology and Experimental Therapeutics (Ferguson & Blakely, 2004).

reported evidence for both HACU and LACU, suggesting that either a single transporter can exist in two states or that multiple carriers/subunits were reconstituted in parallel. Yamada and colleagues in the Coyle lab (K. Yamada, Saltarelli, & Coyle, 1988b), solubilized brain membranes and retained [^{3}H]HC-3 binding sites, suggesting a possible path to a further molecular analysis of CHT protein. Rylett (Rylett, 1988) used [^{3}H]choline mustard to label proteins of the Torpedo electroplax electric organ, a preparation rich in cholinergic terminals, yielding species of 42 kDa, 58 kDa, and 90 kDa, with labeling of the former two species absent when labeling was conducted in the presence of HC-3. Breer and colleagues (Breer, Knipper, & Kahle, 1989; Knipper, Boekhoff, & Breer, 1989) developed monoclonal antibodies that blocked HACU in insect preparations and used these to purify an 80 kDa species that could support HC-3 sensitive HACU on liposome reconstitution. Deglycosylation studies (Knipper, Kahle, & Breer, 1991) indicated that the core protein isolated had a mass of approximately 65 kDa. Although these studies did not yield sequence information or progress toward cDNA or gene isolation, and as such may or may not have reflected CHT isolation, the apparent molecular mass of the species identified was later determined to fit reasonably well with the size of CHT which was determined once antibodies were developed from on the cloned transporter (see below).

Cloning and Characterization of CHT cDNAs and Genes

As noted above, efforts to clone CHT cDNAs that encode CHT accelerated in the early 1990s with the elucidation of founding members of the SLC6 transporter gene family (Broer & Gether, 2012; Guastella et al., 1990; Pacholczyk, Blakely, & Amara, 1991). Both the GAT1 GABA transporter (*SLC6A1*) and the antidepressant-sensitive NE transporter

(NET, *SLC6A2*), as noted earlier, display requirements for extracellular Na^+ and Cl^- to drive neurotransmitter uptake, and thus the Na+/Cl^- dependence of HACU suggested that CHT would also be a member of the SLC6 gene family (Figure 5). Indeed, one lab reported the cloning of a choline transporter as a member of the SLC6 family (Mayser, Schloss, & Betz, 1992), though the Blakely lab could not replicate these findings, and ultimately the cDNA identified turned out to be a transporter for creatine (CT1, SLC6A8) (Guimbal & Kilimann, 1993; Schloss, Mayser, & Betz, 1994).

Okuda and colleagues were the first to report cDNAs for what we now know to represent CHT and that supports HACU (Okuda et al., 2000). These investigations identified CHO-1 in *C. elegans* and a rat species they termed CHT1. We prefer the designation of CHT since there appear to be no other molecular species supporting HACU. Surprisingly, the sequence of these cDNAs identified the transporter as a member of the SLC5 gene family (*SLC5A7*), a family that encodes, among others, Na^+-dependent glucose transporters (SGLTs) (Figure 5). Shortly after Okuda and colleagues reported the cloning of CHT, the Blakely lab reported sequences of human and mouse CHT (Apparsundaram et al., 2001; Apparsundaram et al., 2000). Our studies predicted CHT proteins to contain 580 amino acids folded into an N-glycosylated protein of 13 transmembrane domains (TMD), with an extracellular amino terminus, and an intracellular carboxyl terminus (Figure 6). Canonical phosphorylation sites for protein kinase C and protein kinase A were identified, along with 12 other serines and 10 threonines that hold potential for noncanonical phosphorylation (Apparsundaram et al., 2001). The topology of CHT has been supported by cysteine scanning analysis, and a three-dimensional model of CHT based on vSGLT has been generated (Figure 7), guiding ongoing structure

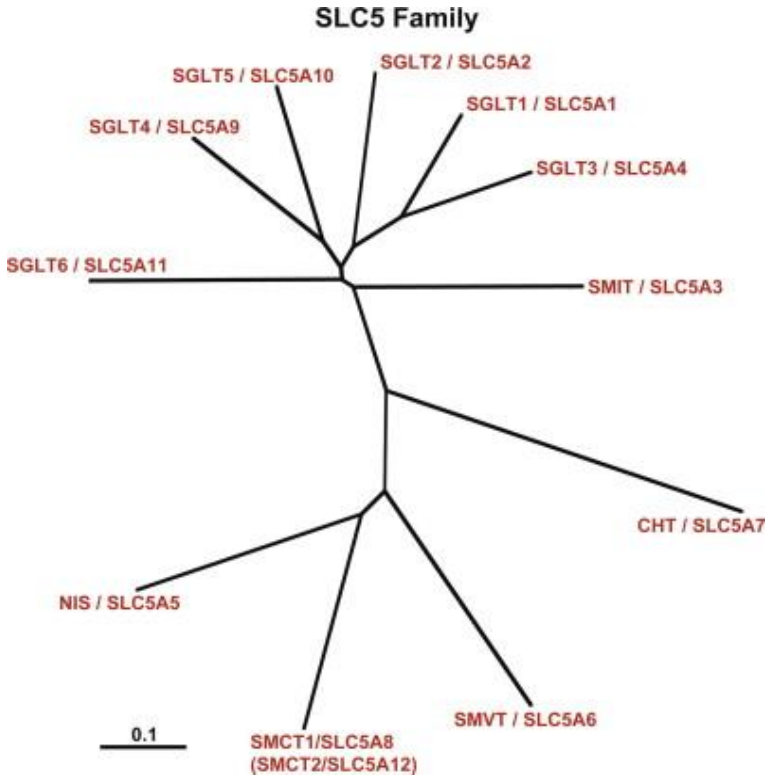

Figure 5. SLC5 gene family containing various glucose transporters and the CHT. Reprinted from Molecular Aspects of Medicine, 34, Ernest M. Wright, Glucose transport families SLC5 and SLC50, 183-196. Figure republish with permission from Elsevier (2013).

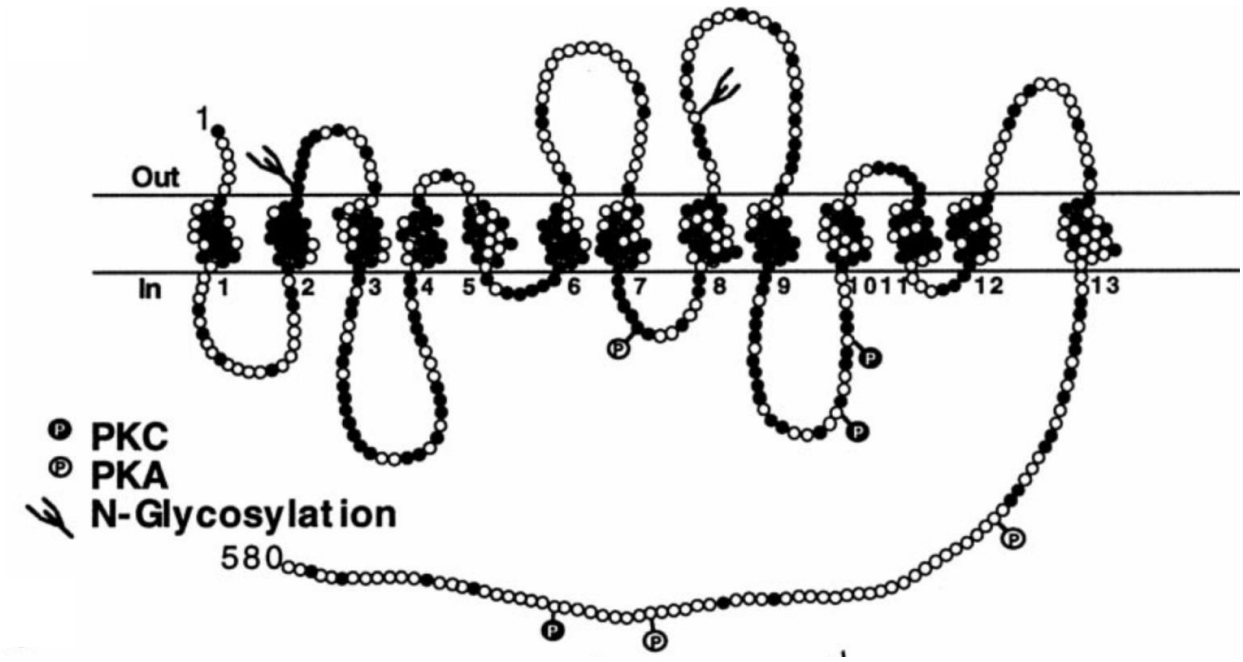

Figure 6. Predicted secondary structure of human CHT with for protein kinase C (PKC), protein kinase A (PKA) and N-linked glycosylation sites indicated. Dark circles indicate amino acid residues conserved in human, mouse, rat and nematode choline transporters. Figure republished with permission from Biochemical and Biophysical Research Communications (Apparsundaram et al, 2000)

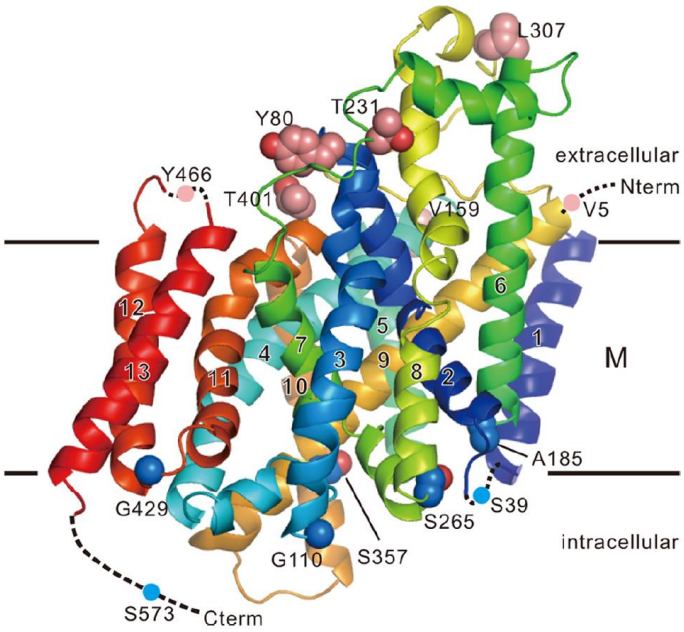

Figure 7. 3D Homology model of human CHT based on *Vibrio parahemeolyticus* Na^+/galactose cotransporter structure. The color of the structure changes from blue to red as the sequence runs from the amino terminus to the carboxyl terminus while the unmodeled loops are indicated by dashed lines. Individual atoms are represented by colored balls with extracellular carbon in pink, inaccessible carbon by cyan, and oxygen in red. Figure republished with permission from American Society for Biochemistry and Molecular Biology (Okuda et al, 2012).

function studies (Okuda et al., 2012). Although a CHT monomer is believed to be the functional unit supporting HACU, many other transporters have been found to exist in homo- and hetero-multimeric complexes and, in this regard, a homodimerization motif, GXXXG (Russ & Engelman, 2000), has been noted in TMD 12. Crosslinking and immunoprecipitation studies (Okuda et al., 2012), and dominant-negative character of human CHT mutations has provided experimental evidence that CHT may oligomerize *in vivo* (Barwick et al., 2012).

Molecular Mechanisms of CHT Regulation

With the sequence of CHT available, highly specific antibodies that detect *bona fide* CHT protein in biochemical and cell biological studies could be produced (Ferguson et al., 2003a; Guidry, Willison, Blakely, Landis, & Habecker, 2005; Harrington, Hutson, & Southwell, 2007; Hoover, Ganote, Ferguson, Blakely, & Parsons, 2004; Kobayashi et al., 2002; Kus et al., 2003; Lips, Pfeil, Haberberger, & Kummer, 2002; Nakata, Okuda, & Misawa, 2004; Proskocil et al., 2004). These studies revealed CHT localization to be highly enriched in the presynaptic terminals of cholinergic neurons, including projections of the mammalian basal forebrain, striatum, medial habenula and motor neurons, providing higher resolution, yet complementary patterns, to the distribution of CHT first defined through [^{3}H]HC-3 autoradiography. The availability of CHT antibodies also led to a discovery of a novel mechanism that supports activity-dependent trafficking of CHT to the presynaptic membrane (Figure 4) (Ferguson & Blakely, 2004; Ferguson et al., 2003a). In the studies of Ferguson et. al., subcellular fractionation studies of brain CHT protein

revealed an enrichment of the transporter in membranes that co-fractionate with synaptic vesicle markers, including VAChT. Immuno-electron microscopy studies confirmed a predominant localization of CHT to synaptic vesicles in cholinergic terminals (Ferguson et al., 2003a; Holmstrand, Asafu-Adjei, Sampson, Blakely, & Sesack, 2010; Nakata et al., 2004), with a much lower expression on the presynaptic plasma membrane under basal conditions. Using a surface biotinylation approach, Ferguson et al. (Ferguson et al., 2003a) also demonstrated that depolarization of synaptosomes with K^+ leads to a translocation of CHT protein to the plasma membrane, an effect dependent on Ca^{2+} influx and synaptic vesicle fusion machinery. These studies led to the model that CHT traffics to the cell surface in an activity-dependent manner due to its high steady-state residence on cholinergic synaptic vesicles, where the transporter, lacking a Na^+ gradient to support choline uptake, is inactive. Interestingly, immuno-depletion studies revealed that CHT protein is present in only a subset (~50% in brain preparations) of cholinergic vesicles labeled with VAChT antibodies, suggesting the existence of a unique sub-population of ACh storage vesicles that are responsible for CHT surface trafficking. Parikh and colleagues in the Sarter group have provided evidence that CHT trafficking through this mechanism is a key feature of activity-dependent elevations in HACU that support the continued ACh release needed for sustained attention (Apparsundaram, Martinez, Parikh, Kozak, & Sarter, 2005b; Parikh, St Peters, Blakely, & Sarter, 2013; Sarter & Parikh, 2005).

The presence of CHT on cholinergic synaptic vesicles suggests that CHT may target to presynaptic regions via the same mechanism that traffics synaptic vesicle proteins from the cell soma to neuronal terminals. Support for this idea has been provided

in studies by Matthies and colleagues (Matthies, Fleming, Wilkes, & Blakely, 2006) who observed somatic retention of *C. elegans* CHO-1 in a kinesin mutant (*unc-104*) that results in retention of other synaptic vesicle proteins. Evidence has also accumulated that the synthesis and export of CHT to cholinergic terminals is under retrograde influences by target-derived signals (Krishnaswamy & Cooper, 2009). High steady-state localization of CHT to synaptic vesicles also raises the question as to how the transporter localizes to this compartment. Studies in transfected cells with CHT mutants have revealed evidence for a dileucine motif in the CHT C-terminus that promotes efficient clathrin mediated endocytosis of surface transporters (Ribeiro et al., 2003; Ribeiro et al., 2005; Ribeiro et al., 2006). Using a genetic mouse model system, Misawa and colleagues have presented evidence that the clathrin adaptor protein AP-3 may be responsible for CHT export from intracellular membranes and endocytosis (Misawa et al., 2008). Rylett's group (Cuddy et al., 2012) has provided evidence that the peroxynitrite donor SIN-1 can influence CHT endocytosis, ubiquitiylation and degradation, suggesting that oxidative stress may be able to influence cholinergic signaling capacity by targeting CHT away from synaptic vesicles and to a degradative, proteosomal pathway.

Prior to the cloning of CHT and the identification of putative phosphorylation sites, the ability of kinases and phosophatases to regulate ACh synthesis had been documented. Thus, the Ser/Thr phosphatase inhibitors calyculin A and okadaic acid dose-dependently reduce ACh synthesis in rat hippocampal slices (Issa, Gauthier, & Collier, 1996). The mechanism of action for these agents was not due to inhibition of ChAT but could, in part, be explained by a decrease in HACU. The availability of CHT antibodies has permitted metabolic phosphate labeling of CHT proteins followed by

immunoprecipitation, with evidence from such studies supporting phosphorylation of hippocampal and striatal CHT after calyculin A and okadaic acid treatment that parallel reductions in HACU and surface CHT levels (Gates, Ferguson, Blakely, & Apparsundaram, 2004a). The kinases responsible for CHT phosphorylation, as well as whether phosphorylation is a critical determinant of activity-dependent trafficking, have yet to be defined. An emerging area of CHT research, with regulatory and clinical implications, concerns the identification of proteins associated with the transporter (Bales et al., 2006; Fishwick & Rylett, 2015; Misawa et al., 2008; Okuda, Konishi, Misawa, & Haga, 2011; Ribeiro et al., 2003; Xie & Guo, 2004; H. Yamada, Imajoh-Ohmi, & Haga, 2012). Given the evidence for CHT phosphorylation noted above, and evidence for a localization of CHT to cholesterol-rich plasma membrane microdomains (Cuddy, Winick-Ng, & Rylett, 2014), it will be interesting to see whether, or which, of these protein associations are modulated by the state of CHT phosphorylation, and whether specific membrane compartments support these interactions.

CHT Contributions to Cholinergic Function and Dysfunction *In Vivo*

CHT Genetic Animal Models

As noted above, HC-3 administration to animals *in vivo* can be lethal, presumably due to an inability to sustain ACh synthesis and release. To validate an essential requirement for CHT in sustaining cholinergic signaling, the Blakely lab genetically ablated the *Slc5a7* locus in mice to produce animals with no functional capacity to

synthesize the transporter (CHT KO), or with only one functional allele (CHT HET) (Ferguson, Bazalakova, et al., 2004). At birth, CHT KO pups appear grossly normal, but within 30 minutes they demonstrate abnormal breathing and cyanosis (Figure 8) as well as limited movements that progress to full paralysis, resulting in death within an hour. These studies also detected a complete loss of HC-3 sensitive [^{3}H]ACh synthesis from exogenous [^{3}H]choline. Though there is a complete loss of CHT protein (Figure 8) in the KO, cholinergic signaling at the neuromuscular junction *ex vivo* appears normal at the beginning of recordings, but progressively demonstrates a loss of spontaneous and evoked end plate potentials, consistent with a failure to synthesize and release ACh. Compensatory changes in AChE or ChAT activity were not detected. Interestingly, Ferguson and colleagues detected alterations in the organization of axonal inputs to muscle fibers in the CHT KO, with a broader spread and increased branching of motor axons, consistent with a role for ACh in the development of cholinergic inputs to muscle. A similar pattern has also been observed for ChAT KO mice (Lin et al., 2005), consistent with a developmental requirement of ACh signaling during neuromuscular synapse development.

Although these studies clearly demonstrated an essential requirement for CHT in cholinergic signaling capacity, the lack of viability of CHT KO mice obviously precluded tests of a requirement for CHT in older animals, experiments that in mammals await the development of animals supporting conditional gene elimination. However, in *C. elegans*, many genes essential to life in vertebrates do not have such devastating effects, and the Blakely lab therefore examined the contribution of the transporter to cholinergic biology and behavior in worms deficient in expression of the CHT ortholog CHO-1 (Matthies et

al., 2006). Because the standard culture of worms on a lawn of OP-50 bacteria provides these animals with a food source high in choline, *cho-1* mutant worms lack an essential requirement for HACU, though they did observe a significant, 40% reduction in whole animal ACh levels. In the worm, as in man, ACh supports neuromuscular contraction and thus movement assays can be used to examine modulation of cholinergic signaling *in vivo.* When grown on OP-50, *cho-1* mutant animals display normal movement patterns. When grown on HB101 bacteria that contain low amounts of free choline, and when subjected to conditions that require high-rates of movement, Matthies et. al. (Matthies et al., 2006) detected premature fatigue in cho-1 animals, consistent with a time-dependent loss of neuromuscular cholinergic signaling capacity. Together, these studies demonstrate the critical role played by CHT and its phylogenetic orthologs in sustaining ACh synthesis and release *in vivo*.

The lethality caused by a full CHT KO in the mouse established an essential requirement for CHT in sustaining life. The site(s) of cholinergic signaling responsible for this lethality may be multifold (e.g. neuromuscular junction, spinal and brainstem cholinergic control of motor circuits, CNS cholinergic signaling) and cannot be ascertained solely through this model. The Blakely lab therefore pursued a rescue strategy, expressing CHT selectively in motor neurons of CHT KO mice under the control the Hb9 promoter (Lund et al., 2010). This effort succeeded in prolonging life in CHT KO animals by as much as 24 hrs. Possibly, the limited strength of the Hb9 promoter and the low amount of CHT produced in the rescue line may have been insufficient to sustain animals for a longer period of time. Alternatively, descending CNS/spinal cholinergic circuits that do not rely on Hb9 for expression become critical after the first day of life for driving the

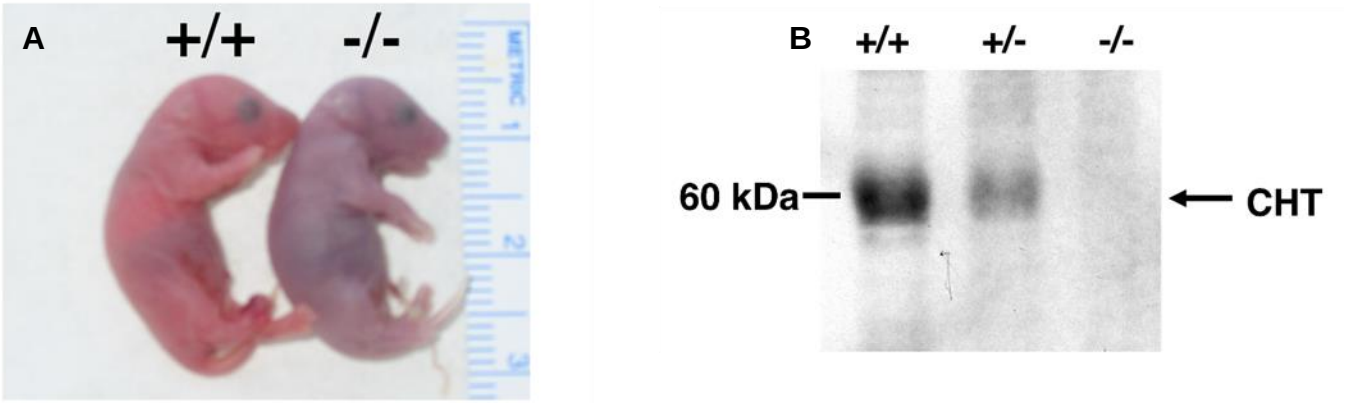

Figure 8. A. Photograph of high affinity choline transporter knock out mouse next to a wild type mouse four hours after birth. B. Representative western blot showing decreased CHT protein levels in CHT KO mice compared to their littermates while VAChT protein levels are unchanged. Figure utilized with permission from the Proceeding of the National Academy of Science USA (Ferguson et al 2004). Copyright (2004) National Academy of Sciences, U.S.A.

necessary motor rhythms needed for respiration, versus the contributions that motor neurons make to the execution of muscle contraction.

The CHT KO mouse line also affords a unique opportunity to evaluate the impact of reduced CHT availability on ACh synthesis, signaling and behavior via the study of CHT HET animals (Bazalakova et al., 2007; Ferguson, Bazalakova, et al., 2004). In their initial CHT KO study, Ferguson and colleagues found that forebrain [^{3}H]HC-3 binding and synaptosomal uptake were unaffected by loss of one copy of the *Slc5a7* gene, even though CHT protein levels were reduced by half, as revealed with CHT antibodies. The results suggested that post-translational mechanisms could compensate for reduced total protein expression, later validated in studies that revealed a shift in the proportion of CHT proteins from intracellular pools to the cell surface, permitting expression of a normal level of HACU (Parikh et al., 2013). The normal level of HC-3 binding observed in CHT HET mice reveals clearly that HC-3 cannot be used, without validation, to infer CHT protein density. Rather, HC-3 binding appears to reflect the density of surface resident transporters, where the HC-3 binding site becomes exposed in an “open out” conformation. Reflecting back also on the earlier Coyle group studies where *in vitro* manipulations could rapidly change [^{3}H]HC-3 density, it seems likely that binding changes arose in these studies due to the induced fusion of cholinergic synaptic vesicles tethered to plasma membrane fragments, or to a shift in conformation of plasma membrane-resident CHT, from an inactive, inward facing conformation that cannot bind the ligand, to an active, outward facing conformation, competent for HC-3 binding. Further studies are needed to explore these possibilities, though results may be very revealing with respect to the mechanics of CHT regulation.

As to phenotypes of CHT HET mice, these mice on first analysis appear grossly normal, growing to normal size, with a normal lifespan and normal fertility (Bazalakova et al., 2007). CHT HET KO mice also exhibit normal rates of horizontal locomotion, though they demonstrate an increase in vertical activity (rearing). Normal behavior was observed in the rotarod test, in the Morris water maze, and elevated plus maze and light-dark test, suggesting a lack of effect of loss of one *Slc5a7* allele on balance and motor learning, spatial learning and memory, or anxiety. These data indicate that the compensations that maintain normal rates of HACU in the CHT HET mouse also preclude the emergence of gross behavioral alterations. Despite these compensations, reductions are evident in striatal M1 receptors as well as cortical and striatal M2 muscarinic receptors (Bazalakova et al., 2007) whereas elevations are evident in cortical α4β2 nicotinic receptors. These findings suggest that demands for normal cholinergic signaling are not fully met in the CHT HET context. Notably, CHT HET mice demonstrated premature fatigue on the treadmill test (Bazalakova et al., 2007) (Figure 9), reminiscent of the motor deficits seen in *cho-1* mutant nematodes where animals fail to sustain normal rates of swimming behavior (Matthies et al., 2006). CHT HET mice also demonstrated reductions in scopolamine-induced hyperactivity (Bazalakova et al., 2007), as well as cocaine and nicotine-induced DA release *in vivo* (Dong, Dani, & Blakely, 2013), though whether these changes derive from ongoing deficits in ACh release (Paolone et al., 2013) or involve changes in synapse structure imposed by CHT heterozygozity during development needs to be explored. CHT HET mice demonstrate a basal tachycardia, though they mount a normal heart rate elevation upon exercise (English et al., 2010). Strikingly, when CHT HET mice are removed from the treadmill, they fail to reset their heart rates as quickly as

wild type animals, reinforcing the demand-dependent contribution of CHT to cholinergic signaling, in this case for vagally-mediated slowing of the heart. The hearts of CHT HET mice demonstrate enlargement and ventricular thickening, as well as age-dependent fibrosis, suggesting that the basal tachycardia throughout life remodels structural features of the heart, reminiscent of changes observed in cardiovascular disease in humans (English et al., 2010). Finally, CHT HET mice also demonstrate deficits in attention-demanding cognitive tasks (Parikh et al., 2013; Zurkovsky et al., 2013).

Genetic manipulations have also afforded insights into the consequences of abnormally *elevated* CHT expression. In the course of the studies by Lund and colleagues that sought to restore motor neuron CHT expression in CHT KO animals, breeding efforts also generated motor neuron specific overexpression of CHT(Lund et al., 2010). Analysis of these animals revealed an increased capacity for treadmill running, as well as increased compound muscle action potentials. In a separate effort, the Blakely lab also established a model of global, constitutive CHT overexpression, via genomic integration of a bacterial artificial chromosome (BAC) containing the full length *Slc5a7* gene (Holmstrand et al., 2014). CHT BAC mice express 2-3 fold more CHT protein binding throughout the body and a comparable elevation in neuronal HACU. Immunocytochemical analyses revealed a lack of ectopic transporter expression. In unpublished studies, the Blakely lab has found CHT BAC mice to support elevated depolarization-induced ACh release (Iwamoto, Calcutt and Blakely, submitted). Like the motor-neuron specific CHT overexpressors (CHT expressed by the Hb9 promotor on an otherwise wild type backgrounds), CHT BAC mice display reduced fatigue in the treadmill test (Figure 9). Additionally, these mice demonstrate increased horizontal activity in the

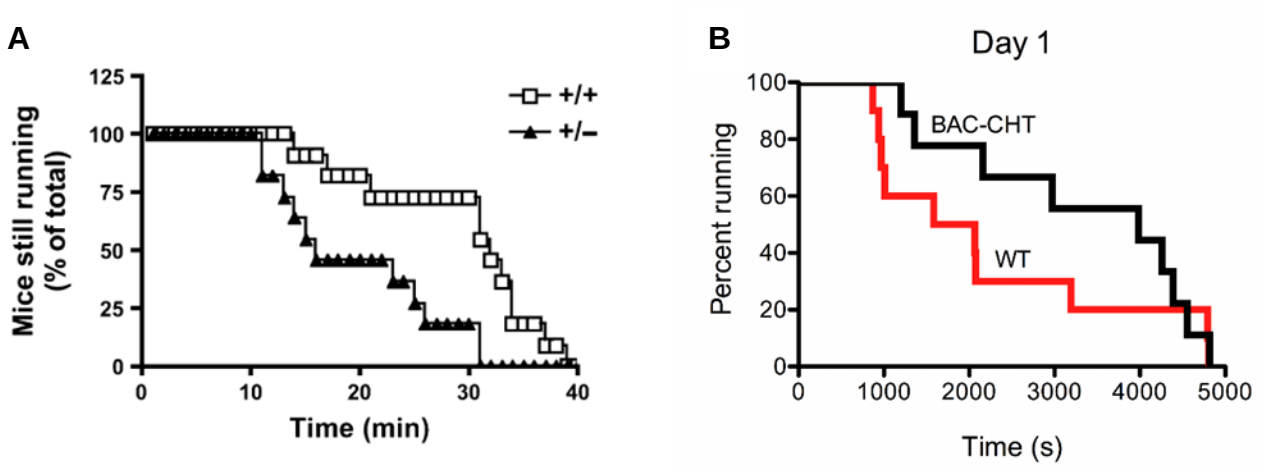

Figure 9. Behavioral phenotype of CHT HET and CHT BAC mice on treadmill task. A.CHT HET mice remained on a treadmill for shorter periods that litter mate controls revealing a locomotor phenotype. Graph taken from Bazalakova et. al. 2007. B. BAC-CHT mice demonstrated enhanced treadmill endurance at a fixed speed, over two sessions compared to wild type controls. Figures republished with permission from Elsevier (Holmstrand et. al. 2014).

open field, decreased spontaneous alterations in the Y-maze, and reduced time in the open arms of the elevated plus maze, consistent with an anxiety phenotype. Together, the CHT HET and CHT BAC mouse models represent important new tools in the study of contributions made by alterations in CHT expression and/or activity to cholinergic physiology and behavior.

CHT Gene Contributions to Human Disorders

The cloning of human CHT cDNAs and mapping of the *SLC5A7* chromosomal locus (2q12.3) (Apparsundaram et al., 2001; Apparsundaram et al., 2000; Okuda et al., 2000) has allowed for a search for potential functional polymorphisms and mutations that could impact disease risk. The first such polymorphism to be identified (rs1013940) was an A to G transition at nucleotide 265 of the cDNA that produces an Ile to Val substitution at amino acid 89 in TM3, reported to be present with an allele frequency of 6% in a small Ashkenazi Jewish cohort. Significant ethnic differences exist in allele frequency (http://www.ncbi.nlm.nih.gov/projects/SNP/snp_ref.cgi?rs=rs1013940), ranging from 1-15%. This is a significantly higher frequency for coding variation than observed for other neurotransmitter transporter coding variants, raising questions as to whether significant population risk for one or more disorders associated with disrupted cholinergic signaling might be impacted by CHT dysfunction. Indeed, the Blakely lab and our colleagues have found the Val89 variant to be overrepresented in subjects with major depressive disorder (Hahn et al., 2008) and ADHD (particularly the combined type) (English et al., 2009; Okuda, Okamura, Kaitsuka, Haga, & Gurwitz, 2002). With respect to depression, preclinical studies point to both a role for elevated cholinergic signaling in mood/anxiety

like behaviors in mice (Mineur et al., 2013), and differential *Slc5a7* expression may contribute to behavioral changes in rats bred for low vs high anxiety traits (Diaz-Moran et al., 2013). In relation to attentional dysfunction, Berry and colleagues (Berry et al., 2014) have reported a significant association of the Ile89Val polymorphism with distractibility, both in self-reports and in psychometric evaluations. This same group, using a functional magnetic resonance imaging approach found evidence that the Val89 variant associated with a redistribution of cortical activation in an attention-demanding task (Berry, Blakely, Sarter, & Lustig, 2015). A 3' untranslated region variant in the human SLC5A7 transcript (rs333229) has been associated with heart rate variability (Neumann, Lawrence, Jennings, Ferrell, & Manuck, 2005), reminiscent of the support for heart rate under basal and stress conditions observed in CHT HET mice (English et al., 2010). This variant has also been associated with subclinical measures of carotid atherosclerosis (Neumann et al., 2012). Most recently, Barwick and colleagues identified a loss of function, dominantly-acting coding mutation that truncates the transporter's C-terminus, producing a hereditary motor disorder (Barwick et al., 2012). *In vitro* functional studies in the Barwick et. al. studies indicate a likelihood that this mutation appears to influence the assembly of CHT oligomers, impacting protein levels and CHT trafficking.

Other studies of relevance to human disorders have provided evidence of changes in gene or protein expression accompanying the mutation of other genes or traits linked to brain disease. Thus, CHT gene expression, as well as that of the nicotinic alpha 7 receptor, has been reported to be significantly downregulated in mice deficient in maternal Ube3a expression, a model of Angelman's syndrome (Low & Chen, 2010), though whether these changes reflect Ube3a-linked ubiquitination pathways or other

mechanisms remains unclear. Although, only RNA changes in CHT were detected in the latter study, Yamada and colleagues found the ubiquitin ligase Nedd4-2 protein to interact with CHT and modulate transporter surface expression and activity in transfected cells (H. Yamada et al., 2012). Altogether, evidence suggests that both direct and indirect effects on CHT expression and function may contribute to motor, cardiovascular, mood and cognitive disturbances. Further investigation of molecular pathways that associated with CHT gene expression (Ye et al., 2014) may pay dividends in elucidating the broader impact of CHT gene and protein modulation underlying disease risk.

Advances in CHT Pharmacology

The Search for Novel CHT Modulators: MKC-23

As noted above, HC-3 has, for over 50 years, been the primary pharmacological tool employed for the contribution of CHT to HACU and cholinergic signaling. Due to its dual quaternary amines, HC-3 has limited CNS penetration and, though the reagent effectively targets CHT in accessible preparations, it can also interact with other targets with varying affinity (Mandl & Kiss, 2006; Yuan, Wagner, Poloumienko, & Bakovic, 2004). HC-3 is also a competitive CHT antagonist, binding to the same site that recognizes ACh, encourages to identify novel CHT-targeting pharmacologies. The compound (2-(2-oxopyrrolidin-1-yl)-N-(2,3-dimethyl-5,6,7,8-tetrahydrofuro[2,3-b]quinolin-4-yl)acetoamide (MKC-231), has been advanced as a positive modulator of CHT and cholinergic signaling *in vivo* (Murai et al., 1994). In this study, MKC-231 reversed hippocampal ACh depletion after lesion of cholinergic projections and improved working memory deficits as studied

Genetic Manipulation	Species	Observed changes	Reference
CHT KO	mouse	Early postnatal lethality	(Ferguson et al., 2004)
CHT KO	C. elegans	40 percent less ACh than wild-type animals Exhibit premature paralysis in choline free envriomeent	(Matthies, Fleming, Wilkes, & Blakely, 2006)
CHT HET KO	mouse	Grossly normal Impaired performance on the treadmill Reduced sensitivity to scopolamine in the open field task Density of M1 and M2 mAChRs in specific brain regions	(Bazalakova et al., 2007)
		Decreased ACh release after basal forebrain stimulation Impaired performance on sustained attention task	(Parikh, St Peters, Blakely, & Sarter, 2013)
		Attenuated ACh release during SAT task concurrent with normal performance Increased α4β2 nAChR density in cortex Diminished dopamine levels in the NAc Decreased DA levels after nicotine or cocaine administration	(Paolone et al., 2013)
		Tachardyia and hypertension at rest in mice	(English et al., 2010)
Hb:9	mouse	Increased survival time on CHT KO background Increased performance on treadmill task	(Lund et al., 2010)
HET KO & 6-OHDA treated	mouse	Impaired performance on object recognition Impaired performance on attentional set shifting paradigm	(Zurkovsky et al., 2013)
Overexpression	mouse	Diminished fatigue and increased speeds on treadmill task Decreased time in open arms of elevated plus maze	(Holmstrand et al., 2014)

Table 1. Summary of mouse lines with genetic alterations of CHT and highlights of the changes observed in these lines.

in the T-maze. Additionally, MKC-231 was found to elevate HACU after lesion and improve deficits in a spatial learning task (Bessho et al., 1996), Additional studies indicated that the drug improved evoked ACh release and HC-3 binding *in vivo.* However, the drug did not cause biochemical or behavioral effects in non-lesioned preparations, suggesting either a ceiling effect on HACU in normal animals or indirect linked to targeting pathological states (Bessho, Takashina, Eguchi, Komatsu, & Saito, 2008; Takashina, Bessho, Mori, Eguchi, & Saito, 2008). Since effects of the drug are long-lived, past the point of MKC-231 residency in the brain, the effects, at least of repeated dosing, would appear to be either indirect or a consequence of CHT-dependent compensations induced that can overcome the deleterious effects of a lesion. A mechanism supporting the latter effects has yet to be advanced. Although experiments with unlabeled MKC-231 and surface plasmon resonance suggest that the ligand has measurable affinity for CHT (Takashina, Bessho, Mori, Kawai, et al., 2008), studies are lacking that demonstrate specificity against other targets, that interactions correlate with CHT distribution, or are lost with cholinergic lesions that reduce CHT levels. Additionally, studies with radiolabeled MKC-231 that could allow further evaluation of ligand binding kinetics, and modes of CHT interactions, are lacking. Given that virtually all of the literature with the compound arises from *in vivo* studies with lesioned preparations, and that modulation of HACU and HC-3 binding is highly sensitive to the state of cholinergic neuron activation, it seems likely that MKC-231 effects derive from indirect actions, rather than a direct targeting of CHT.

The Search for Novel CHT Modulators: ML352

The findings for MKC-231, despite the concerns noted, helped maintain awareness that a new CHT pharmacology could provide insights into transporter physiology and regulation, as well as potential therapeutic leads. The emergence of an allosteric pharmacology targeting G-protein coupled receptors (GPCRs) (Conn, Lindsley, Meiler, & Niswender, 2014; Nickols & Conn, 2014) suggested to us that drugs could be developed that target CHT with increased specificity and brain penetration than HC-3, by capitalizing on interactions outside the orthosteric choline binding site, where a quaternary amine to drive high-affinity interactions would likely be needed. In order to pursue this idea, the Blakely lab first sought to overcome obstacles that limit the use of traditional high-throughput screens (HTS), specifically 1) the low surface expression of CHT at steady state in transfected cells and 2) the reliance to date on CHT assays based on radioactive choline uptake. Following transferring the human CHT C-terminus onto a plasma membrane reporter protein, Ruggiero et. al used site-directed mutagenesis studies with this construct or the full length protein to identify two amino acids (Leu531Val532) that meet criteria as a dileucine motif and that, when mutated to alanine (LVAA), lead to significantly elevated CHT surface expression, overcoming the first concern (Figure 10) (Ruggiero et al., 2012). These studies identified overlapping sequences to those found by Ribeiro and colleagues who identified sites in the CHT C-terminus determining endocytic control of CHT surface expression (Ribeiro et al., 2003; Ribeiro et al., 2005; Ribeiro et al., 2007).

To address the need for a nonisotopic CHT activity assay that would be compatible with an HTS format, the Blakely lab considered the possibility that the electrogenicity of

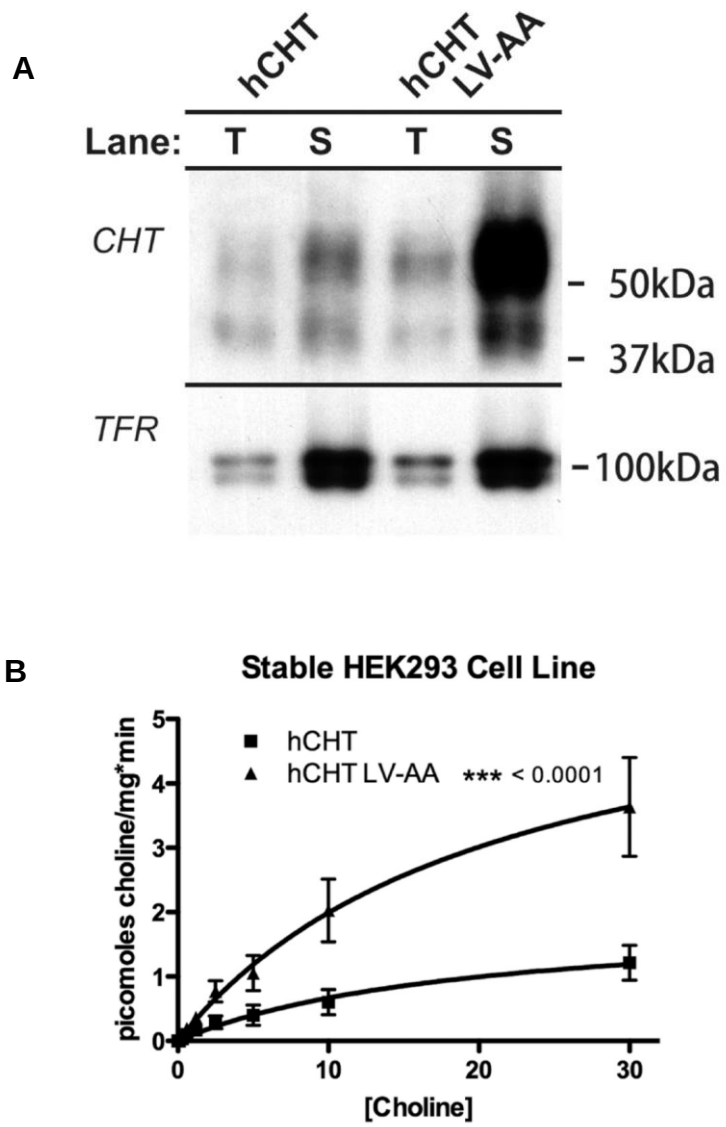

Figure 10. Characterization of the HEK 293 LVAA-CHT cell line. A. Western blot of HEK 293 cells transfected with WT and LVAA-CHT show that surface (S) levels of LVAA-CHT are significantly higher than the surface levels of wild type (WT) CHT while total levels of the respective CHT, total and surface levels of transferrin receptor (TFR) remain unchanged. B. Saturation kinetics analysis of LVAA-CHT stably expressed in HEK 293 cells reveal a 3-fold increase in V_{max} compared to WT CHT. Figure utilized with permission from ACS Chemical Neuroscience (Ruggiero et.al. 2012).

the CHT transport cycle might allow for such an approach (Iwamoto, Blakely, & De Felice, 2006). Indeed, when we incubated HEK-293 cells stably transfected with the LVAA-CHT mutant were incubated with a membrane potential-sensitive dye, significant elevations in whole cell fluorescence could be detected upon addition of choline (Figure 11) (Ruggiero et al., 2012). As will be described below, a screen of over 300,000 compounds identified multiple compounds that could augment or inhibit choline-induced fluorescence and that failed to induce nonspecific changes in membrane potential in either the absence of choline or in cells lacking CHT (Ennis, Wright, Retzlaff, McManus, Lin, Huang, Wu, Li, et al., 2015).

Outline of the Dissertation

My goals in pursuing this thesis research was to use a HTS approach to identify novel CHT directed small molecules and characterize the molecular pharmacology and pharmacokinetics of a CHT inhibitor developed from HTS leads and subsequent SAR studies, and, then to, utilize this CHT inhibitor to determine the effects of CHT mediated cholinergic inhibition in basal physiology and disease states using mouse model. The work presented here begins after the endocytosis-deficient LVAA mutation in CHT and the electrogenic nature of CHT were described. These discoveries were the building blocks of the HTS which made it possible to embark on an endeavor to create novel CHT pharmacology. In chapter 2, the one structural class of inhibitors identified through out HTS and the SAR studies based on that class are of CHT inhibitors is detailed. The details on the other structural classes of inhibitors are located in Appendix 1 while efforts to identify leads for CHT activators is described in Appendix 2. Chapter 3 describes a novel,

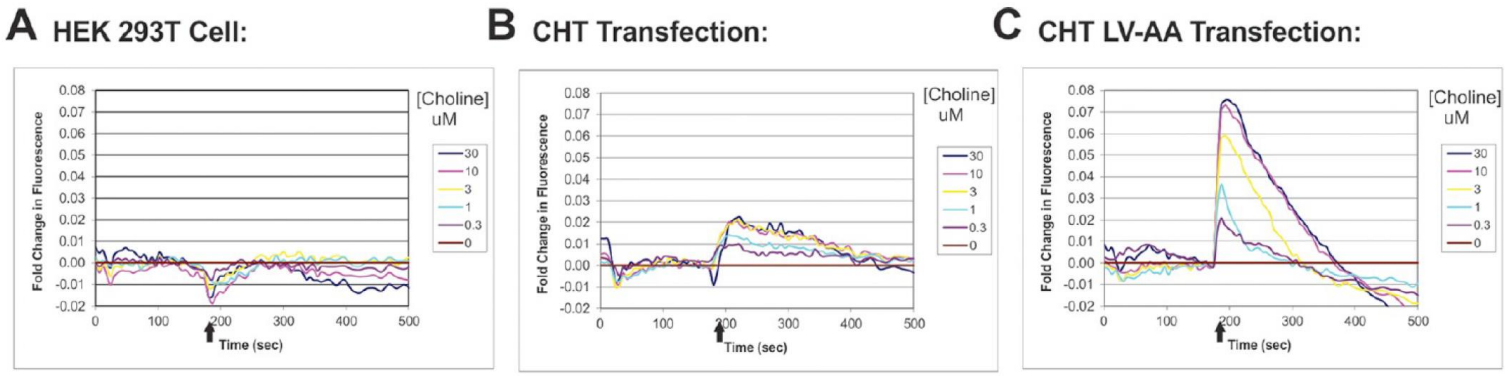

Figure 11. Fluorescent membrane potential assay in transiently transfected HEK293 cells following application of choline. A. HEK 293 cells alone do not generate a fluorescent signal after the addition of choline and hence do not have a choline-induced membrane depolarization. B-C. HEK 293 cells transiently transfected with wild type (WT) CHT, B, or LVAA-CHT, C, demonstrate a choline induced membrane depolarization in a dose dependent manner. Figure A, B, and C republished from Ruggiero et. el. 2012.

non-choline-based, CHT-targeted inhibitor (ML352) that demonstrates nanomolar CHT antagonism, as well as selectivity for CHT in relation to multiple transporters, ion channels, and receptors. In addition, Chapter 3 includes our kinetic studies with ML352 that provides evidence of allosteric modulation of the transporter and, providing a novel path to the development of cholinergic therapeutics. The *in vitro*, and *ex vivo* data on ML352 is followed in Chapter 4 by the initial efforts to characterize ML352 *in vivo*. Pharmacological characterization of ML352 in wild type mice allowed for planning of future studies in the DYT1 dystonia mice, described in Appendix 3.

CHAPTER 2

THE IDENTIFICATION OF ML352 THROUGH SAR STUDIES BASED ON HTS LEAD COMPOUNDS*

Introduction

The neurotransmitter acetylcholine (ACh) plays a critical role in autonomic function, motor control, attention, learning, and memory, and reward (Hasselmo & Sarter, 2011; Mark, Shabani, Dobbs, & Hansen, 2011). Consequently, multiple, devastating disorders have been linked to perturbations of cholinergic signaling, including Alzheimer's disease (AD) (Doody, 2003), Parkinson's disease (PD) (Manganelli et al., 2009), dystonia (Sciamanna, Hollis, et al., 2012; Sciamanna, Tassone, et al., 2012), myasthenia (Pisani, Bernardi, Ding, & Surmeier, 2007), schizophrenia (Higley & Picciotto, 2014), and addiction (Williams & Adinoff, 2008), among others. Cholinergic agents, including acetylcholinesterase inhibitors (AChEIs) and muscarinic/nicotinic receptor agonists and antagonists, are used to treat symptoms in diseases with either diminished or excessive cholinergic signaling, as in AD, nicotine addiction (Koegelenberg et al., 2014), and dystonia (Jankovic, 2013). Although these agents have proven to be useful, their efficacy is reduced by dose-limiting side effects and, in some cases, a constitutive mode of cholinergic manipulation. Sustained synthesis of ACh is dependent on the efficient acquisition of choline by cholinergic terminals, an activity exclusively mediated by the

* Research described in this chapter was previously published in Bioorganic & Medicinal Chemistry Letters (Bollinger et. al., 2015)

high-affinity choline transporter (CHT, SLC5A7) (Apparsundaram et al., 2001; Apparsundaram et al., 2000; Haga, 2014; Okuda et al., 2000). Not surprisingly, full loss of CHT in transgenic mice produces a time-dependent elimination of cholinergic signaling that is incompatible with life (Bazalakova & Blakely, 2006; Ferguson, Bazalakova, et al., 2004). Less radical genetic manipulations of CHT also result in significant biochemical, physiological, and behavioral effects, in keeping with a key contribution of the transporter to ACh signaling.

Thus, CHT heterozygous animals exhibit reduced ACh levels and ACh release, basal and exercise-induced tachycardia (English et al., 2010), and diminished neuromuscular signaling and motor endurance. Elevated CHT expression leads to increased ACh levels and reduced motor fatigue (Holmstrand et al., 2014; Lund et al., 2010). With respect to CNS function, CHT heterozygous animals demonstrate reduced performance on tasks that require sustained attention in the presence of distraction and in tests of behavioral flexibility as well as diminished dopamine elevations following cocaine or nicotine challenge, whereas CHT overexpressing mice exhibit anxiety/depression behaviors. In keeping with these rodent studies, functional polymorphisms in the SLC5A7 gene have been linked to neuromuscular disorders, elevated distractibility and ADHD, and depression.

CHT is conspicuous in being absent from current efforts to pharmacologically manipulate cholinergic function, but it may possess advantages in therapeutic targeting related to its activity-dependent support of cholinergic signaling, mediated by a steady-state enrichment on cholinergic synaptic vesicles, where it can move to the plasma membrane in response to cholinergic neuron activation. This feature also suggests that

CHT-targeted antagonists may display use dependence, thereby limiting drug effects to states of intense cholinergic signaling. CHT-mediated choline transport can be effectively attenuated by the competitive antagonist HC-3. Unfortunately, many of the properties of HC-3, including the presence of two choline-like quaternary nitrogens as well as its limited CNS penetrance and challenging chemical synthesis, restrict the use of the molecule as a tool for mechanistic studies or as a starting point for the development of imaging or therapeutic agents. However, in the more than 50 years since the first synthesis of HC-3, no other widely utilized CHT-targeted agents have been developed. To expand CHT pharmacology, we took advantage of the electrogenic nature of CHT-supported choline uptake to implement a membrane potential-based, high-throughput screen for CHT modulators (Iwamoto et al., 2006; Ruggiero et al., 2012).

Although CHT has been known to play a critical role in dictating cholinergic signaling capacity for many decades (Birks & Macintosh, 1957; Collier & Katz, 1974; Mulder et al., 1974), the transporter is conspicuously absent from targets engaged for the therapeutic manipulation of cholinergic signaling. In part, this may be due to the understanding that full elimination of transporter function in vertebrates, as seen with CHT knockout mice, is incompatible with life. In CHT knockout mice, however, loss of CHT expression occurs throughout life, irrespective of demand, and thus the model may poorly represent the therapeutic limitations associated with CHT antagonism. Possibly, attenuated cholinergic signaling, rather than full inhibition, may offer an effective treatment for disorders where hypercholinergic function has been proposed as a major etiological component. For example, the uncontrolled movements associated with dystonia are commonly treated with anticholinergic agents to reduce both central and

peripheral control of motor function. Hypercholinergic function has also been associated with depression and anxiety behaviors (Mineur et al., 2013; Picciotto, Higley, & Mineur, 2012). In the latter case, the nonspecific muscarinic ACh receptor antagonist scopolamine has received significant attention as a rapidly acting antidepressant. Finally, ACh receptor stimulation is intimately involved in the modulation of reward circuits, where anticholinergics have been shown to reduce aspects of reward signaling (Crooks et al., 2004; Shinohara, Kihara, Ide, Minami, & Kaneda, 2014) and CHT heterozygous mice have been found to demonstrate reduced dopamine release in response to cocaine and nicotine (Dong et al., 2013).

The importance of CHT in determining ACh signaling capacity, the therapeutic potential of CHT antagonism, and the limitations of HC-3 noted above encouraged us to pursue a high-throughput screen to identify novel CHT modulators. Here, we report the results of our screen for CHT inhibitors. We describe a novel, non-choline-based, CHT-targeted inhibitor (ML352) that demonstrates nanomolar CHT antagonism as well as selectivity for CHT in relation to multiple transporters, ion channels, and receptors. Our kinetic studies with ML352 are the first to demonstrate the possibility of allosteric modulation of the transporter and offer a novel path to the development of cholinergic therapeutics.

Here, I report the results of the HTS effort, including further diversification of initial hits. Out of our structure activity relationship studies (SAR) (Figure 12), we identified a novel, non-choline based, CHT- targeted inhibitor (ML352) (Figure 13). These studies that yielded ML352 and its analogs are the first to provide pharmacology, other than HC-3, to modulate the transporter, and offer pathways to new tools for the study of CHT

contributions to cholinergic signaling, as well as a path to the development of novel tools that afford imaging and/or therapeutic manipulation of cholinergic synapses. We characterize the mechanism of ML352 inhibitory action on CHT in Chapter 3.

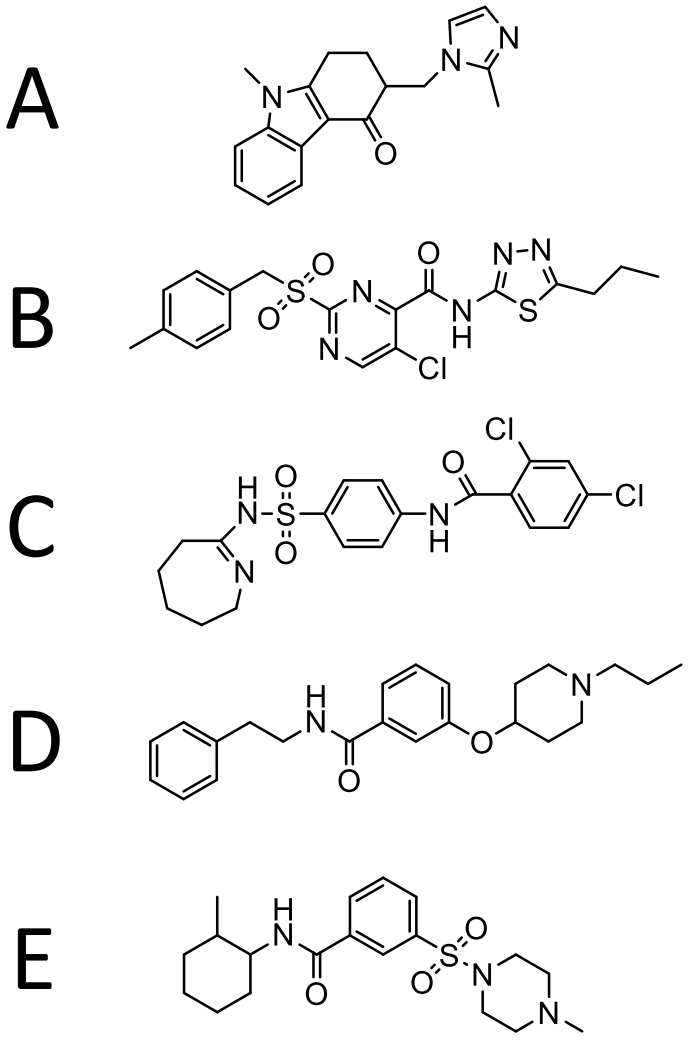

Figure 12. Five structures that are representative the 5 structural classes identified in the high-throughput screen.

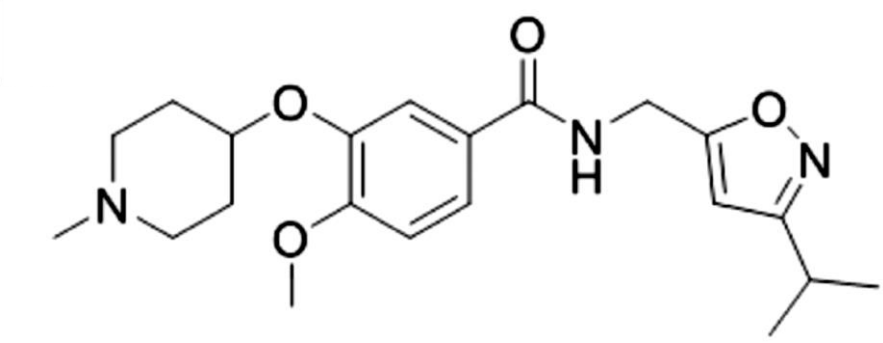

Figure 13. Chemical structure of ML352.

Materials and Methods

Reagents and Cells

All biochemical reagents were of research grade and, unless stated otherwise, obtained from Sigma Aldrich (St. Louis, MO, US). Commercially available replicates and derivatives of molecules identified as hits in our HTS screen were obtained from Ambinter (Orleans, France) as dry powders. HEK 293 cells stably transfected with either the human CHT (CHT) or a mutant, LVAA-CHT (L531A, V532A), were described previously (Ruggiero et al., 2012) and maintained according to American Type Culture Collection (ATCC, Manassas, VA, USA) guidelines using MEM Earles media containing 1X fetal bovine serum, 2mM glutamine, 100IU penicillin and 100 µg/mL streptomycin (Fisher-Scientific, Pittsburgh, PA, USA). All studies used cells cultured at 70−100% confluency.

Choline-Induced Membrane Potential Assay (96-Well Flex-Station Format)

HEK 293T cells stably expressing LVAA-CHT or control cells were assessed for choline-induced membrane depolarization as previously described (Ruggiero et al., 2012). Cells were plated into 96 well, black walled, clear bottom poly-D lysine coated plates (BioCoat BD Biosciences). Cells were plated in 50 µL/well at 45,000 cells/well and allowed to grow for 48 hrs. Cells were pre-incubated in HBSS/HEPES 1X dye (60 µL of Blue membrane potential dye, R8042 at 1.67 µg/mL, Molecular Devices, Sunnyvale, CA, USA) for 30 min at 37 °C in an atmosphere of 95% air/5% CO_2. Tested compounds were added at this pre-incubation step. Membrane potential-associated fluorescence was detected using a FlexStation (Molecular Devices) microplate fluorimeter, recording the

baseline (1 min), and following automated addition of choline (20 µL) to achieve 100 nM and 10 µM final concentrations in HBSS/HEPES 1X dye. Fluorescence was recorded for 2−4 min with sampling every 1.5 seconds. Data were analyzed by SoftMax Pro (Molecular Devices) and exported to Microsoft Excel for further evaluation.

Neurotransmitter Transport Activity Assay (96-Well Format)

Cells were plated onto poly-D-lysine coated, 96 well, white cell culture plates (Culturplate-96, Perkin-Elmer, Waltham, MA, USA) at 45,000 HEK 293 LVAA-CHT cells, or 20,000 HEK 293 hDAT, hNET, or hSERT cells in 100 µL/well and allowed to grow for 48 hours at 37 °C in an atmosphere of 95% air/5% CO_2. Each plate was washed 3X with 100µL KRH using a Biotek 405 Touch microplate washer (Winooski, Vermont, USA). Wells were filled with 40 µL of KRH buffer with or without drugs using a multichannel pipet. Plates were incubated at 37°C in an atmosphere of 95% air/5% CO_2 for 15 minutes for choline uptake assays and 10 minutes for DA, NE, and 5-HT uptake assays. Following the first incubation, an addition of 10 µL of either 100 nM or 10 µM (final concentrations) [^{3}H]-choline chloride (Perkin-Elmer, Waltham, MA, USA, NET109001MC,1 mCi/mL) or 50nM (final concentrations) [^{3}H]DA, (dihydroxyphenylethylamine,3,4-[Ring-2,5,6-^{3}H]) (Perkin-Elmer, NET673001MC, 1mCi/mL), ([^{3}H]NE] (norepinephrine hydrochloride, DL-[7-^{3}H(N)]) (Perkin-Elmer, NET048001MC, 1mCi/mL) or [^{3}H]5-HT (hydroxytryptamine creatinine sulfate) (5-HT),5-[1,2-^{3}H(N)] (Perkin-Elmer, NET498001MC, 1mCi/mL) in KRH buffer. Final concentrations of substrates solutions were made using 1% radioligand with 99% unlabeled neurotransmitter stock solution. After a 10-15 min incubation with radiolabeled substrates, each plate was washed 3X with 100 µL of KRH buffer using a

Biotek (Winooski, VT, USA) 405 Touch microplate washer. A volume of 100 µL of MicroScint™-20 (Perkin-Elmer, Waltham, MA, USA) was added to wells and uptake quantified by scintillation spectrometry using a TopCount instrument (Perkin-Elmer, Waltham, MA, USA). Counts obtained from wells incubated as noted above in the presence of inhibitors of CHT (HC-3, 10µM), DAT (Cocaine, 1uM), NET (mazindol, 1uM), and SERT (citalopram, 1uM) were subtracted from total uptake values to obtained specific uptake values. In saturation choline transport studies, serial dilutions from a 1-5% mix of radiolabeled and unlabeled choline was used to maintain specific activity. Choline transport velocity (V_{MAX}) and half saturation concentrations (K_M), and antagonist K_I values, were determined using non-linear curve fits in Prism 5 (GraphPad Inc, San Diego, CA USA).

Synthesis of 3-hydroxy-N-((3-isopropylisoxazol-5-yl)methyl)-4-methoxybenzamide (2)

To a round-bottomed flask was added 3-hydroxy-4-methoxybenzoic acid (1) (0.43 g, 2.55 mmol, 1.0 eq), (3-isopropylisoxazol-5-yl)methanamine hydrochloride (0.45 g, 2.55 mmol, 1.0 eq), Hünig's base (1.33 mL, 7.65 mmol, 3.0 eq) and DMF (15 mL) at rt. To the solution was added HATU (0.97 g, 2.55 mmol, 1.0 eq). After 8h at rt, the rxn was added to EtOAc:H_2O (1:1, 150 mL). The separated organic layer was washed with 1N HCl (50 mL), H_2O (2 x 50 mL), Brine (50 mL) and dried ($MgSO_4$). The mixture was filtered and the solvent removed under reduced pressure. The material was taken forward without further purification. LCMS: R_T = 0.766 min, >98% @ 215 and 254 nM, m/z = 290.8 $[M + H]^+$.

Synthesis of N-((3-isopropylisoxazol-5-yl)methyl)-4-methoxy-3-((1-methylpiperidin-4-yl)oxy)benzamide (3m, ML352)

To a solution of PPh_3 (0.72 g, 2.76 mmol, 2.0 eq) in THF (15 mL) at 0°C was added diethyl azodicarboxylate (DEAD) (0.44 mL, 2.76 mmol, 2.0 eq), followed by 4-hydroxy-*N*-methylpiperidine (0.27 g, 2.33 mmol, 1.7 eq). After 15 min, a solution of **2** (0.40 g, 1.37 mmol, 1.0 eq) in THF (5 mL) was added and the ice bath was removed. After an additional 24 hours at room temperature, the reaction was added to EtOAc:H_2O (1:1, 200 mL). The separated organic layer was washed with H_2O (50 mL), Brine (50 mL) and dried ($MgSO_4$). The mixture was filtered and the solvent removed in vacuo. The residue was purified by reverse-phase HPLC (15-55% acetonitrile: H_2O w/ 0.1% TFA) to afford ML352 (0.29 g, 55% yield over 2 steps). LCMS: R_T = 0.741 min, >98% @ 215 and 254 nM, m/z = 387.8 $[M + H]^+$; ^1H NMR (500 MHz, , 333K, DMSO-d_6): μ 8.81 (t, *J* = 5.8 Hz, 1 H), 7.60 (d, *J* = 8.4 Hz, 1 H), 7.56 (br s, 1 H), 7.10 (d, *J* = 8.5 Hz, 1 H), 6.24 (s, 1 H), 4.62-4.40 (m, 1 H), 4.54 (d, *J* = 5.7 Hz, 2 H), 3.85 (s, 3 H), 3.55-3.29 (m, 4 H), 2.96 (septet, *J* = 7.0 Hz, 1 H), 2.82 (br s, 3 H), 2.26-1.74 (m, 4 H), 1.20 (d, *J* = 7.0 Hz, 6 H); HRMS, calc'd for $C_{21}H_{30}N_3O_4$ $[M + H]^+$, 388.2236; found 388.2238.

Results and Discussion

Original HTS Hits

To establish a screen for novel CHT inhibitors, we capitalized on the significantly elevated surface expression of the human transporter bearing Ala substitutions for two amino acids, L531 and V532, that constitute a strong dileucine-type endocytic sequence.

In addition to the greatly enhanced choline activated membrane depolarization achieved in CHT LV-AA cells, the removal of strong endocytic sequences lessens the possibility that compounds that reduce choline-induced membrane depolarization do so by triggering transporter endocytosis. Using these cells, we instituted a triple-add protocol (Figure 14) that involved addition of vehicle or inhibitor in the absence of choline, followed 1 min later by the addition of an EC_{20} concentration (500 nM) of choline, followed 2 min later by the addition of an EC_{80} concentration (60 μM) of choline. To identify noncompetitive and potentially allosteric inhibitors distinct from HC-3, we focused on compounds that reduced signal at the EC_{80} choline concentration, also capturing the superior signal/noise characteristics associated with signals generated at or near the CHT Vmax. Figure 11A demonstrates the fluorescence emission from the triple-add protocol following addition of choline alone or choline in the presence of an inhibitor, a structural predecessor to the focus of this article, ML352. Using the triple-add format, we screened >300,000 compounds (Figure 15) from the NIH Molecular Library Small Molecule Repository (MLSMR) compound collection (http://mli.nih.gov/mli/secondary-menu/mlscn/ml-small-molecule repository/) at 60 μM, and, based on a cutoff criteria of 3 SD from the mean EC80 choline-induced fluorescence, we identified 2635 preliminary hits, a 0.86% hit rate. We were able to validate CHT depolarization inhibition by 1,714 of these compounds available for retesting, an ~65% replication rate. These compounds were then tested in a counter screen against nontransfected HEK 293 cells, where we found that 90% of these compounds lacked CHT-independent depolarization inducing activity, yielding 1,544 molecules for further analysis. Next, 5-point concentration response curves (CRC)

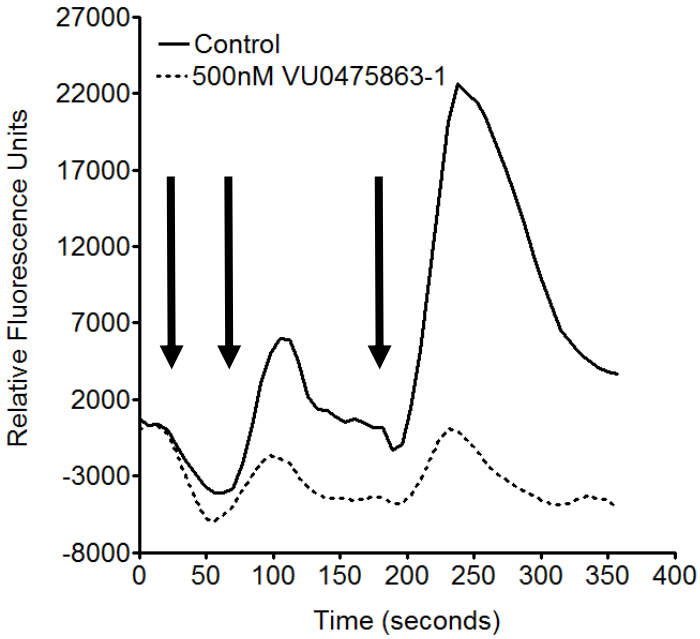

Figure 14. Example of the triple add fluorescence assay used in the HTS. The time course of the triple add protocol shows the depolarization of the HEK 293 cells stably transfected with LVAA-CHT after the addition of choline as indicated by the increase in random fluorescence units. Each arrow, going from left to right, represents the first addition containing compound or vehicle, followed by an EC_{20} choline (500 nM), and finally an EC_{80} choline (60 µM). The presence of 500nM VU0475863-1, one of the final 15 hits compounds and a progenitor of ML352, shows an inhibition of the depolarization during the triple add protocol (dotted line). Figure utilized with permission from ACS Chemical Neuroscience (Ennis et al 2015).

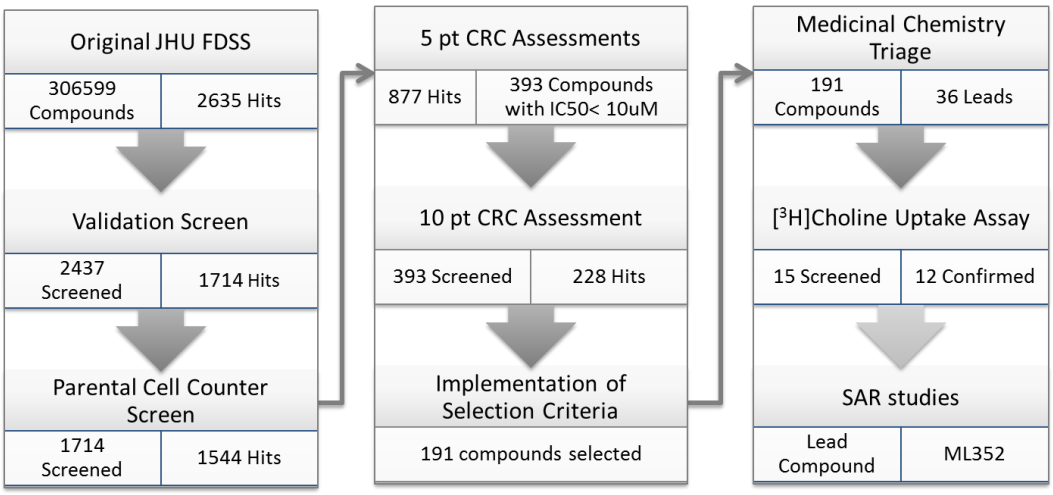

Figure 15. Workflow of the high-throughput screen. Our progress through the 9 major stages of the screen with the respective number of compounds that entered (small left-hand boxes) and exited (small right-hand boxes) each phase. Figure utilized with permission from ACS Chemical Neuroscience (Ennis et al 2015).

were performed using the CHT LV-AA based membrane depolarization assay. In this effort, we found that 57%, or 877, of the compounds displayed dose-dependent inhibitory activity. From this group, we selected 393 molecules based on having IC_{50} values lower than 10 μM to more carefully analyze in 10-point CRC assays, which yielded 228 molecules that retained high potency for inhibition of choline-induced depolarization. Of these compounds, 191 displayed no inherit fluorescence and retained their EC80 inhibitory potency upon repeat testing. Inspection of the molecules in this group revealed five major structural classes, comprising 36 molecules, whose structures also indicated suitability for chemical modifications and *in vivo* use. As membrane depolarization that arises with CHT activity is nonstoichiometrically linked to choline flux, we next selected 15 molecules derived from 3 of these classes for 5-point CRC tests, now targeting inhibition of [^{3}H]choline uptake, again using CHT LV-AA cells. In the latter tests, 12 molecules demonstrated significant, dose dependent inhibitory activity, of which belong to the one f2 class selected for chemical diversification. Details of our chemical diversification efforts will be described elsewhere. In this effort, we produced VU0476328 *N*-((3187isopropylisoxazol-5-yl)methyl)-4-methoxy-3-((1-methylpiperidin-4-yl)oxy)benzamide (Figure 13; hereafter designated ML352) as our most potent derivative and describe its characterization below.

Chemical synthesis for diversification of lead scaffold

The synthesis of the lead scaffold followed known procedures and is outlined in Figure 16. The commercially available 3-hydroxy-4-methoxybenzoic acid, 8, was converted to the appropriate amide, 9, via HATU coupling conditions. The common

intermediate amide, 9, could then be converted to the final compounds by either: a) standard Mitsunobu conditions (R_2OH, DEAD, PPh_3)9, or b) through a standard displacement reaction (R_2Br, Cs_2CO_3, KI, DMF). The final compounds, 10a-o, were isolated in modest to good yield.

Chemical Diversification of Lead Scaffold

The SAR assessment started with the evaluation of the right-hand amide portion of the molecule (Table 3). As many of these compounds were available from commercial sources, the SAR was performed via a combination of SAR by catalog and synthesis. The compounds were evaluated in a [^{3}H] choline transport assay utilizing a low (100 nM, sub-K_M) and high (10 µM, V_{MAX}) concentration of choline. We first measured the % activity remaining at both concentrations of choline (with a standard 5 µM concentration of compound), and those compounds that retained less than fifty percent activity were then progressed to CRC formats for IC_{50} determinations, again, at both concentrations. Since the lead compound from the HTS evaluation contained an isoxazole ring system, our first compounds evaluated similar 5-membered heteroaryl groups (**10a-h**). The thiazole and pyrazole compounds were active at both choline concentrations, albeit with modest potency (> 1 µM). The thiophene analog was inactive at the low concentration and modest inhibitory activity at the high concentration, **10c**. The 3-isopropylisoxazole methyl derivative, **10e**, a compound similar to the HTS hit compound was very potent at both concentrations (290 nM and 90 nM at the low and high choline concentrations, respectively). Moving to a six-membered heteroaryl (**10i**) or extending the chain length (**10j-k**) was only moderately tolerated.

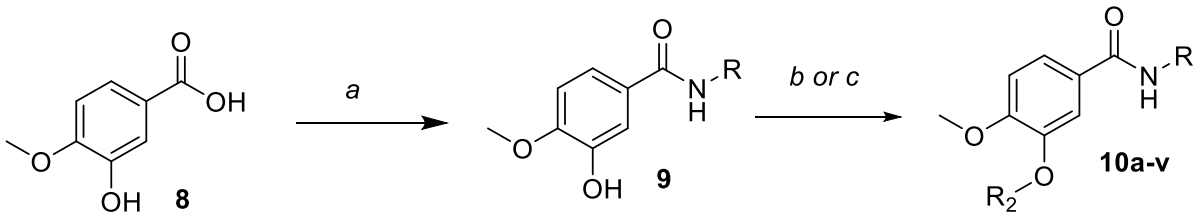

Figure 16. Reagents and conditions for SAR synthesis: (a) R-NH_2, HATU, DIEA, DMF, room temperature; (b) R_2OH, DEAD, PPh_3, THF, 0°C → room temperature, 41–59%; (c) R_2Br, Cs_2CO_3, KI, DMF, 120°C, 30 minutes, µW, 23–93%. Figure utilized with permission from *Bioorganic & Medicinal Chemistry Letters* (Bollinger et. al. 2015).

Having evaluated and identified an optimal amide group, we next turned our attention to the 4-isopropylpiperidine ether moiety (Table 4). The synthesis of these compounds follows that outlined in Figure 16. The SAR around this portion of the molecule was quite narrow as substituents such as the cyclohexyl, **10o**, and cyclopentyl, **10p**, were inactive. Replacements that were tolerated included the (2-piperidin-1-yl)ethoxy, **10q**, (IC_{50} = 0.76 and 0.53 μM, respectively) and 2-morpholinoethoxy, **10r**, (IC_{50} = 6.12 and 1.77 μM, respectively). However, the morpholine was ~10-fold less active than the piperidine analog. Removal of the isopropyl group from the piperidine ether led to a much less active compound (NH, **10l**). However, the methylpiperidine ether analog, **10m**, was an active compound – equipotent with the isopropyl analog. Moving the *N*-methylpiperidine from the 4-position to the 3-position, **10n**, was tolerated, but less active. Lastly, the unsubstituted phenol, **10v**, was inactive. Based on the potency at both concentrations of choline studied, **10m**, was declared an MLPCN probe compound, ML352, and further profiled as outlined in the next chapter.

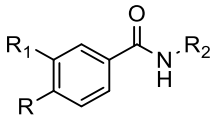

Compound	R	R_1	R_2	IC_{50} (μM)[a]
1	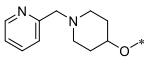	H		1.26
2	H	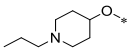		4.22
3	OMe	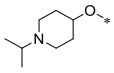		3.36
4	OMe	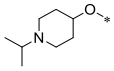		4.47
5	OMe	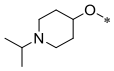		3.16
6	OMe	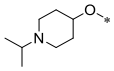		0.60
7	OMe	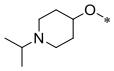		0.76

Table 2. Structures of initial 4-methoxybenzamide scaffold. [a] IC50s were generated from the membrane depolarization assay utilizing HEK 293 cells stably transfected with an endocytic mutant of human CHT. 10-point concentration response curved were performed at 100nM choline concentration

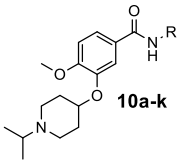

		% Activity remaining[a]		IC50 (μM)[a]	
		Choline concentration			
Compound	**R_1**	**100 nM**	**10 μM**	**100 nM**	**10 μM**
10a		42.2	13.2	3.48 ± 0.40	1.02 ± 0.06
10b		42.6	18.9	4.93 ± 1.40	1.64 ± 0.30
10c		76.4	36.7	-	-
10d		49.9	29.4	8.09 ± 0.80	2.51± 0.22
10e		10.9	-2.8	0.24 ± 0.05	0.10 ± 0.02
10f	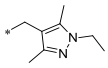	45.8	15.9	1.58 ± 0.29	0.91 ± 0.11
10g	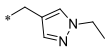	41.8	24.8	9.27 ± 1.83	1.85± 0.17
10h		64.8	47.5	-	-
10i		87.7	71.8	-	-
10j		37.4	9.9	2.13 ± 0.22	1.56 ± 0.14
10k		46.3	20.4	4.12 ± 1.36	1.73 ± 0.28

Table 3. SAR of the amide analogs. [a] IC_{50}s were generated from radiolabeled choline chloride uptake experiments in HEK 293 cells stably transfected with an endocytic mutant of human CHT. 10-point concentration response curves were performed in triplicate with 2-fold dilutions starting from the maximal concentration (20 μM). Inhibition definition: The compounds were defined as inactive if greater than 50% of basal activity remained at 5 μM compound concentration at 100 nM choline chloride solution. Otherwise, the compounds were defined as an inhibitor with the calculated IC_{50} value. IC_{50} values are expressed as IC_{50} ± SD, using estimated standard deviations provided by the fitting software (Origin 6.0).

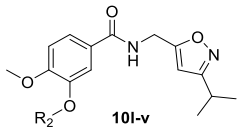

10l-v

Compound	R_2	% Activity remaining[a]		IC50 (μM)[a]	
		Choline concentration			
		100 nM	10 μM	100 nM	10 μM
10l		51.5	18.6	-	-
10m		3.1	-0.9	0.51 ± 0.83	0.09 ± 0.01
10n		51.7	18.4	1.25 ± 0.27	4.54 ± 2.85
10o		83.2	87.6	-	-
10p		82.0	81.3	-	-
10q		38.3	-0.2	0.76 ± 0.70	0.53 ± 0.40
10r		36.7	32.1	6.12 ± 6.47	1.77 ± 0.25
10s		59.7	28.2	-	-
10t		50.1	29.8	-	-
10u		99.8	89.4	-	-
10v	H	86.2	99.4	-	-

Table 4. SAR evaluation of the piperidine replacements. [a] IC_{50}'s were generated from radiolabeled choline chloride uptake experiments in HEK 293 cells stably transfected with an endocytic mutant of human CHT. 10-point concentration response curves were performed in triplicate with 2-fold dilutions starting from the maximal concentration (20μM). Inhibition definition: The compound will be defined as inactive if greater than 50% of basal activity remains at 5 μM compound concentration at 100 nM choline chloride solution. Otherwise, the compound will be defined as an inhibitor with the calculated IC_{50} value. IC_{50} values are expressed as IC_{50} ± SD, using estimated standard deviations provided by the fitting software (Origin 6.0).

Conclusions

The discovery of the electrogenicity of CHT and the mutation of the endocytic sequence in CHT provided fundamental building blocks for the development of an HTS analysis implemented by the Blakely lab, executed by the JHICC (Johns Hopkins Ion Channel Center), and funded by NIH's MLPCN that resulted in the identification of a novel, high potency, CHT antagonist, ML352. Screening over 300,000 compounds, five unique structural classes of inhibitors were identified. The class with the most potent compound was selected for SAR diversification to produce a library of new compounds to be tested for the inhibit potency of CHT. These SAR studies successfully identified a new structure, different from that of HC-3, that more potently inhibited CHT than its parent compound. The most potent compound, ML352, from the SAR studies was selected for further characterization in hopes to produce a compound for future *in vivo* animal studies to elucidate the role of CHT in cholinergic signaling. Portions of the data presented in this chapter were published in Ennis et. al. 2015 (Ennis, Wright, Retzlaff, McManus, Lin, Huang, Wu, Li, et al., 2015), the NIH MLPCN Probe Report, and Bollinger et. al. 2015 (Bollinger et al., 2015). The molecular pharmacology portion of this characterization follows in Chapter 3. Data on the other structural classes of CHT inhibitors can be found in Appendix 1. Also, it should be noted that the HTS identified a subset of activator compounds though their ability to enhance CHT mediated choline transport was never replicated in the Blakely lab. Brief details on the activator compounds are found in Appendix 2.

CHAPTER 3

IN VITRO AND *EX VIVO* CHARACTERIZATION OF ML352

Introduction

Countless common therapeutics are prescribed without completely understanding their mechanism of action. Antihistamines, and serotonin reuptake inhibitors (SSRIs) are prescribed daily to patients. Medical professionals know generally how these drugs work but cannot explain how the off target side effects of antihistamines will effect patients as they age or why SSRIs display delayed efficacy. “How do drugs work?” is an essential question that numerous research projects are founded upon in attempts to better understand and, hopefully, improve upon the therapeutics used to treat the diseases that ail our society. Drug discovery research allows drugs to be developed for specific targets and attempts to know how a drug work prior to its release to a commercial market. The knowledge obtained about the potency, specificity, the nature of the interaction, the drug metabolism, and pharmacokinetics of a molecule can ultimately yield safer and more effective therapeutics. Typical drug discovery projects are initiated by HTS activities, followed by SAR studies, leading to a thorough pharmacological analysis of the basic characteristics of a lead compounds.

Our drug discovery effort, described in the previous chapter, was initiated by a HTS that aimed to expand pharmacology around CHT and provide novel pathways to modulate cholinergic signaling. The HTS resulted in a series of compounds that binned into five structural classes. Diversification of three of these structural classes produced a series of

compounds with varying potency, specificity, and mechanisms of inhibition. Determining the ideal characteristics of a CHT inhibitor was not straight-forward, as other than the research based on HC-3, very little was known about how a CHT inhibitor would affect cholinergic signaling. Given that HC-3 is an extremely toxic competitive inhibitor, we aimed to select non-competitive inhibitors as to avoid the orthosteric binding site and potentially generate a use-dependent inhibitor. Of the compounds with a non-competitive mechanism of action, ML352 was selected from the SAR series of compounds due to its high potency and replicability.

The second phase of our drug discovery program, which involved *in vitro* and *ex vivo* studies of compound potency, specificity, and mechanism of action, is detailed in this chapter. I present evidence that ML352 is a novel, non-choline based, CHT-specific inhibitor that demonstrates nanomolar CHT antagonism, as well as a lack of inhibitory action at multiple transporters, ion channels and receptors. Our kinetic studies with ML352 are the first to demonstrate small molecule induced allosteric modulation of the transporter.

MATERIAL AND METHODS

Reagents and Cells

All biochemical reagents were of research grade and, unless stated otherwise, obtained from Sigma Aldrich (St. Louis, MO, US). Commercially available replicates and derivatives of molecules identified as hits in our HTS screen were obtained from Ambinter (Orleans, France) as dry powders. HEK 293 and HEK 293 cells stably transfected with

either the human CHT (CHT) or a mutant, CHT LV-AA (L531A, V532A), were described previously (Ruggiero et al., 2012) and maintained according to American Type Culture Collection (ATCC, Manassas, VA, USA) guidelines using MEM Earles media containing 1X fetal bovine serum, 2mM glutamine, 100IU penicillin and 100 ug/mL streptomycin (Fisher-Scientific, Pittsburgh, PA, USA). All studies used cells cultured to 70−100% confluency.

Animal Care and Husbandry

All procedures with mice (C57BL/6J mice, Jackson Labs, Bar Harbor, MN, USA) and rats (Sprague Dawley, Harlan, Indianapolis, IN, USA) were performed with animals at 10-20 weeks of age under an approved protocol that is reviewed annually by the Vanderbilt Institutional Animal Care and Use Committee (IACUC). Animals were housed prior to use on a 12:12 light-dark cycle with food and water provided *ad libitum*.

Neurotransmitter Transport Activity Assay (96-Well Format)

Cells were plated onto poly-D-lysine coated, 96 well, white cell culture plates (Culturplate-96, Perkin-Elmer, Waltham, MA, USA) at 45,000 (HEK293 CHT LV-AA), or 20,000 (HEK293 hDAT, hNET, or hSERT) cells/100 µL/well and allowed to grow for 48 hours at 37 °C in an atmosphere of 95% air/5% CO_2. Each plate was washed 3X with 100µL KRH using a Biotek 405 Touch microplate washer (Winooski, Vermont, USA). Wells were filled with 40 µL of KRH buffer with or without drugs using a multichannel pipet. Plates were incubated at 37 °C in an atmosphere of 95% air/5% CO_2 for 15 min for choline uptake assays and 10 min for DA, NE, and 5-HT uptake assays. The first

incubation is followed by an addition of 10 µL of either 100 nM or 10 µM (final concentrations) [^{3}H]-choline chloride (Perkin-Elmer, Waltham, MA, USA, NET109001MC,1 mCi/mL) or 50nM (final concentrations) [^{3}H]DA, (dihydroxyphenylethylamine,3,4-[Ring-2,5,6-^{3}H]; Perkin-Elmer, NET673001MC, 1mCi/mL), ([^{3}H]NE] (norepinephrine hydrochloride, DL-[7-^{3}H(N)]; Perkin-Elmer, NET048001MC, 1mCi/mL) or [^{3}H]5-HT (hydroxytryptamine creatinine sulfate,5-[1,2-^{3}H(N)]; Perkin-Elmer, NET498001MC, 1mCi/mL) in KRH buffer. Final concentrations of substrates solutions were made using 1% radioligand with 99% unlabeled neurotransmitter stock solution. After a 10-15 min incubation with radiolabeled substrates, each plate was washed 3X with 100 µL of KRH buffer using a Biotek (location) 405 Touch microplate washer. A volume of 100 µL of MicroScint™-20 (Perkin-Elmer, Waltham, MA, USA) was added to wells and uptake quantified by scintillation spectrometry using a TopCount instrument (Perkin-Elmer, Waltham, MA, USA). Counts obtained from wells incubated as noted above in the presence of inhibitors of CHT (HC-3, 10µM), DAT (Cocaine, 1uM), NET (mazindol, 1uM), and SERT (citalopram, 1uM) were subtracted from total uptake values to obtain specific uptake values. In saturation choline transport studies, serial dilutions from a 1-5% mix of radiolabeled and unlabeled choline was used to maintain specific activity. Choline transport velocity (V_{MAX}) and half saturation concentrations (K_M), and antagonist K_I values, were determined using non-linear curve fits in Prism 5 (GraphPad Inc, San Diego, CA USA).

Synaptosomal Transport Assays

Male mice (C57BL/6J, Jackson Labs, Bar Harbor, ME, USA) at 8-10 weeks of age were sacrificed by rapid decapitation, brains were removed and brain regions dissected on an ice-cold aluminum plate on ice. Crude synaptosomes (P2) were prepared from isolated forebrain tissue as previously described (Apparsundaram, Martinez, Parikh, Kozak, & Sarter, 2005a), with forebrain defined as all brain tissue anterior to a coronal plane abutting the superior colliculus. Aliquots (100 µL) of crude synaptosomes (P2) were incubated with 100 µL of 100 nM radiolabeled choline, DA or 5-HT (materials noted above) in Kreb's bicarbonate buffer (118 mM NaCl, 4.7 mM KCl, 1.2 mM KH_2PO_4, 25 mM $NaHCO_3$, 1.7 mM $CaCl_2$, 10 mM glucose, 100 mM ascorbic acid) in the presence and absence of 10 µM HC-3, or other inhibitors, also as noted above, for 15 minutes for choline uptake assays and 10 minutes for all other neurotransmitters at 37 °C. Transport assays were terminated by transferring the tubes to an ice bath followed by rapid filtration over a Brandel cell harvester (Brandel Inc., Gaithersburg, MD). Accumulated radioactivity was determined by scintillation spectrometry. Protein concentrations were measured using the Pierce BCA protein assay kit (Thermo Fisher Scientific Inc., Rockford, IL). Specific uptake was defined with parallel incubations with specific transporter inhibitors as noted for transfected cells. Saturation kinetic parameters were determined using Prism 5 as described in cell studies.

Off Target Screen

ML352 was tested in the Lead Profiling Screen (Eurofin, Luxembourg), a binding assay panel of 68 G-protein coupled receptors, ion channels and transporters, at 10 µM.

The Lead Profiling Screen consists of 68 primary molecular targets including several CNS targets recommended by the European Medicines Agency (EMEA) to evaluate drug dependence potential. For full assay details, see www.eurofinspanlabs.com.

ChAT Assays

ChAT activity was evaluated by measuring the formation of [^{14}C] ACh from [^{14}C] acetyl CoA and unlabeled choline chloride. Brain regions were rapidly dissected on ice and homogenized with a Polytron homogenizer (Wheaton Instruments, Millville, NJ, USA) in 50 mM Tris-HCl containing 0.02% Triton X-100 and protease inhibitor cocktail (Sigma). Crude extracts were added to an equal volume of reaction buffer containing 600 mM NaCl, 100 mM NaHPO4 (pH 7.4), 20 mM EDTA, 0.2 mM serine, 0.1 mg/mL BSA, 16 mM choline chloride, 0.4mM acetyl [^{14}C] CoA (40-60 Ci/mmol), Perkin Elmer). Reactions proceeded for 20 minutes at 37^{o}C and were then quenched by the addition of 80 µL of a 17:3 mixture of toluene:acetonitrile with 5 g/L of sodium-tetra-phenylboron. Samples were centrifuged briefly at 13,000 rpm to separate the organic phase containing the [^{14}C]-ACh product. The upper layer was extracted and transferred to scintillation vials containing 7 mL of scintillation fluid. The samples were shaken overnight and counted the next day on a TriCarb liquid scintillation counter. Assays using no tissue were performed in parallel and counts subtracted to yield specific enzyme activity.

AChE Assays

AChE activity was measured using the Amplex Red ACh/AChE Assay Kit (Sigma, A12217). Crude extracts of brain tissue were obtained as detailed in ChAT assays. Equal

volumes of extract and reaction buffer containing 400 µM Amplex Red reagent, 0.2 U/mL choline oxidase, and 100 µM ACh were mixed. Reactions were plated in a 96 well, black walled, clear bottom poly-D lysine coated plates (BioCoat BD Biosciences). Product was detected at 590nM wavelength, elicited with 550 nm wavelength excitation on a Flexstation fluorescence microplate reader (Molecular Devices Corp., Sunnyvale, CA).

Hemicholinium-3 (HC-3) Radioligand Binding Assays

HEK 293 cells stably expressing CHT were plated on 150mm sterile tissue culture dishes and allowed to grow to confluency. Cells were harvested from plates with 50 mM TRIS-HCl buffer (pH 7.5) and homogenized using a Polytron at a speed setting of 4. Homogenates were centrifuged for 15 min at 15,000*xg*. Pellets were resuspended in 10mL of 50mM TRIS-HCl buffer (pH 7.5) and centrifuged again for 15 minute at 15,000*xg* The resulting pellets were resuspended in 2 mL of TRIS base buffer. Protein concentrations were determined using the BCA protein assay (Pierce, Rockford, IL USA). HC-3 diacetate salt, [methyl-^{3}H]- (Perkin Elmer, Waltham, MA, 120 Ci/mmol) binding assays were conducted in 50 mM TRIS-HCl buffer, 200 mM NaCl, pH 7.5 at 37 ^{o}C for 45 min. For saturation assays, serial dilutions from a 1% mix of radiolabeled and unlabeled antagonist were used to maintain specific activity. For ML352 competition binding assays, 100 µg of membranes were incubated for designated times in 10 nM [^{3}H] HC-3 +/- with or without several concentrations of ML352. Nonspecific binding in competition assays was defined in parallel incubations with 20 µM unlabeled HC-3 and subtracted from total counts to define specific HC-3 binding. Nonspecific binding in saturation binding assays was defined using membranes from non-transfected HEK-293 cells. Radioactively-

labeled membranes were harvested on glass fiber filters (Whatman GF/B, Brandel, Gaithersburg, MD) that were pretreated with 0.3% polyethylenimine and 0.2% BSA and rinsed 4X with assay buffer (50 mM Tris–HCl, 200 mM NaCl, pH 7.5). Filters were solubilized in EcoScint H (National Diagnostics, Atlanta, GA), allowed to shake overnight, and bound radiolabel quantified by liquid scintillation counting (TriCarb 2900TR, Perkin Elmer). HC-3 binding capacity (B_{MAX}) and affinity (K_D) and ML352 K_I values were determined using non-linear curve fit to a single site inhibition model using Prism 5.

Evaluation of CHT Surface Expression.

Cell surface biotinylation assays to evaluate impact of selected compounds on CHT surface expression were performed as previously described (Ruggiero et al., 2012) using EZ-Link Sulfo-NHS-SS-Biotin (Pierce, Rockford, IL, USA). Following treatments of CHT transfected HEK 293 cells with or without choline (10 µM), HC-3 (5 µM) or ML352 for 15 minutes, cells were biotinylated on ice for 1 hour, followed by a 30-minute incubation with 1xPBS with calcium, magnesium, and 100mM glycine. Cells were extracted with 500µL of RIPA buffer (10mM TRIS HCl, 100 mM NaCl, 1 mM EDTA, 0.1% SDS, 1% Triton-X 100, 10g/L deoxycholate) and biotinylated proteins were isolated using Ultralink Avidin (Pierce, Rockford, IL, USA), eluted in Laemmli buffer (Black, Ribeiro, Ferguson, & Rylett, 2010; Gates, Ferguson, Blakely, & Apparsundaram, 2004b)), resolved by 10% acrylamide SDS−PAGE, and blotted to PVDF membrane (Millipore, Darmstadt, Germany). PVDF membranes were blocked in PBS-T + 5% non-fat dry milk for one hour and then probed with 10 mL of a polyclonal rabbit anti-CHT antibody (Ferguson et al., 2003b) to CHT (1:500−1:1000) overnight at 4^{o}C. Blots were rinsed 3X

for 5 min in PBST and incubated in HRP-conjugated secondary antibody (goat anti-rabbit, 1:5000 in PBS–TM, Jackson Immunoresearch, West Grove, PA) for 1 hour at room temperature. Blots were rinsed 3X for 5 min in PBST and developed by chemiluminescence (Western Lightning Enhanced Chemiluminescence kit, Perkin Elmer, Waltham, MA). Blots were developed and imaged using a LAS4000 Chemiluminescent and GFP CCD Imager (GE Healthcare, Buckinghamshire, England). ImageQuant software (GE Healthcare, Buckinghamshire, England) was used to determine CHT band densities. In order to compensate for inter-experiment variability, CHT bands were normalized to CHT protein detected in total protein extracts. Results from multiple blot replicates were analyzed by a one-way ANOVA with Dunnett's planned comparisons of drug vs vehicle with $P<.05$ taken as significant (Prism 5.0).

Results and Discussion

Potency of ML352 in Heterologous and Ex Vivo Preparations.

First, we sought to confirm the potency of ML352 for inhibition of CHT LV-AA in transfected HEK293 cells. In these studies (Figure 17), we found ML352 to inhibit [^{3}H]-choline uptake with high affinity (K_I = 92 nM ± 2.8 nM), with data that fit to a single site inhibition model (r=0.935) In Figure 17, we demonstrate that ML352 also inhibits choline uptake in mouse forebrain synaptosomes (K_I = 166 nM ± 12nM).

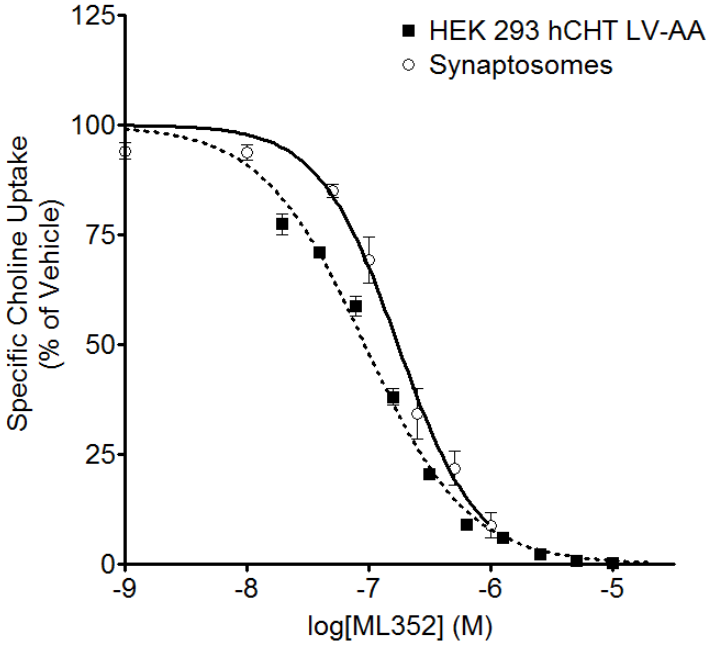

Figure 17. *In vitro* inhibitory potency evaluation of ML352. Inhibition of choline transport by ML352 in transfected HEK 293 LVAA-CHT cells and mouse forebrain synaptosomes. ML352 inhibited choline uptake with a K_I = 92 +/- 2.8 nM (n=3) and in mouse forebrain synaptosomes with a K_I = 172 nM +/- 12 nM (n=3). Figure utilized with permission from ACS Chemical Neuroscience (Ennis et al 2015).

Specificity of ML352 in Heterologous and Ex Vivo Preparations.

We tested the specificity of ML352 by monitoring the function of other neurotransmitter transporters in a HEK 293 heterologous cell system. We observed a lack of inhibitory activity at DAT, NET and SERT in transfected HEK cells (Figure 18). These results indicate it is unlikely that a nonspecific effect on membrane integrity or alterations of ion gradients is the basis for CHT inhibition. Additionally, little or no activity (>50% inhibition at 10 μM) was detected against 68 GPCRs, ion channels and transporters in the EuroFin Lead Profiling Screen (see Methods for list of targets), highlighting a clean ancillary pharmacology profile. In brain preparations, we also assessed the ability of ML352 to inhibit two enzymes involved in ACh homeostasis, the biosynthetic enzyme ChAT and the metabolizing enzyme AChE. Again, at concentrations of ML352 well above the CHT K_I, no inhibition of these enzymes was evident (Figure 19).

Michaelis-Menten Kinetics of ML352 in Heterologous and Ex Vivo Preparations

Next, we explored the kinetic basis of ML352 actions at CHT and interactions of the drug with the binding site labeled by [^{3}H] HC-3 (Figure 20). In studies examining the activity of the inhibitor at varying concentrations of choline in transport assays with CHT LV-AA transfected cells, we observed saturable choline transport with a choline K_M of 2.5 μM +/-0.4, consistent with prior reports (Haga et al., 1973; Yamamura et al., 1972) (Figure 20A). When fixed concentrations of ML352 were included in the assay, we observed no significant effect on the choline K_M, whereas a concentration-dependent reduction in transport V_{MAX} was evident. Analysis of ML352 inhibitory actions on choline uptake in mouse forebrain synaptosomes yielded similar effects (Figure 20B). Together, these

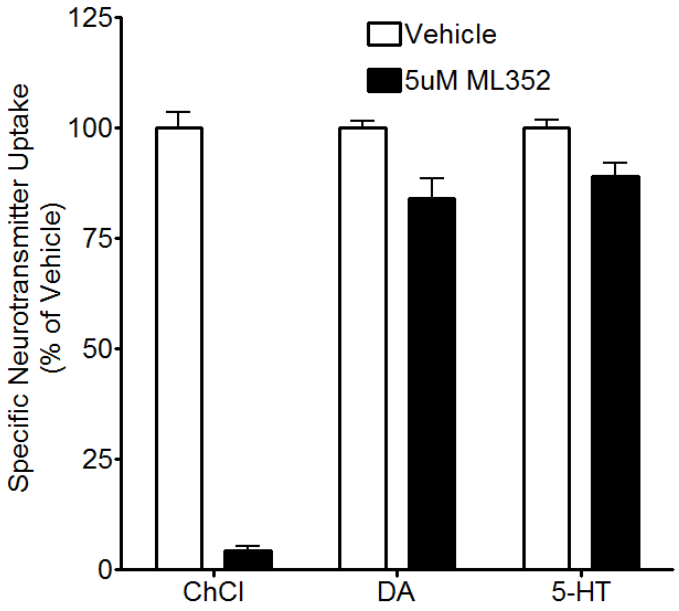

Figure 18. *In vitro* specificity evaluation of ML352. ML352 at 5 µM fails to inhibit DAT, NET, and SERT in mouse forebrain synaptosomes (n=3). Figure utilized with permission from ACS Chemical Neuroscience (Ennis et al 2015).

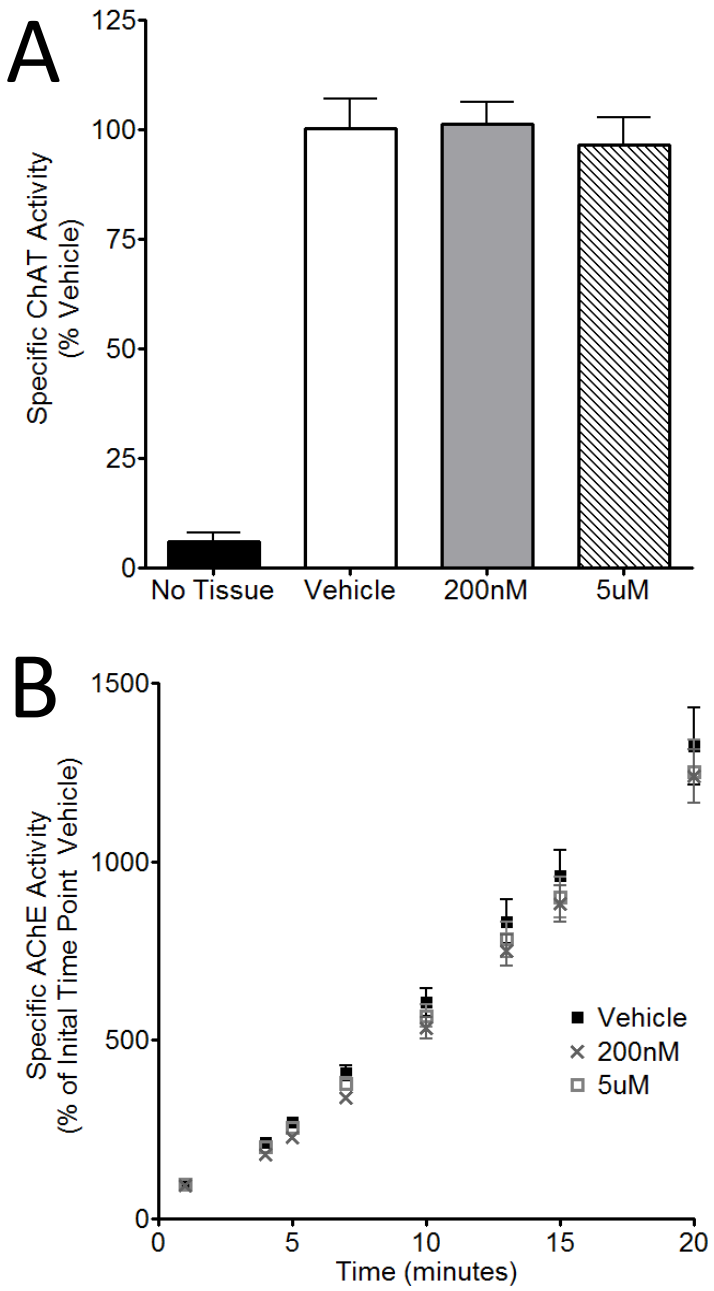

Figure 19. Specificity evaluation of ML352 against cholinergic enzymes. A) ML352 lacks activity for inhibition of ChAT activity in mouse forebrain extracts (n=3). B) ML352 lacks activity for inhibition of AChE in mouse forebrain extracts (n=3). Figure utilized with permission from ACS Chemical Neuroscience (Ennis et al 2015).

Target	%* Inhibition	Target	%* Inhibition
Adenosine A_1	-5	Histamine, H_3	7
Adenosine A_{2A}	0	Imidazoline I_2, Central	16
Adenosine A_3	4	Interleukin IL-1	-2
Adrenergic α_{1A}	23	Leukotriene, Cysteinyl $CysLT_1$	-3
Adrenergic α_{1B}	3	Melatonin MT_1	5
Adrenergic α_{1D}	24	Muscarinic M_1	32
Adrenergic α_{2A}	43	Muscarinic M_2	12
Adrenergic β_1	2	Muscarinic M_3	26
Adrenergic β_2	43	Neuropeptide Y Y_1	-2
Androgen (Testosterone) AR	8	Neuropeptide Y Y_2	7
Bradykinin B_1	6	Nicotinic Acetylcholine	13
Bradykinin B_2	-3	Nicotinic Acetylcholine α1, Bungarotoxin	7
Calcium Channel L-Type, Bensothiazepine	3	Opiate δ_1 (OP1, DOP)	-2
Calcium Channel L-Type, Dihydropyridine	13	Opiate κ (OP2, KOP)	22
Calcium Channel N-Type	-1	Opiate μ (OP3, MOP)	8
Cannabinoid CB_1	4	Phorbol Ester	5
Dopamine D_1	9	Platelet Activating Factor (PAF)	-4
Dopamine D_{28}	18	Potassium Channel [K_{ATP}]	4
Dopamine D_3	15	Potassium Channel Herg	16
Dopamine D_{42}	-3	Prostanoid EP_4	-7
Endothelin ET_A	-3	Purinergic P2X	22
Endothelin ET_B	-2	Purinergic P2Y	19
Epidermal Growth Factor (EGF)	5	Rolipram	1
Estrogen Erα	4	Sertonin (5-Hydroxytrptamine) 5-HT_{1A}	40
$GABA_A$, Flunitrazepam, Central	6	Sertonin (5-Hydroxytrptamine) 5-HT_{2B}	-7
$GABA_A$, Muscimol, Central	9	Sertonin (5-Hydroxytrptamine) 5-HT3	2
$GABA_{B1A}$	-9	Sigma σ_1	-1
Glucocorticoid	-1	Sodium Channel, Site 2	20
Glutamate, Kainate	-2	Tachykinin NK_1	22
Glutamate, NMDA, Agonism	1	Thyroid Hormone	6
Glutamate, NMDA, Glycine	4	Transporter, Dopamine (DAT)	4
Glutamate, NMDA, Phancyclidine	-5	Transporter, GABA	11
Histamine, H_1	37	Transporter, Norepinephrine (NET)	12
Histamine, H_2	20	Transporter, Serotonin (5-hydroxytryptamine) (SERT)	2

Table 5. Off-target interactions of ML352. *Values represent the % inhibition of radioligand binding to designated targets at 10 μM ML352. Figure utilized with permission from ACS Chemical Neuroscience (Ennis et al 2015).

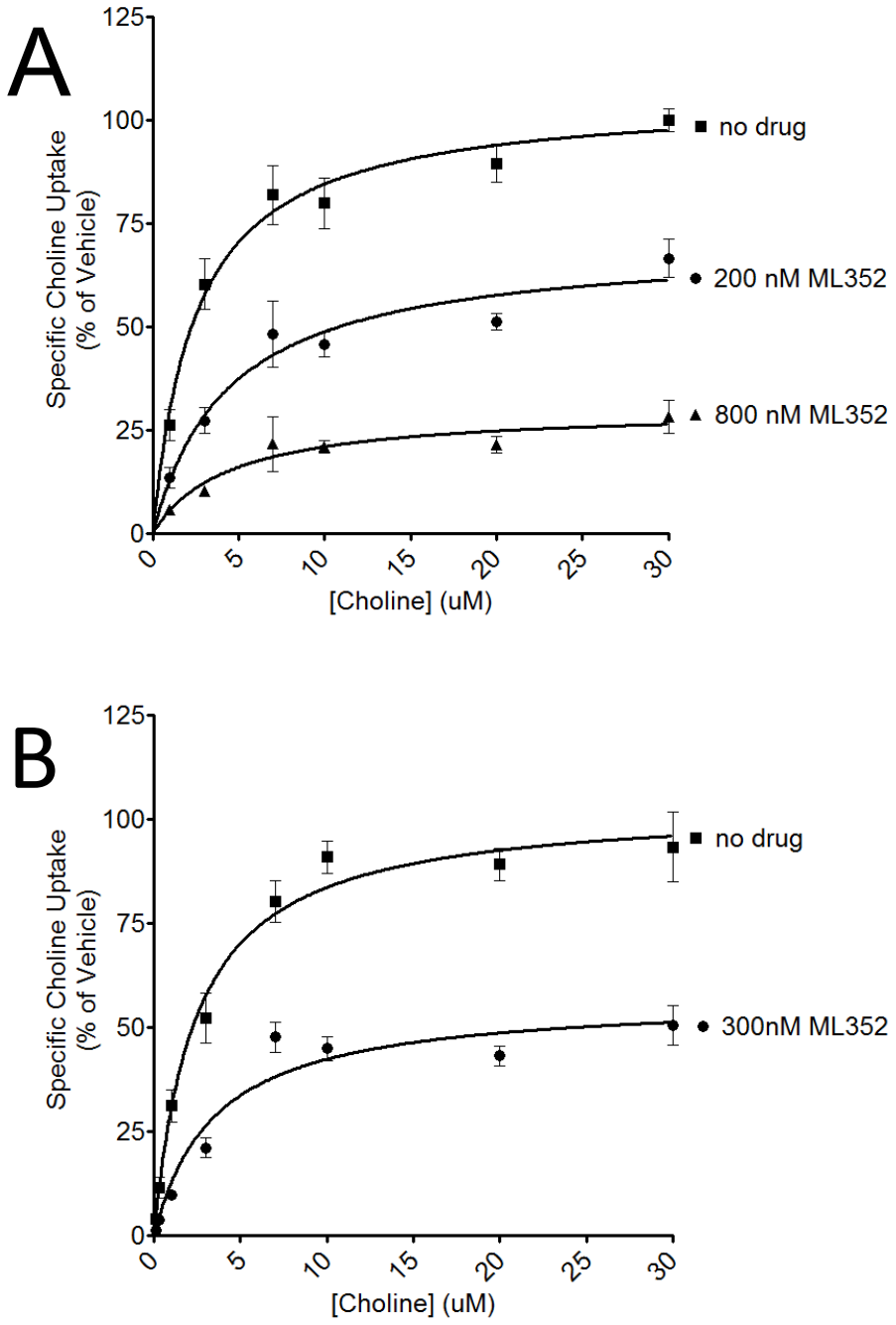

Figure 20. Kinetic mechanism supporting ML352 antagonism of CHT. A) ML352 noncompetitively inhibits choline uptake in HEK 293 LVAA-CHT cells. Inclusion of ML352 at 200 or 800 nM in saturation choline transport assays reveals a progressive decrease in the choline transport V_{MAX} without changing choline K_M (n=3). B) ML352 noncompetitively inhibits choline uptake in mouse forebrain synaptosomes. Inclusion of ML352 at 300 nM in saturation choline transport assays reveals a decrease in the choline transport V_{MAX} without a change in choline K_M (n=3). Figure utilized with permission from ACS Chemical Neuroscience (Ennis et al 2015).

findings point to a non-competitive mode of CHT inhibition, distinct from the competitive mode of inhibition shown by HC-3 (Happe & Murrin, 1992, 1993).

ML352 Inhibition of CHT is Rapid, and Reversible.

The protocol of the tritium-based uptake assay used to determine the potency of ML352 was altered to determine the reversibility of ML352 inhibition (Figure 21)**.** As in the other uptake assays, the cells were incubated for 15 minutes with a concentration of ML352. Unlikely in the previous uptake assays, after the first incubation, the cells were washed with KRH buffer and three different conditions were added, the same concentration curve of ML352, KRH buffer, or HC-3. These three conditions determined ML352 inhibition of CHT, the reversibility of ML353 inhibition, and a non-specific uptake. The time periods that the plates incubated in these three conditions were varied to determine the speed at which ML352 came to equilibrium and reached its maximum inhibition of CHT. Previous experiments that varied the periods of compounds incubation demonstrated that ML352's interaction with CHT reached equilibrium within minutes and elongating the period of ML352 exposure did not increase the potency (data not shown). By introducing a washout step in between, the compound incubation and [^{3}H] choline uptake, we were able to observe that the inhibition ML352 was reversible within minutes. The reversible inhibition of CHT by ML352 could be a critical characteristic in *in vivo* experiments, and as a therapeutic, as permanently inhibiting the transporter would mirror the lethal results seen in the CHT KO mice. The temporary inhibition of CHT may transiently reduce cholinergic signaling which would provide moderate reduction that may

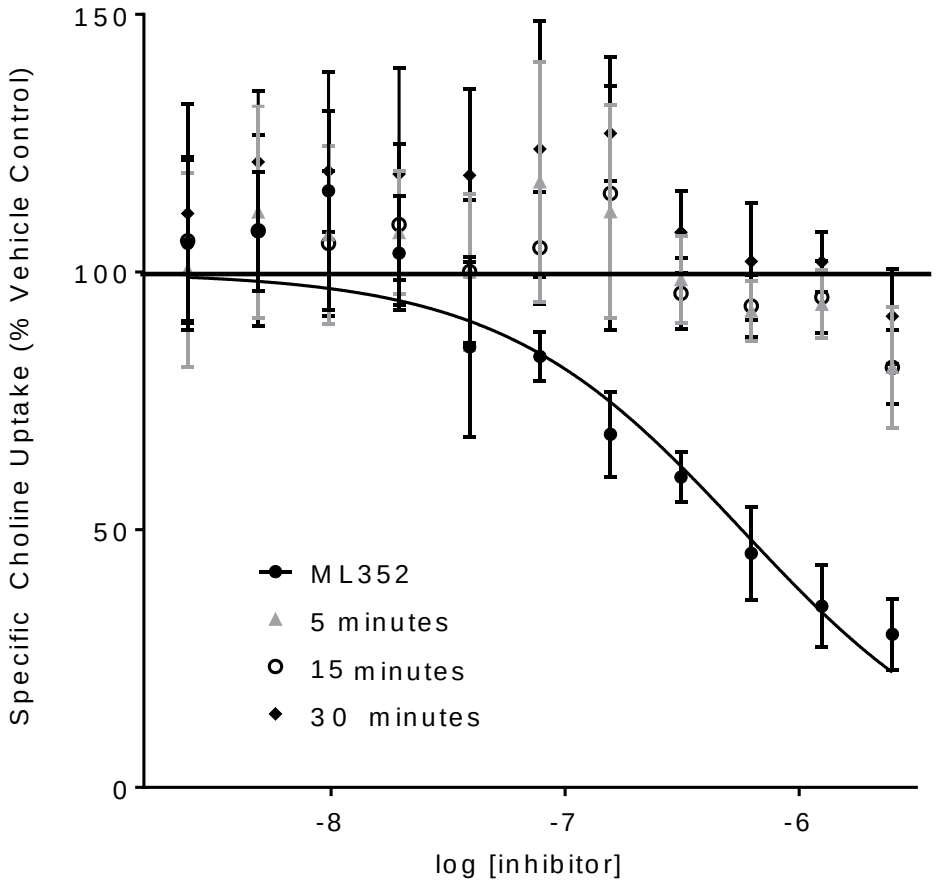

Figure 21. ML352 inhibition of CHT is reversible. ML352 inhibition shown by the ML352 condition in these assays was shown to be comparable to previous experiments. Upon removal of ML352 from the assay solution, the bound ML352 disassociates during the 5, 15, and 30-minute time periods that allow for full HACU by CHT to be restored to untreated levels.

not effect total cholinergic signaling but could greatly effect sites of hypercholinergic signaling.

Binding interactions of ML352 and HC-3 in heterologous and ex vivo preparations.

To assess whether the binding site occupied by ML352 is independent of that occupied by HC-3, we pursued inhibition binding studies using membranes from CHT LV-AA cells. First, we observed that ML352 demonstrated dose-dependent inhibition of HC-3 binding, well fit by a single-site inhibition model ($r = 0.948$) with a K_i of 128.6 +/- 15.3 nM (Figure 22A) similar to that found in uptake inhibition studies. Next, we performed saturation binding studies using [^{3}H]HC-3, observing good, single-site fit to binding data with a K_D of 102.2 +/- 0.04 nM (Figure 22B), similar to previous observations (Happe et al., 1993). In contrast to uptake inhibition findings, HC-3 inhibition by ML352 appeared competitive, with fixed concentrations of the inhibitor inducing an increase in the HC-3 K_D but no change in binding B_{MAX} (Figure 22B).

Evaluation of CHT Surface Expression following ML352 Treatment using In Vitro Preparations

Recently**,** HC-3 was reported to induce elevated surface expression of CHT (Okuda et al., 2011). To determine whether this property is shared by ML352, we performed cell-surface biotinylation studies, testing ML352 after 15 min incubations, in parallel with vehicle, HC-3 or choline treated cells. We used HEK 293 cells stably transfected with wild type CHT for these studies as the CHT LV-AA mutant carries a compromised trafficking sequence that could obscure drug-induced changes in cell-

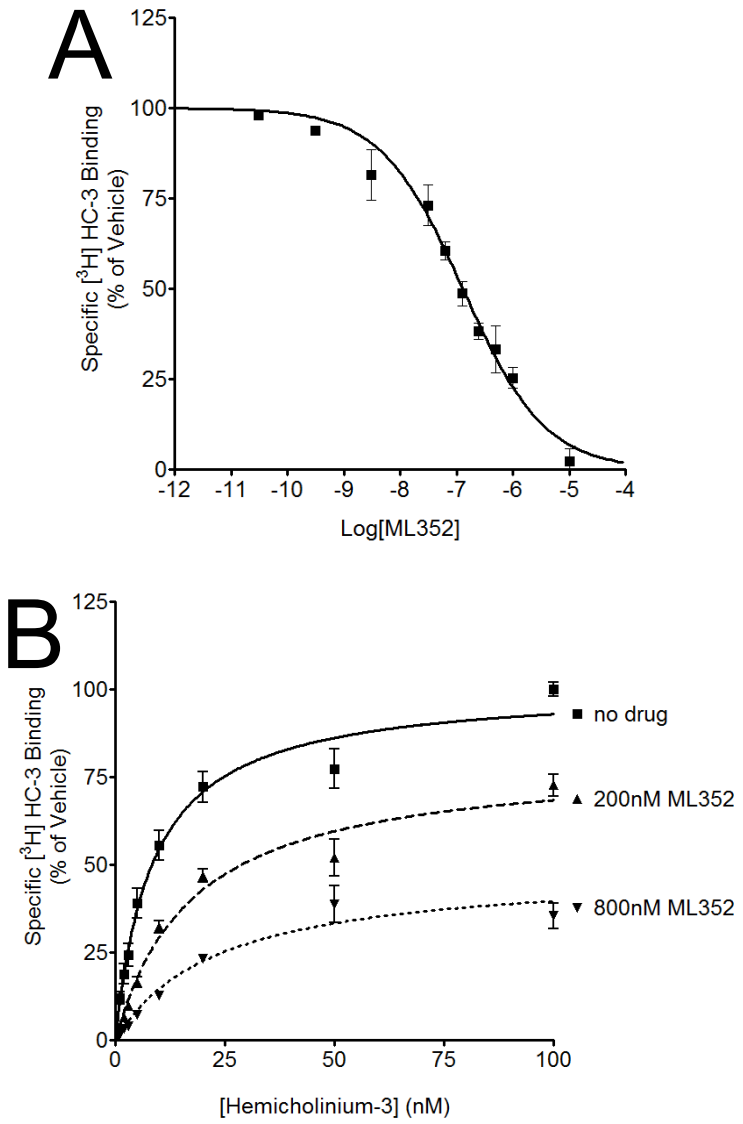

Figure 22. Interaction between [^{3}H] HC-3 binding and ML352. A) Inhibition of [^{3}H]-HC-3 binding to transfected cell membranes by ML352. Binding assays revealed a ML352 K_I of 128.6 +/- 15.3 nM (n=3). B) ML352 exhibits non-competitive inhibition of [^{3}H]-HC-3 binding to transfected cell membranes. Increasing concentrations of [^{3}H]-HC-3 +/- 200 nM ML352 yielded a significant reduction in binding B_{MAX} with no change in [^{3}H]-HC-3 K_D. At 800 nM ML352, a further reduction in B_{MAX} was detected along with an increase in [^{3}H]-HC-3 K_D (n=4). Figure utilized with permission from ACS Chemical Neuroscience (Ennis et al 2015).

surface expression. As shown in Figure 23, we replicated the findings that HC-3 elevates steady-state CHT surface expression (76 +/- 16% of control), although we obtained no evidence for the previously reported choline-dependent reductions (Okuda et al., 2011). ML352 at saturating concentrations (5 μM) also induced a significant increase in CHT surface expression (43.4+/- 4.7% of control). No impact of drugs was seen on total CHT protein expression (data not shown).

Discussion

In our functional studies, ML352 demonstrated activity as a high-affinity, non-competitive antagonist of choline transport. These observations are consistent with the potent antagonism of CHT-dependent membrane potential of ML352 precursors when tested at the EC_{80} choline concentration. This is a potentially useful property in that extracellular choline has been reported to be at near saturating levels in brain extracellular fluid, and much higher concentrations of competitive antagonists might be needed to effect CHT antagonism *in vivo*, leading to off-target actions. Interestingly, ML352 did display non-competitive actions with respect to HC-3 binding, suggesting that the two antagonists bind to mutually exclusive, but interacting sites. Studies that make use of both agents to assess conformations stabilized in either direction may be useful in understanding the structural dynamics supporting choline transport, and thus will be interesting to pursue in the future. In this regard, Okuda and colleagues (Okuda et al., 2011) reported that acute HC-3 application to cells or nerve terminal preparations, leads to elevated CHT surface levels. ML352 also induces an elevation in CHT surface levels. Further studies are needed to determine the basis for this inhibitor-induced increase in CHT surface expression, for

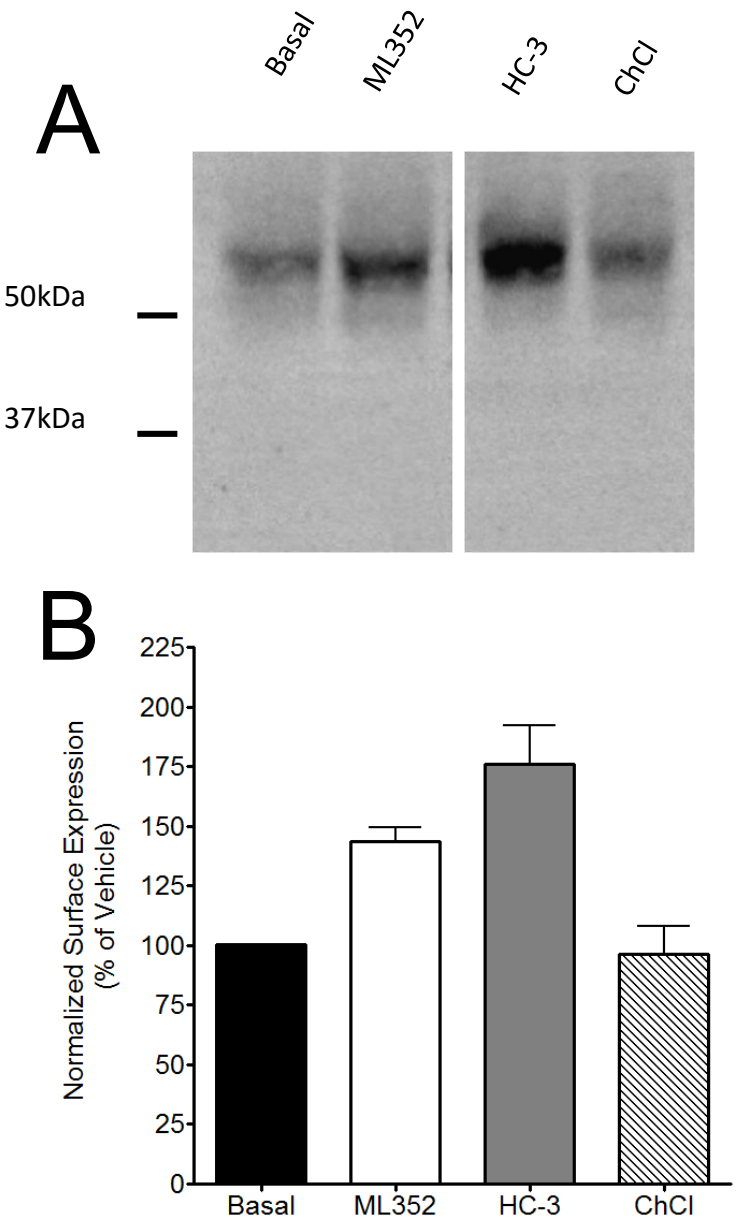

Figure 23. ML352 causes an increase in CHT surface expression in CHT transfected cells. A) Saturating concentrations, 5 µM, of ML352 or HC-3 were incubated for 15 min with wild type CHT transfected HEK 293 cells, followed by cell surface biotinylation and analysis of surface proteins as described in Methods. A representative western blot of surface protein levels is shown. B) Quantitation of CHT surface expression studies. Both HC-3 and ML352 significantly elevated CHT surface protein levels. (* = P<.05 Dunnett's post-hoc comparison vs vehicle treated samples (n=4) following a significant one-way ANOVA treatment effect (P<.001). Figure utilized with permission from ACS Chemical Neuroscience (Ennis et al 2015).

example whether ML352 and HC-3 induced similar protein conformations or/and whether they derive from enhanced rates of surface delivery or recycling, vs diminished endocytosis. Here, methods that label specific extracellular amino acids cells may be particularly helpful in monitoring the conformational effects of ligand binding.

The lack of choline (and HC-3)-mimicking quaternary nitrogens in the progenitor of ML352 suggested the possibility of limited interactions with other cholinergic targets. Indeed, ML352 demonstrated a lack of antagonism of the ACh biosynthetic enzyme ChAT and the metabolic enzyme AChE. Furthermore, our screen of other targets, which includes multiple muscarinic receptors, revealed little or no interactions with these proteins. Portions of this chapter that included the characterization and pharmacological evaluation of ML352 was detailed in a 2015 edition of the American Chemistry Society's journal, Chemical Neuroscience, written my Ennis and colleagues (Ennis, Wright, Retzlaff, McManus, Lin, Huang, Wu, Li, et al., 2015). Evaluation of ML352 for interactions with other targets is of course incomplete, and more extensive evaluations, both *in vitro* and *in vivo*, should now be pursued, as should studies using these agents to manipulate cholinergic physiology and behavior.

CHAPTER 4

THE *IN VIVO* CHARACTERIZATION OF ML352 IN MOUSE MODELS

Introduction

HACU has been shown to be a critical element to cholinergic signaling across phylogeny (Sullivan et al., 2014). The process that led to the discovery of CHT, the protein responsible for the HACU necessary for ACh synthesis, took more than 40 years, limited in part by reliance on a sole pharmacological reagent, HC-3. The use of pharmacological agents, not only in cholinergic system but also many others, has proven key to tease apart the function of specific proteins within a larger system. Though HC-3 was initially extremely useful, the core structure of HC-3 lends it to cross-reactivity with other cholinergic proteins, including those that support both LACU and HACU, and a limited ability to cross the blood brain barrier all of which diminish HC-3's utility in *in vivo* experiments and therapeutic utility. To expand upon the pharmacology that targets CHT, we conducted a HTS, identified hit compounds that underwent SAR studies, and characterized one lead CHT inhibitor.

In vitro and *ex vivo* characterization of ML352 revealed potent, non-competitive inhibition of CHT in a heterologous, and synaptosomal preparations while having little effect on other neurotransmitter transporters, and a variety of other common protein receptors and transporters. With a structure and mechanism of inhibition distinct from that of HC-3, we hoped that ML352 would present with additional characteristics that would

make it a better tool for *in vivo* investigation to the role of CHT in cholinergic signaling. The *in vivo* investigations utilized rats, and three mouse lines, wild type, CHT BAC, and CHT HET mice. The use of different species aided in creating a detailed picture of the pharmacokinetic profile while utilizing multiple mouse lines tested our CHT inhibitor in models of hypercholinergic and hypocholinergic states, CHT BAC and CHT HET mice, respectively. This chapter is a continuation of the characterization of ML352 found in Chapter 3, though the characterization here is focused on an initial evaluation of the pharmacological parameters or the physiological effects of ML352 in rodents.

Materials and Methods

Animal Care and Husbandry

All procedures with mice (C57BL/6J mice, Jackson Labs, Bar Harbor, MN, USA) and rats (Sprague Dawley, Harlan, Indianapolis, IN, USA) were performed with animals at 10-20 weeks of age under an approved protocol that is reviewed annually by the Vanderbilt Institutional Animal Care and Use Committee (IACUC). Animals were housed prior to use on a 12:12 light-dark cycle with food and water provided *ad libitum*.

Metabolism and Disposition Methods

The metabolism of CHT inhibitors was investigated *in vitro* in rat hepatic microsomes (BD Biosciences, Billerica, MA) using substrate depletion methodology (% test article remaining). A potassium phosphate-buffered reaction mixture (0.1 M, pH 7.4) of test article (1 µM) and microsomes (0.5 mg/mL) was pre-incubated (5 minutes) at

37°C prior to the addition of NADPH (1 mM). The incubations, performed in 96-well plates, were continued at 37º C under ambient oxygenation and aliquots (80 µL) were removed at selected time intervals (0, 3, 7, 15, 25 and 45 minutes). Protein was precipitated by the addition of chilled acetonitrile (160 µL), containing carbamazepine as an internal standard (50 ng/mL), and centrifuged at 3000 rpm (4 °C) for 10 min. Resulting supernatants were transferred to new 96-well plates in preparation for Liquid Chromatography (LC)/Mass Spectrometry (MS)/Mass Spectrometry (MS) analysis. The *in vitro* half-life ($t_{1/2}$, min, Eq. 1), intrinsic clearance (CL_{int}, mL/min/kg, Eq. 2) and subsequent predicted hepatic clearance (CL_{hep}, mL/min/kg, Eq. 3) were determined employing the following equations:

(1) $t_{1/2}$ = Ln(2) / k ; where k represents the slope from linear regression analysis (% test article remaining)

(2) CL_{int} = (0.693 / $t_{1/2}$) (reaction volume / mg of microsomes) (45 mg microsomes / gram of liver) (20[a] gm of liver / kg body weight); [a]scale-up factors of 20 (human) and 45 (rat)

(3) $$CLhep = \frac{Q \cdot CL_{\text{int}}}{Q + CL_{\text{int}}}$$

Plasma Protein Binding

Protein binding of CHT inhibitors were determined in rat plasma via equilibrium dialysis employing Single-Use RED Plates with inserts (ThermoFisher Scientific, Rochester, NY). Briefly, commercially available rat plasma (220 µL) was added to the 96 well plate containing test article (5 µL) and mixed thoroughly. Subsequently, 200 µL of the plasma-test article mixture was transferred to the *cis* chamber (red) of the RED plate, with an accompanying 350 µL of phosphate buffer (25 mM, pH 7.4) in the *trans* chamber. The RED plate was sealed and incubated for 4 hours at 37 °C with shaking. At completion,

50 µL aliquots from each chamber were diluted 1:1 (50 µL) with either plasma (*cis*) or buffer (*trans*) and transferred to a new 96 well plate, at which time ice-cold acetonitrile (2 volumes), containing carbamazepine as internal standard (50 ng/mL), was added to extract the matrices. The plate was centrifuged (3000 rpm, 10 minutes) and supernatants transferred to a new 96 well plate. The sealed plate was stored at -20 °C until LC/MS/MS analysis.

Pharmacokinetics and Brain Tissue Distribution Studies in Sprague-Dawley Rats

CHT inhibitors were formulated in 10% EtOH:50% PEG400 and 40% saline, as well as 0.5% methylcellulose/0.1% Tween 80, in preparation from intravenous (IV) and oral (PO) dosing, respectively. The IV dose was administered via the jugular vein to 4 dual-cannulated (carotid artery and jugular vein) adult male Sprague-Dawley rats, each weighing between 250 and 350 g (Harlan, Indianapolis, IN) for a final dose of 1 mg/kg ML352; the PO dose was administered via oral gavage to 4 dual-cannulated (carotid artery and jugular vein) adult male Sprague-Dawley rats, each weighing between 250 and 350 g for a final dose of 2.3 mg/kg dose of ML352. Whole blood collections from the IV study via the carotid artery were performed at 0.033, 0.117, 0.25, 0.5, 1, 2, 4, 7, and 24 hours post dose; the PO sampling times were 0.25, 0.5, 1, 2, 3, 4, 6, 8, and 24 hours post dose. Following the 24 hour sample collection, rats were redosed with ML352 (1 mg/kg) followed by isoflurane treatment (0.75 min) 15 minutes post second-dose in order to obtain blood and CNS tissue for the $K_{p,Brain}$ determinations. The samples for pharmacokinetic analysis were collected into chilled, EDTA-fortified tubes and centrifuged for 10 minutes (3000 rcf, 4 °C), with the resulting separated plasma stored at -80 ºC until

LC/MS/MS bioanalysis. The samples for brain tissue distribution analysis were collected at the time of euthanization, with the whole brain being removed and thoroughly rinsed with cold phosphate-buffered saline prior to freezing on dry ice. Whole brains were weighed and diluted (3 mL) with 70:30 isopropanol:water (v/v). The mixture was subjected to mechanical homogenation employing a Mini-Beadbeater™ and 1.0 mm Zirconia/Silica Beads (BioSpec Products Inc., Bartlesville, OK) followed by centrifugation (3500 rcf, 20 °C, 5 min). The liquid extraction of plasma (40 µL) and brain homogenate supernatant diluted (4X) in plasma (40 µL) was performed by conventional protein precipitation using three volumes of ice-cold acetonitrile containing an internal standard (50 nM carbamazepine). The samples were centrifuged (3500 rcf, 20 °C, 5 min) and the supernatants diluted (1:1; v/v) via transfer into a fresh 96-well plate containing deionized water for LC/MS/MS bioanalysis (*vide infra*).

LC/MS Analysis for DMPK

Compounds were analyzed via electrospray ionization (ESI) on an AB Sciex API-5500 (Foster City, CA) triple-quadruple linear ion trap instrument that was coupled with Shimadzu LC-20AD pumps (Columbia, MD) and a Leap Technologies CTC PAL auto-sampler (Carrboro, NC). Analytes were separated by gradient elution using a Fortis C18 2.1 x 50 mm, 3.5 µm column (Fortis Technologies Ltd, Cheshire, UK) thermostated at 40°C. HPLC mobile phase A was 0.1% NH_4OH (pH unadjusted), mobile phase B was acetonitrile. The gradient started at 30% B after a 0.2 min hold and was linearly increased to 90% B over 0.8 min; held at 90% B for 0.5 min and returned to 30% B in 0.1 min followed by a re-equilibration (0.9 min). The total run time was 2.5 min and the HPLC flow

rate was 0.5 mL/min. The source temperature was set at 500°C and mass spectral analyses were performed using multiple reaction monitoring (MRM) utilizing a Turbo-Ionspray® source in positive ionization mode (5.0 kV spray voltage). LC/MS/MS analysis was performed employing a TSQ Quantum^{ULTRA} that was coupled to a ThermoSurveyor LC system (Thermoelectron Corp., San Jose, CA) and a Leap Technologies CTC PAL auto-sampler (Carrboro, NC). Chromatographic separation of analytes was achieved with an Acquity BEH C18 2.1 x 50 mm, 1.7 µm column (Waters, Taunton, MA).

ML352 solution Formulation for Mouse Experiments with i.p. Injections

ML352 was synthesized by the Lindsley lab in Cool Springs, TN and given to the Blakely lab in a glass tube in its free base form. ML352 was stored in a closed glass tube in a desiccator at room temperature. Before each experiment, flakes of the ML352 crystal were removed from the stock container and placed in a new glass tube. The amount of ML352 transferred to the new glass tube was weighed and enough dimethyl sulfoxide (DMSO) was added to the tube to yield a final ML352 concentration of 100 mM. A 100 mM ML352 solution was used to prepare injection solution for mouse experiments by creating a 4 mg/kg solution in saline and then serial diluting the 4 mg/kg solution to produce the other doses desired. Efforts were made to keep the concentration of DMSO in each dose the same across experiments though this was not feasible for the high concentrations required for the LD50 experiments in the CHT BAC mice.

Determination of the Dose of ML352 that Kills 50 Percent of Mice (LD50)

Groups of wild type, CHT BAC, or CHT HET mice at 7 or more weeks of age were injected i.p. with ML352 formulated as previously indicated. Mice were injected one group of mice at a time and the doses were increased sequentially until a dose was found that proved lethal to fifty percent of the mice. Predicted toxicity based on HC-3 involved seizures or cessation of breathing within 15 minutes of injection. Mice were observed constantly until toxicity was presented as seizure for 1 minute or cessation of breathing for 1 minute, both situations that resulted in euthanasia by rapid decapitation.

LC/MS/MS Bioanalysis of Samples from In Vivo Assays for Brain Time Course of ML352

In vivo samples were analyzed via electrospray ionization (ESI) on an AB Sciex API-4000 (Foster City, CA) triple-quadrupole instrument that was coupled with Shimadzu LC-10AD pumps (Columbia, MD) and a Leap Technologies CTC PAL auto-sampler (Carrboro, NC). Analytes were separated by gradient elution using a Fortis C18 3.0 x 50 mm, 3 µm column (Fortis Technologies Ltd, Cheshire, UK) thermostated at 40 ºC. HPLC mobile phase A was 0.1% formic acid in water (pH unadjusted), mobile phase B was 0.1% formic acid in acetonitrile (pH unadjusted). The source temperature was set at 500 ºC and mass spectral analyses were performed using multiple reaction monitoring (MRM), with transitions specific for each compound utilizing a Turbo-Ionspray® source in positive ionization mode (5.0 kV spray voltage). The calibration curves were constructed, and linear response was obtained by spiking known amounts of test compound in blank brain homogenate or plasma. All data were analyzed using AB Sciex Analyst software v1.5.1.

The final PK parameters were calculated by non-compartmental analysis using Phoenix (version 6.2) (Pharsight Inc., Mountain View, CA).

ACh, DA, and choline levels in synaptosomes after acute ML353 i.p. administration

Groups of wild type mice at 8 or more weeks of age were injected i.p. with ML352 formulated as previously indicated. Mice were injected one group of mice at a time and allowed to move freely in a white transport bucket for either 30 minutes, or 1 hour after which time they were sacrificed by rapid decapitation, and their brains harvested. Striatum, hippocampus and cortex were dissected on an ice-cold aluminum plate from the brains and placed into separate tubes containing 1mL sucrose solution and kept on ice. The brain regions were then homogenized with a Wheaton Instrument Overhead Stirrer on setting 4.5 for 8-10 strokes. These homogenates were used to produce crude synaptosomes (P2) prepared as previously described (Apparsundaram et al., 2005a). The supernatant was removed from the top of the P2 pellet and snap frozen on dry ice and subjected to LC/MS/MS to Dr. Ginger Milne in the Vanderbilt Neurochemistry Core.

Locomotor activity assay following ML352 administration

Basal locomotor activity was evaluated in an open field by using activity monitors in clear Plexiglas chambers measuring 27.9 x 27.9 cm (MED Associates). Each chamber contains 16 photocells in each horizontal direction, as well as 16 photocells elevated 4.0 cm to measure rearing that automatically record activity. A five-day experimental protocol was developed to observe changes in basal activity after the preliminary exploratory locomotor activity ceased. On day one, the mice acclimated to the chamber without injection and allowed to move freely for 3 hours while the MED Associates software

recorded their behavior. Analysis of the data with MED Associates software and Graphpad Prism 6 determined the time at which the exploratory phase of the mice behavior ended. The time at which the exploratory phase ended was used on subsequent days for the time of compound injection. On day 2, the mice were placed into the chambers and allowed to move freely for 90 minutes. At the 90-minute time point, each mouse was injected with saline and placed back into the chamber to move freely for an additional 2.5 hours while the MED Associates software recorded their behavior. On subsequent days, each of the mice was subjected to the same protocol but received one of four doses in a random order, 2, 1.5, 1, or 0.5 mg/kg, of ML352. By the end of the experiment, each mouse had received an equal amount of ML352.

Results and Discussion

Pharmacokinetics of ML352 in Rat, Mouse, and Humans Models

First, we profiled ML352 and a group of analogs in a variety of drug metabolism and pharmacokinetic (DMPK) assays in mice in order to provide essential information for future behavioral experiments with ML352 and its analogs. ML352 and its analogs were tested in a battery of pharmacokinetic assays (Table 6) including an assessment of intrinsic clearance (CL_{INT}) in liver microsomes and plasma protein binding in the mouse. We chose to continue to characterize several of the ML352 analogs in case the PK profile of ML352 had been unfavorable pharmacokinetic profile. The ML352 analogs would have

	10m, ML352	10q	10b	10k	10e	10f
MW	387.2	401.5	403.2	411.3	415.2	428.3
CLogP	2.49	2.85	4.11	3.56	3.41	3.82
TPSA	77.1	77.1	63.7	63.7	77.1	68.6
In vitro PK parameter, mouse [a]						
CL_{INT} (mL/min/kg)	43.7	167	979	106	781	29.9
CL_{HEP} (mL/min/kg)	29.4	58.4	82.4	48.8	80.7	22.4
PPB (f_u)	0.48	0.71	0.39	0.35	0.57	0.57
Cytochrome P450 inhibition (IC_{50}, µM)						
1A2	>30	>30	10.3	>30	>30	>30
2C9	>30	>30	>30	>30	>30	>30
2D6	>30	>30	>30	27.1	>30	6.7
3A4	>30	>30	>30	28.2	>30	>30
Tissue Distribution (1.0 mg/kg per compound intraperitoneal cassette dose to mice, 10%EtOH:85%PEG400:5%DMSO, n = 3)						
Plasma (ng/mL)	15.5	25.9	8.8	4.3	10.5	12.8
Brain (ng/g)	3.3	1.8	1.5	4.0	BLQ	BLQ
Mean B:P	0.28	0.07	0.19	1.1	<0.06	<0.05
BLQ=Below level of quantitation						

Table 6. *In vitro* and *in vivo* pharmacokinetic properties of ML352 and analogs in mice. Parameters are inherent to the structure of the compounds. MW: molecular weight. cLogP: partition coefficient. TSPA: total polar surface area. [a] *In vitro* data was acquired through the treatment of mouse microsomes with 1µM compound. Figure utilized with permission from Bioorganic & Medicinal Chemistry Letters (Bollinger et al 2015).

in vitro PK parameters	Human	Rat
CL_{INT} (mL/min/kg)	10.4	95.0
CL_{HEP} (mL/min/kg)	6.9	40.3
PPB (% fu)	67	35
PBS Solubility	98.2± 1.1 µM	
P450 1A2	>30 µM	
P450 2C9	>30 µM	
P450 2D6	>30 µM	
P450 3A4	>30 µM	
in vitro PK parameters (Sprague-Dawley Rats)		
IV (1mg/kg)		
CL(mL/min/kg)		107
$T_{1/2}$ (min)		33
V_{ss} (L/kg)		3.2
AUC (hr·ng/mL)		150
PO (2.3 mg/kg)		
C_{max} (ng/mL)		32.6
T_{max} (hr)		0.25
AUC (hr·ng/mL)		77.5
F (%)		22
tissue distribution (IV, 1 mg/kg, 0.25 hr)		
Plasma (ng/mL)		129
Brain (ng/g)		23.4
CSF (ng/g)		11.8
$K_{p,brain}$		0.2

Table 7. *In vitro* human and rat, and *in vivo rat* pharmacokinetic properties of ML352. Figure utilized with permission from ACS Chemical Neuroscience (Ennis et al 2015).

provided a foundation to select a new lead CHT inhibitor or to continue SAR studies to improve upon the PK profile of ML352. ML352 was shown to have low-to-moderate intrinsic clearance in the mouse (CL_{INT} = 43.7 mL/min/kg using 87.5 g liver/kg of body weight) with subsequent low predicted hepatic clearance (CL_{HEP} = 29.4 mL/min/kg using 90 mL/min/kg for mouse liver blood flow). Interestingly, the closely related analog, **10e** (isopropyl analog) (Table 3) was highly cleared in liver microsomes, CL_{INT} = 781 mL/min/kg. Compound **10f** (pyrazole analog) (Table 3) also displayed low intrinsic clearance (CL_{INT} = 29.9 mL/min/kg) and predicted hepatic clearance (CL_{HEP} = 22.4 mL/min/kg). ML352 possesses excellent free fraction in mouse (0.48) as did all of the analogs tested (>30%, f_u) in mouse equilibrium dialysis plasma protein binding studies. In addition, all of the analogs tested displayed low potential for human cytochrome P450 inhibition as demonstrated by IC_{50} values for 1A2, 2C9, 2D6, 3A4 being >10 µM, except for compound **10f** against 2D6 (6.7 µM). Moreover, ML352 was highly soluble in PBS (98.2 µM) and displayed no inhibition of the four major P450s (>30 µM) (Ennis, Wright, Retzlaff, McManus, Lin, Huang, Wu, Li, et al., 2015). Lastly, ML352 and analogs were evaluated in a cassette tissue distribution study in mice. ML352 was shown to have low B:P in this study (0.28), similar to results in the rat (Ennis, Wright, Retzlaff, McManus, Lin, Huang, Wu, Daniels, et al., 2015). Of all the analogs tested in mice, ML352 and **10k** (Table 3) had the highest B:P and total brain concentrations.

Then, we evaluated ML352 in an additional battery of pharmacokinetic assays (Table 7) to predict rat and human PK parameters, including an assessment of CL_{int} in hepatic microsomes, allowing for the prediction of clearance, CL, and half-life, $t_{1/2}$. From these data, ML352 is predicted to have moderate clearance in rat (CL_{int} = 326 95.0

mL/min/kg, CL_{hep} = 40.3 mL/min/kg) and low clearance in human (CL_{int} = 10.4 mL/min/kg, CL_{hep} = 6.9 mL/min/kg), possessing an elevated f_u (0.67 in human, 329 0.35 in rat), as assessed via equilibrium dialysis in plasma. We also found that ML352 displayed no inhibition of four principal xenobiotic-metabolizing cytochrome P450s (3A4 (>30 μM), 332 2D6 (>30 μM), 2C9 (>30 μM), and 1A2 (>30 μM)). In addition to its *in vitro* profiling, the *in vivo* pharmacokinetic properties of ML352 were evaluated in male Sprague-Dawley rats. The compound displayed plasma clearance in rats that exceeded hepatic output (CL, 107 mL/min/kg), an observation that correlated to the *in vitro* CL_{int} values obtained in rat hepatic microsomes (95 mL/min/ 339 kg); the elevated plasma clearance and high volume of distribution predicted at steady state (V_{ss}) are consistent with a 30-minute half-life. In a tissue distribution study, ML352 displayed modest brain penetration (brain K_p = 0.2). The predicted concentration achieved suggests a potential for use in localizing and probing CNS components of CHT function *in vivo*. Studies are underway to further diversify the structure, with a goal of reducing clearance rates and improving CNS penetration while maintaining the CHT inhibitory potency, and limited off-target effects.

Lethal Dose of ML352 Scales with the Levels of CHT Protein

We evaluated the lethality of ML352 in three lines of mice, C57B6/J, CHT HET, and CHT BAC. The lethality of ML352 was determined by dosing mice with increasing amounts of ML352 until fifty percent of the mice demonstrated signs of distress that would lead to death (LD_{50}). The LD_{50} of ML352 was found to be approximately 3.5 mg/kg in wild type mice, and 1.5 mg/kg in CHT HET mice. The CHT BAC mice began to demonstrate lethality at 5 mg/kg but we did not continue to increase the dosage to find the LD50 of

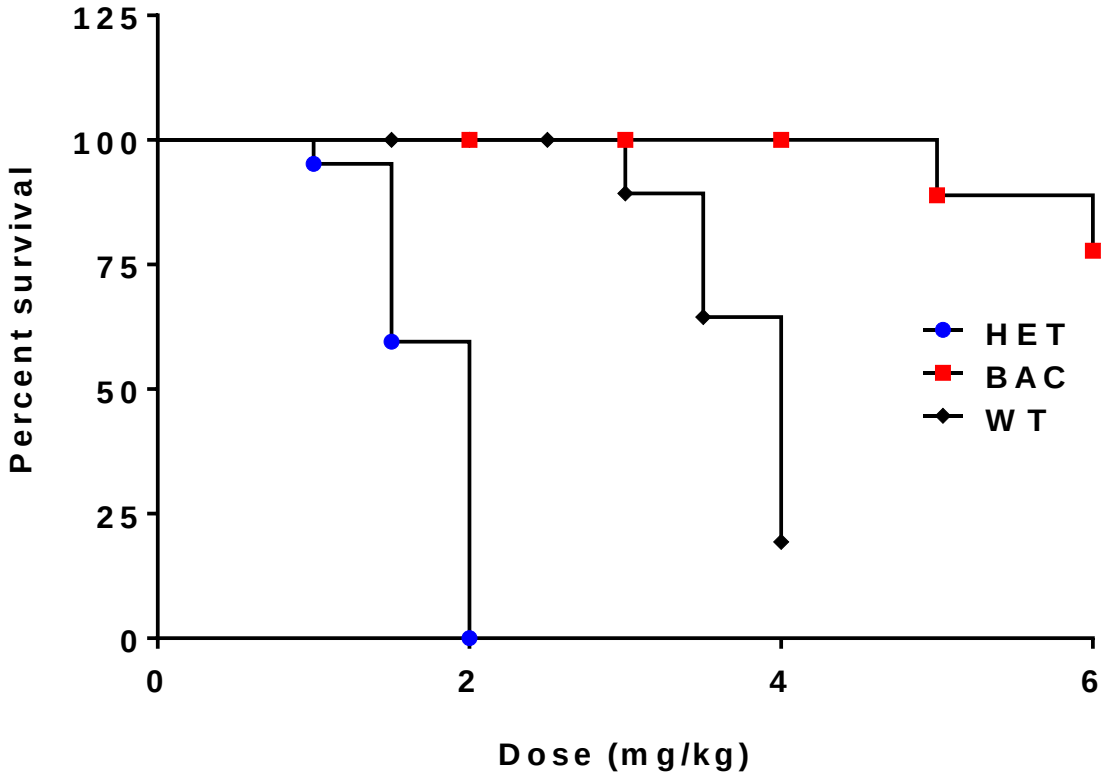

Figure 24. ML352 lethality scales with CHT protein levels. WT, CHT HET, and CHT BAC mice were dose with increasing doses of ML352 until specific signs of toxicity were observed. CHT HET mice displayed significantly increased sensitivity towards ML352 with an LD50 of approximately 2 mg/kg when compare to WT, LD50 ≈ 3.5 mg/kg, and CHT BAC mice. Toxicity is measured along the y-axis in the number of mice that survived each i.p. injection of the ML352 dose specified on the x-axis.

ML352 in consideration of the number of additional mice such studies would require. The difference in the LD50 between the wild type, CHT HET, and CHT BAC mice scales with the amount of CHT available, supporting our conclusion that ML352 specifically targets CHT (Figure 24).

The nature of the ML352 lethality was recorded in detail and videotaped records so that it could be compared to other CHT inhibitors, and anticholinergics in the future. Here is a description of the physical signs animals exhibited after ML352 administration. After i.p. injection of doses approaching the LD50 or at the LD50, the mice moved freely and without struggle from 10 to 30 minutes in a white cardboard chamber. The length of time that the mice moved freely without struggle appeared to correlate inversely with the amount of movement. The activity levels of the mice would decrease and the mice would lay against an edge of the chamber with legs slightly spraddle and their front paws underneath them. The mice would raise their heads and bodies slightly, as if it was exhausting to move. Alternatively, some mice switched between laying and walking around, though they were significantly less agile. It was also common to observe piloerection, and tail rattling. Laying behavior appeared similar to sleep, and could last a few minutes before the next stage of the lethality, through it could also could last longer periods of time after which the mice would resume completely normal behavior and survive through the time period allotted for assessments. Some period of time after the laying behavior began, the sides of the mice above the hips below the rib cage would thump as though their hearts were struggling and beating harder than normal. If the thumping movement of the sides of the mouse persisted, the mice would begin to slightly bend in on themselves, open their mouths as if gasping for breath, and make a low

clicking sound. This sound is often described as a death throw, and an indicator of suffocation. If the death throw sound persisted for longer than a minute, the behavior was taken as a side of distress and, according to our protocol we were require to humanely sacrifice the animals. This was the measure that we decided to indicate lethality. The notes from the LD_{50} experiment included the time at which the mice began the death throws and their time of death. The majority of mice that died from ML352 administration would begin death throws after 12-17 minutes and die within 5 minutes of beginning death throws. At higher doses or ML352 or in mice that were extremely active at the beginning of the experiment, some mice would not exhibit the laying behavior and then exhibit a minor clonic seizure. The mice would be freely moving and, with very few other signs of distress, would shake. The seizures observed ranged from a shake of the head to a whole body shake. Mice that had seizures were closely observed for additional clonic seizures. Most mice would transition straight into death throws and they were immediately humanely sacrificed though a small fraction would reduce their activity and never show additional signs of distress. The progression of ML352 lethality mirrored the lethality of other anticholinergics previously noted by Dale (Dale, 1906). The appearance of this lethality was identical in all of the genotypes tested.

ML352 Brain and Plasma Levels over Time in the Mouse

To determine the exposure to ML352 at a non-lethal dose through the method of administration that would be used in future experiments, mice were dosed with 1.5 mg/kg ML352 i.p. and after a designated amount of time we obtained trunk blood and whole brain tissue (Figure 25). Each time point in this experiment represents at least 4 mice.

Plasma from the whole blood showed a C_{MAX} of 321.4 ng/mL at 5 minutes and a T_{MAX} of approximately 5 minutes. The C_{MAX} achieved by i.p. administration of ML352 reached much higher levels much more quickly than P.O. administration of a much higher dose of ML352. Whole brain analysis showed a C_{MAX} of 13.6 ng/g at 20 minutes, substantially lower that the levels reached via IV in rat (23.4 ng/g at 15 minutes) after a lower dose of 1mg/kg. The brain C_{MAX} from our mouse studies was closer to the CSF levels, obtained in the previously rat IV studies (11.8 ng/g). The time course of clearance of ML352 in mice via i.p. injection was similar to that described by the DMPK parameters determined from the human, mouse, and rat *in vitro* and *in vivo,* though the quantities of ML352 greatly varied over the time course depending on the route of administration. These experiments were also conducted with CHT BAC and CHT HET mice at 20-minute time point, and the 1.5 mg/kg ML352 dose. The concentrations of ML352 achieved in the plasma and the brain tissue did not vary from the concentrations achieved in wild type mice revealing a lack in genotype effect on the pharmacokinetics of ML352.

ACh, DA, and Choline Levels in Synaptosomes after Acute ML353 Administration

In our assessment of the effects of ML352, we attempted to determine if acute administration of ML352 changed levels of ACh, choline, and DA in mouse brain synaptosomes using three brain regions, hippocampus, striatum, and cortex. Following with the experimental design used in the LD_{50} experiments, the P2 fractions were prepared from mouse brains, showed no differences in the synaptosomal levels of Ch, ACh, or DA compared to the saline injected mice. This observation held true for both of the time points assessed 1 hour and 30 minutes post injection.

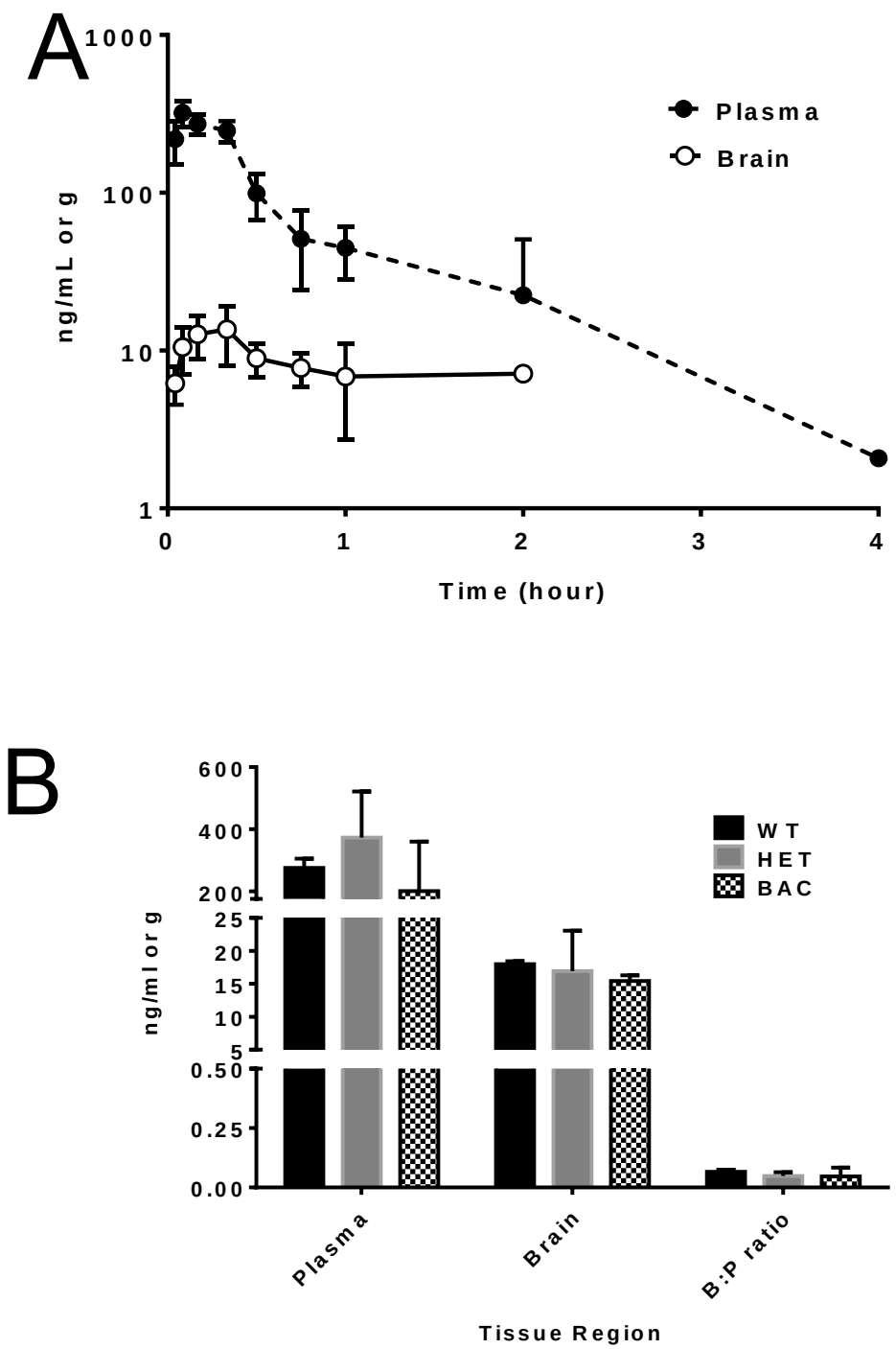

Figure 25. Concentration of ML352 in mouse brain and plasma over time. A. Brain time course of ML352 after 1.5 mg/kg i.p. injection into WT mice. B. Comparison of the concentration of ML352 in brain and plasma levels across genotypes. WT, CHT HET and CHT BAC mice were injected with 1.5 mg/kg. Concentration of ML352 in tissue and trunk blood samples were compared at the 20-minute time point.

ML352 does not Change Locomotor Activity in Wild Type Mice over Various Doses

Prior to using ML352 in other behavioral paradigms, we determined the effects of ML352 on basal locomotor activity as changes in activity may greatly influence the outcomes of other behavioral paradigms such as the tail suspension paradigm. Our first attempt to determine the effects of ML352 on basal activity was designed based on standard protocols that allow mice to acclimate to the chamber 20 minutes prior to injection and monitor their activity for the following 2 hours (data not shown). Analysis of these data showed that the activity of the mice was still declining at the 20-minute time point when the i.p. injections were administered. We decided to change our protocol to inject the mice at a later time point in the experiment where their activity had completely stabilized. The later injection time point removed the possibility that our data would be confounded by acclimation behaviors (Figure 26).

Injection of the mice with various doses of ML352 at the 90-minute time point did not change the level of activity that the mice exhibited when injected with saline. The spraddle behavior seen in the LD_{50} experiment supported the hypothesis that, if ML352 were to have an effect on the basal locomotor activity of mice, ML352 would have decreased activity. An increase in locomotor due to acute ML352 exposure would have been surprising as ML352 should work to inhibit CHT, decrease ACh levels, and limit the ACh available for release that is needed for muscle contraction.

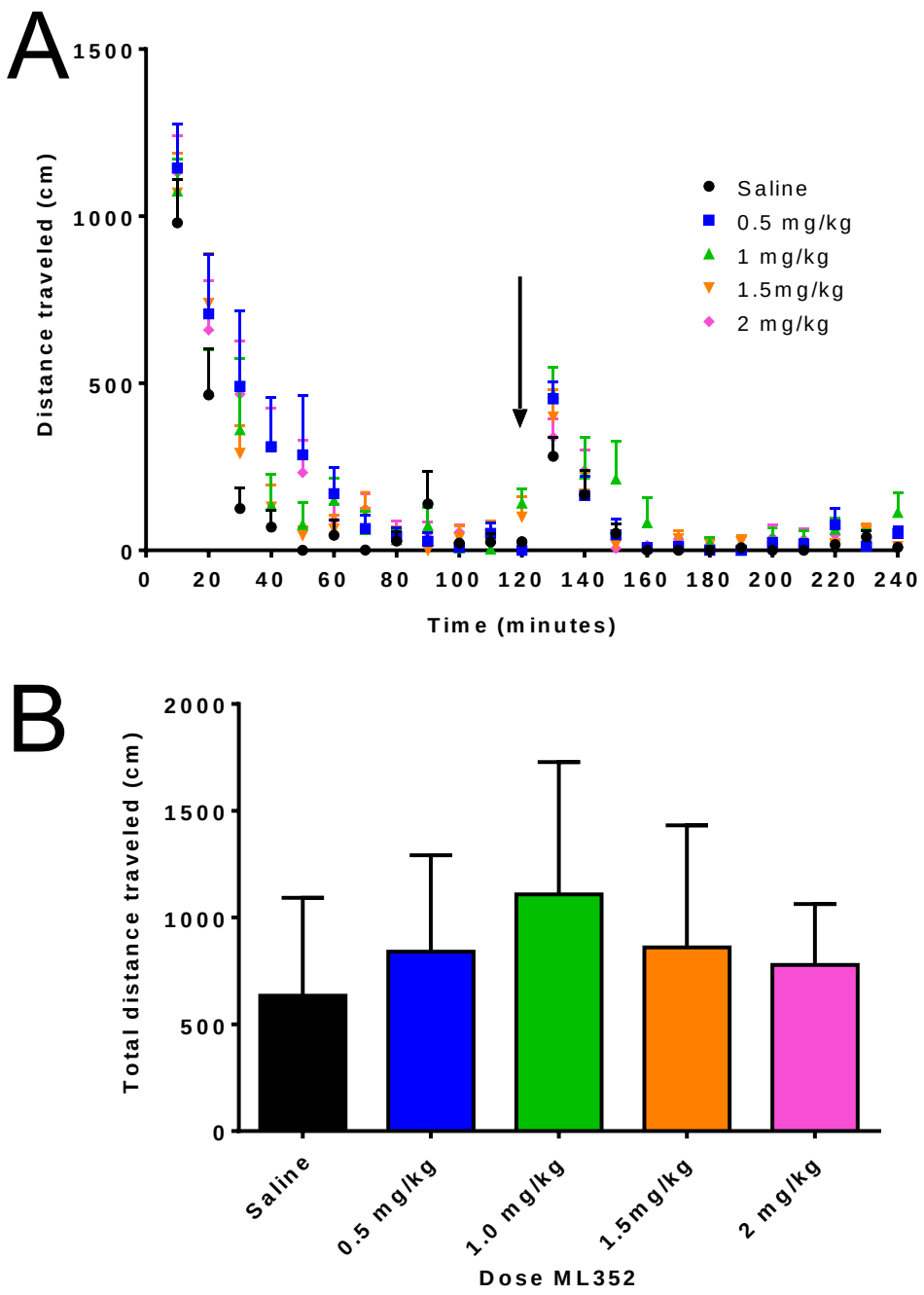

Figure 26. Evaluation of ML352 on basal locomotor activity in freely moving mice. A. Mice were i.p. injected with either saline or 1 of 4 doses of ML352, indicated above, after 120 minutes of acclimation to the open field chambers. The data acquired through monitoring their behavior before and after ML352 administration reveals that ML352 has no effect on basal locomotor activity. B. Bar graph for the cumulative distance traveled after the injection of ML352. A Tukey's multiple comparisons test (P<.05, n=9) determined the differences in total distance traveled between treatments was insignificant.

Conclusions

ML352 is the result of an extensive academic drug discovery project that encompassed numerous universities, cores, research lab, and researchers and brought together a variety of field of study. The final efforts to characterize ML352 initially pursued many different aspect of physiology that were known to be involved in cholinergic signaling. This chapter detailed those *in vivo* experiments conducted in mice and discovered that ML352 had a short half-life, penetrated the blood brain barrier, and displayed a toxicity that scaled with the quantity of CHT protein. The toxicity of ML352 was not unexpected as previously anticholinergic exhibited toxicity and reductions in cholinergic signaling cause by CHT inhibition interferes with critical physiological processes. The increased range of nonlethal ML352 doses allows for lower doses to be utilized for behavioral paradigms and avoid toxicity. The decreased toxicity of ML352, when compared to HC-3, may be due to a decrease in toxicity given the difference in potency. *In vivo* binding studies that evaluate the occupancy of ML352 at CHT *in vivo* over a range of doses are needed to make a direct comparison of the toxicity of ML352 versus HC-3. Currently, our collaborators at the University of Michigan have produced the first radiolabeled ML352 and are preparing to inject the molecule at tracer levels into rodents and non-human primates.

In addition to our goal to make a CHT inhibitor with fewer off target side effects, we also aimed to change the mechanism of action from a orthosteric competitive inhibition seen with HC-3 to an allosteric modulatory inhibition. By aiming for an allosteric mechanism of action, we hoped to develop a compound with increased specificity and

decreased off target effects with in the cholinergic system. Additionally, we had hoped an allosteric inhibitor would be able to more delicately inhibit CHT function and therefore be less toxic than HC-3. ML352 exhibited aspects of allosteric inhibition and was 20 fold less toxic than HC-3 in wild type C57B6/J mice, though this may be a reflection of the decrease in the potency of ML352 compared to HC-3 (Ferguson, Bazalakova, et al., 2004). With the data obtained for the DMPK studies, we are able to predict that we are reaching concentrations of 3.3 nanograms of ML352 per gram of brain tissue in the brain. These concentrations of ML352 are equivalent to 8.5 nanomoles per gram of brain tissue. We would predict that these levels of CHT inhibition, and that the concentrations of ML352 in the brain prior to lethality would most likely not be high enough to reach therapeutic efficacy. Though, without additional information about the free fraction of ML352 in brain tissue calculating the amount of ML352 to inhibit CHT is difficult.

The similarities between the data obtained from the ML352 *in vitro* pharmacokinetic experiments and the *in vivo* DMPK experiments that described the DMPK profile of ML352 supports the use of ML352 *in vitro* experiments as a facile, rapid analysis of a compounds DMPK profile. Nonetheless, the differences between the predicted and measured brain concentrations of ML352, and the difference through route of administration should not be overlooked when utilizing the data to design future experiments. Monitoring of ML352 in the brain and blood in these time course experiments should be used as a point of reference for the rest of the *in vivo* experiments in this dissertation as it used the i.p. route of administration and will most closely reflect the amount of ML352 the mice are experiencing.

Acute exposure to ML352 appeared to have no effect on brain tissue levels of ACh, choline, or DA though these experiments were preliminary evaluations and should be repeated. The lack of change in neurochemistry was not surprising as it is known that neurotransmitters reside in stable vesicle pools that may not have been impacted by the drug over the time of the experiment. Repeated stimulation of the cholinergic system may be need to completely deplete the stores of ACh in the presence of CHT inhibitor. This explanation assumes that ML352 reached high enough levels, and resided at the site of action long enough, to substantially inhibit CHT and affect brain neurochemistry. With these caveats considered, we cannot assume that ML352 does not possess therapeutic value. These results invite the hypothesis that chronic dosing of ML352 may effect brain neurochemistry and could be studied in models of cholinergic hyperactivity, such as the CHT BAC mouse line. The results of these neurochemical experiments are preliminary and have yet to be repeated to a level to determine significance though our collaborators, the Sarter lab at University of Michigan, have been conducting *in vivo* amperometry experiments to compliment the neurochemical experiments previously described. Dr. Sarter's lab has shown that acute local administration of ML352 decreased choline clearance in mice.

Additionally, no change was seen in the basal locomotor activity in mice. Though, the lack of change in basal locomotor activity may not have been due to a lack of ML352 efficacy but instead a limited range of measurable activity or low levels of ML352. The mice had quite little basal activity, when only injected with saline, possibly limiting the ability to see a depression in activity due to ML352 though making it quite apparent that ML352 did not cause hyperactivity. An alternative protocol will have to be employed in

future experiments to monitor a decrease in activity caused by the administration of ML352. The DMPK profile of ML352 suggests that ML352 may not reach concentrations that would elicit physiological effects with acute dosing. Multiple doses and a chronic administration protocol prior to the open field assay or other behavioral paradigms may be better suited to evaluate the effects of acute exposure to ML352.

Throughout the *in vivo* experiments conducted to characterize the effects of ML352 *in vivo*, the CHT BAC and CHT HET mice were also utilized as models of hypercholinergic, and hypocholinergic states, respectively, to determine how CHT inhibitors variations in cholinergic tone. ML352 toxicity inversely scaled to the levels of CHT protein in the CHT BAC and CHT HET mice though no changes in the pharmacological profile of ML352 was seen. Future experiments with these mouse lines may help determine the therapeutic doses necessary to alter cholinergic tone without causing toxic side effects.

Even though ML352 displayed high clearance, it crossed the blood-brain barrier after IV and i.p. administration, reinforcing its potential use in probing CNS components of CHT function *in vivo*. However, the DMPK profile leaves much to be desired before it could be considered a viable compound for therapeutic development. Particularly, the low brain concentrations have encouraged us to continue compound diversification. Studies are underway to further diversify the structure, with a goal of reducing clearance rates and enhancing CNS penetration while maintaining CHT inhibitory potency, limited off-target effects. Currently, these studies have resulted in an analog of ML352 where the meth-oxy functional group has been replaced with a chloride ion. In summary, we have successfully broadened the pharmacology of CHT antagonism, providing a novel tool for

the study of CHT in both heterologous and native preparations, *in vivo* studies, and a platform for further drug development.

CHAPTER 5

CONCLUSIONS AND FUTURE DIRECTIONS

Although CHT has been known to play a critical role in dictating cholinergic signaling capacity for many decades, the transporter is conspicuously absent from targets engaged for the identification and monitoring of cholinergic pathways or therapeutic manipulation of cholinergic signaling. In part, this may be due to the understanding that full elimination of transporter function, as seen with CHT knockout mice (Ferguson, Bazalakova, et al., 2004), is incompatible with life, at least for vertebrates (Matthies et al., 2006). In CHT knockout mice, loss of CHT expression occurs throughout life, irrespective of demand, and thus the model may poorly represent the therapeutic limitations associated with CHT antagonism. Additionally, attenuated cholinergic signaling, rather than full inhibition, may offer an effective treatment for disorders where hypercholinergic function has been proposed as a major etiological component. For example, the uncontrolled movements associated with dystonia are commonly treated with anticholinergic agents to reduce both central and peripheral control of motor function (Jankovic, 2013; Ramirez-Castaneda & Jankovic, 2013). Hypercholinergic function has also been associated with depression and anxiety behaviors (Mineur et al., 2013; Picciotto et al., 2012). The association between enhanced cholinergic tone and anxiety behaviors have further supported by the CHT BAC mice, a model of hypercholinergic states which demonstrated basal anxiety-like behaviors in behavioral paradigms. In the case of anxiety behaviors, the nonspecific muscarinic ACh receptor antagonist

scopolamine has received significant attention as a rapidly acting antidepressant (Drevets, Zarate, & Furey, 2013; Voleti et al., 2013). Finally, ACh receptor stimulation is intimately involved in the modulation of reward circuits, where anticholinergics have been shown to reduce aspects of reward signaling (Crooks et al., 2004; Shinohara et al., 2014) and CHT heterozygous mice have been found to demonstrate reduced DA release in response to cocaine and nicotine (Dong et al., 2013).

For the past fifty years, HC-3 has been essentially the sole CHT antagonist in common use, limited essentially to mechanistic studies of cholinergic signaling (Bonsi et al., 2008). Developed in the late 1950's by Long and colleagues, HC-3 is a bicyclic structure with two choline mimicking quaternary nitrogens. The latter property affords orthosteric, high-affinity interactions with CHT. The choline features of HC-3, however, also provide for interactions with other choline targets such as CTL1 type choline transporters involved in choline lipid biosynthesis (Michel, Yuan, Ramsubir, & Bakovic, 2006) as well as choline kinase (Ansell & Spanner, 1974). With respect to *in vivo* utility, constitutive positive charge of HC-3 impedes CNS penetration, and thus limits the use to the molecule in the potential treatment of brain disorders, or in imaging CNS cholinergic innervation (Zheng et al., 2007). Thus, whereas HC-3 has proved useful in documenting CHT density in both membrane binding assays (Sandberg et al., 1985) and autoradiographic studies (Manaker et al., 1986), PET studies that document cholinergic neuron projections and/or terminals are currently limited, with a primary focus on derivatives of the vesicular choline transporter antagonist vesamicol (Giboureau, Som, Boucher-Arnold, Guilloteau, & Kassiou, 2010). Depending on access of novel CHT ligands to intracellular versus extracellular conformations, targeting CHT may afford

labeling of activated cholinergic neurons where synaptic CHT density is elevated relative to less active states (Apparsundaram et al., 2005b; Ferguson et al., 2003a; Parikh et al., 2013).

The importance of CHT in determining ACh signaling capacity, the therapeutic potential of CHT antagonism, and the limitations of HC-3 noted above encouraged us to pursue a high-throughput screen for novel CHT modulators. Our screen made use of the electrogenic properties of choline transport by CHT (Iwamoto et al., 2006; Ruggiero et al., 2012)rather than the more expensive and labor intensive assessment of radiolabeled choline transport. As membrane depolarization that arises with CHT activity is nonstoichiometrically linked to choline flux (Iwamoto et al., 2006), we counter-screened at later stages in our screen for the actions of our agents on [^{3}H]choline uptake. Because CHT is predominantly intracellularly localized in transfected cells as it is *in vivo*, we made use in our screen of a stable cell line expressing the CHT LV-AA mutant, where a strong dileucine-type endocytic motif has been modified to afford constitutively high levels of CHT expression. Not only does this maneuver elevate CHT-dependent signals in our screen, but it also reduces the likelihood that the hits in our screen target generic endocytic pathways. We used a triple add protocol involving vehicle addition, followed by an EC_{20} choline addition followed by an EC_{80} choline addition, in the presence or absence of individual library molecules. Using this design, we were able to exclude molecules with nonspecific actions on membrane potential that could lead to false positives in a screen based on electrogenicity, as well as potentially identify both positive and negative modulators of CHT activity. We also validated hits with traditional [^{3}H]choline uptake assays. With respect to CHT inhibitors, the focus of our current report, the use of both

sub- and near-saturating concentrations of choline permits an initial inspection of the kinetic features of hits identified. Thus, molecules that effectively antagonizes choline-induced membrane depolarization at low choline concentrations, but less so at high concentrations, would be expected to reflect competitive antagonism, such as that arising from HC-3, whereas sustained inhibitory activity at high concentrations could reflect non-competitive antagonism. Finally, we screened all potential hits against non-transfected cells to insure that inhibitors were not affording reductions in choline-induced depolarization through nonspecific actions on membrane ion transporters/channels.

The high-throughput screen used the more than 300,000 compounds in the NIH Molecular Library Small Molecule Repository (MLSMR) collection, and from this we identified five distinct structural scaffolds. We have explored the SAR around a series of 3-methoxy-4-(piperidin-4-yl)oxy benazmides based on a core scaffold identified from our HTS to identify CHT inhibitors. Within this series, it was noted that benzylic heteroaromatic amide moieties were the most potent. In addition, 3-(piperidin-4-yl)oxy substituents were favored over alkyl ether changes. From this work, ML352 was discovered as a potent inhibitor of CHT at both a low and high concentration of choline (100 nM and 10 μM, respectively). In addition, we have fully characterized ML352 and additional analogs in a variety of selectivity and *in vitro* and *in vivo* DMPK studies. In this effort, we identified and submitted *N*-((3-isopropylisoxazol-5-yl)methyl)-4-methoxy-3-((1-methylpiperidin-4-yl)oxy)benzamide (ML352) to the NIH Molecular Libraries Program as our lead compound for further analysis, and describe its characterization in Chapter 3.

Tests of many other GPCRs, ion channels and transporters, including ACh receptors and LACU, revealed specificity of ML352 interactions for HACU/CHT (Ennis, Wright,

Retzlaff, McManus, Lin, Huang, Wu, Li, et al., 2015). Pharmacokinetic studies indicated a favorable profile for potential *in vivo* use, with limited metabolism and significant brain penetration (Ennis, Wright, Retzlaff, McManus, Lin, Huang, Wu, Li, et al., 2015). Acute exposure to ML352 has no short term effects on brain neurochemistry though these studies are preliminary and should be replicated. Behavioral paradigms also revealed no change in basal activity of mice and no change has yet to be detected in heart rate and blood pressure of mice in our studies (data not shown). Our *in vivo* studies with ML352 are just beginning to define the physiological and behavioral effects of the drug, with an ultimate goal of using the molecule to attenuate symptoms of disorders suggested to involve excess cholinergic signaling.

Our HTS and molecular pharmacology studies have provided new pathways to understand and manipulate multiple dimensions of cholinergic signaling. Key areas for future studies include the identification of high-resolution structures of CHT in distinct states, and when complexed with ligands (e.g. choline, HC-3, ML352), the mechanisms by which CHT is targeted to synaptic vesicles, and the identification of CNS circuits where human *SLC5A7* polymorphisms influence disease risk. To pursue these future studies, we have initiated collaborations with the laboratory of Dr. Martin Sarter, and Dr. Michael R. Kilbourn and Peter J. H. Scott, to further evaluate the effects of CHT inhibition on cholinergic signaling. The Sarter lab conducted *in vivo* amperometry with ML352 in both wild type and CHT BAC mice to determine the effects of ML352 on the clearance of choline at the synapse. The results show ML352 and HC-3 reduced the clearance of exogenous choline as illustrated by elevated choline current peak amplitudes, though a paradoxical increase in evoked ACh release events was seen in the CHT BAC mice,

suggesting that CHT antagonism leads to a (compensatory) increase in the levels of functional CHT in synaptic plasma membrane. Under the direction of Dr. Michael R. Kilbourn and Peter J. H. Scott at the University of Michigan, researchers have synthesized [^{11}C]ML352 from the desmethyl piperidinic precursor by treatment with [^{11}C]methyl triflate in an automated radiochemistry synthesis module. Experiments by are underway to determine if radiolabeled ML352 is able to monitor CHT-1 activity using PET imaging. The implications of this achievement are immense for both researchers and the medical field. A viable radio tracer for CHT would, for the first time, allow scientists to monitor CHT *in vivo* in murine or non-human primates to evaluate the specific role of CHT in different pathways, and, maybe someday, in humans to determine the levels of CHT in different diseases, potentially allowing us to develop techniques to better diagnosis hypercholinergic and hypocholinergic diseases.

Certainly issues related to the potential broad actions of CHT antagonism must be considered in terms of their potential clinical utility, though relatively nonspecific reagents are commonly used in medical practice (e.g. amphetamines for the treatment of ADHD, clozapine for the treatment of schizophrenia). As I have highlighted previously, CHT is highly regulated with respect to its contribution to cholinergic signaling, due to a steady-state enrichment of the transporter on cholinergic synaptic vesicles (Ferguson & Blakely, 2004; Ferguson et al., 2003a; Nakata et al., 2004), and as a consequence, activity-dependent shuttling to the plasma membrane in response to presynaptic excitation. We predict that latter property may afford a measure of activity-dependent inhibition of cholinergic signaling by CHT antagonists, versus classical cholinergic modulators that act

constitutively and thereby reduce the toxicity by the potentially broad actions of CHT antagonism.

We hypothesize that the novel CHT pharmacology we have developed can be further expanded to include additional CHT inhibitors and CHT activators that could be beneficial in disorders with reduced cholinergic tone, as with Alzheimer's disease. Expansion upon the novel CHT pharmacology represented by ML352 to include other CHT inhibitors that exhibit different mechanisms of action could expand the therapeutic value of CHT inhibitors. Other CHT inhibitors could exhibit lower potencies at CHT compared to ML352 and therefore exhibit more delicate modulation of cholinergic tone that may be required to avoid detrimentally influencing the broad actions of CHT antagonism. Concurrent with the work presented here, the Blakely and Lindsley labs have conducted studies to further diversify the structure of ML352 and expand CHT pharmacology, with a goal of improving the pharmacokinetic profile of ML352 by reducing clearance rates, limiting off-target effects, and enhancing CNS penetration. One compound, the chloro-ML352 analog, to date has improved upon the pharmacological profile of ML352. The chloro-ML352 analog replaces the methoxy group on the central benzene ring for a chloride molecule. This simple structural modification maintained the *in vitro* potency of CHT inhibition, and the clean CYP450 profile nor the great free fraction in both human and rat (as well as rat brain homogenate binding) but fortunately significantly lowered the *in vitro* predicted clearance (CL_{HEP}) from hepatic microsomes (Bertron et. al. 2016 manuscript in preparation). Moreover, the change in pharmacological profile of the chloro-ML352 analog doubled the CNS penetration is doubled for 4c (Kp = 0.34) compared to ML352 (Kp = 0.18). Chlor-ML352 has become a heightened point of

interest and may emerge as a better probe to study CHT modulation *in vivo*. Chloro-ML352 was first tested for *in vivo* utility in the novel object paradigm in rats which, after 3mg/kg and 10 mg/kg doses, revealed an enhancement in cognitive performance while having no toxicity at the 3mg/kg dose and some toxic side effects at the 10mg/kg dose. These findings would suggest a CHT inhibitor enhanced cognitive performance which is generally a quality attributed to cholinergic agonist, AChE inhibitors, and incites the question to whether chloro-ML352 causes an increase in CHT surface expression like ML352. As shown in Chapter 3, ML352 was shown to cause an increase in CHT surface expression in a heterologous system. Though efforts were made, these effects were never validated in native tissue which would have elucidated if the effects could also happen *in vivo*. An *in vivo* elevation of CHT surface expression by ML352 or chloro-ML352 at presynaptic terminals could provide enhanced choline transport into the presynaptic terminal, if the inhibitors were not saturating CHT binding sites. Though, we do not know how a CHT antagonist would act *in vivo*, we hypothesize that decreased presynaptic choline levels will result in decreased presynaptic ACh levels, and possibly reduce cholinergic tone. The results found in the novel object behavior paradigm with chloro-ML352 are contrary to our hypothesis on how a typically CHT inhibitor would act. Though with the effects of ML352 on CHT localization, we can adjust our hypothesis to explain how an *in vitro* CHT inhibitor to be an *in vivo* CHT agonist. The implication of this hypothesis would suggest that CHT inhibitors act as we would predict and diminish cholinergic tone, and the reason for the observed cognitive enhancement by cholor-ML352 in the novel object recognition task is due to its ability to increase CHT surface expression and not its action as a CHT inhibitor.

Outside of the experiments detailed here, two other major experiments to evaluate the *in vivo* effects of ML352 had been initiated by the Blakely lab, microdialysis and *in vivo* heart rate and blood pressure monitoring. The *in vivo* microdialysis experiments were meant to complement out neurochemical studies in synaptosomes but the data has to date demonstrated too much variation to derive conclusions as to the meaning of the results. In collaboration with Dr. Robertson's laboratory at Vanderbilt University and the gracious help of Charlene Finney, wild type and CHT BAC mice were implanted with telemeters and underwent a four-day protocol where the mice acclimated to injections of saline and, finally, exposed to ML352. We hoped to determine the effects of ML352 on the heart rate and blood pressure of freely moving mice. Injection alone causes significant changes in heart rate that persisted for approximately 20 minute, coinciding with the period of time where we expected ML352 to have its greatest effects, obscuring the results. We observed some changed in the slopes of the heart rate and blood pressure recovery after injection but these data need to be replicated before any conclusions can be made. These heart rate and blood pressure experiment were not only designed to probe the effects of ML352 but also to evaluate the basal heart rate and blood pressure of the CHT BAC mice, which had not been previously recorded. Preliminary analysis of these experiments revealed that the CHT BAC mice had an elevated heart rate contrary to our predictions as CHT HET mice show basal tachycardia and elevated cholinergic tone.

In summary, we have successfully broadened the pharmacology of CHT antagonism, providing a novel set of tools for the study of CHT in both heterologous and native preparations and a platform for further drug development. As our collaborations

have indicated, there is still much to learn about ML352 and its impact on cholinergic biology. These efforts were founded by the efforts of “Team Choline” in the Blakely lab and will be carried on by our collaborators and researchers to come.

APPENDIX 1

OTHER STRUCTURAL CLASSES OF HTS LEAD COMPOUNDS FOR THE POTENTIAL DEVELOPMENT OF CHT INHIBITORS

Introduction

Our HTS effort identified five novel structural classes of compounds that inhibit CHT. Structures different from HC-3 have the potential to lead to novel mechanisms of inhibition that may avoid the dose dependent side effects seen with other CHT inhibitors. We pursued only one of the structural classes found by the HTS due to the limitations of time and of resources available to this project. The majority of this document describes the properties of ML352, a compound developed from one of the structural classes.

Prior to choosing ML352, we had in parallel performed SAR studies around two of the other structural classes to see if we could quickly identify a non-competitive compound of increased potency compared to the original HTS hits. Using the HEK 293 LV-AA CHT cells, we tested numerous other compounds for their potency to inhibit CHT and their mechanism of inhibitions through saturation analysis. These preliminary studies revealed other avenues that we could have pursued and that could still lead to novel inhibitors of CHT.

An outline of the data collected on the one of the other structural classes is documented in this Appendix. The data includes limited SAR studies and cell based experiments, as well as, a few studies of their mechanism of action. The different

structures of each of these compounds could result in changes in effects on the potency of CHT inhibition which could translate to differences in the therapeutic efficacy. As such, these compounds should be considered as valuable as starting points for future expansion of CHT pharmacology.

Materials and Methods

See Chapter 2.

Results and Discussion

Organizational Note for Cross Referencing this Dissertation with the Raw Data

The structural classes were color coded in the original tabulations, identifying the 5 structural classes. Group 1 was yellow, group 2 was blue, and group 3 was green. This of importance because the early data was organized according to this color scheme.

Diversification of Group 2 and their Potency Evaluation

Structural analogs based on the core structure of the group 2 compounds were purchased from commercial vendors and synthesized by chemists at Vanderbilt University. Group 2 compounds were tested in the 96-well [^{3}H]choline based CHT inhibition assay, and revealed a variety of potencies (Figure 27). Some compounds retained the ability to inhibit choline uptake, 1PXN, 1PYK, and 1PXQ, while others showed an ability to increase choline uptake, 1PXU, and 1PY1. The potency of these

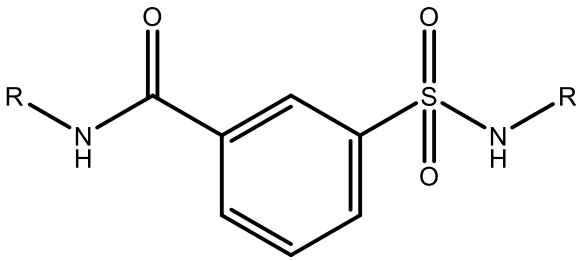

Figure 27. Core structure of the group 2 CHT inhibitor identified in the high-throughput screen.

compounds were tested at both high, 10 µM, and low, 100 nM, concentrations of choline to obtain a preliminary evaluation of their mechanism of action. Compounds such as 1PYL that demonstrate an ability to inhibit choline uptake at 10 uM verses 100 nM may indicate a selective impact on CHT V_{MAX} and a noncompetitive mechanism of action (Figure 28).

Michaelis-Menten Kinetics of ML352 in Heterologous Preparations

We explored the kinetics of some of the inhibitors from group 2. In these studies, the activity of the inhibitor was evaluated at varying concentrations of choline in transport assays with CHT LV-AA transfected cells. When combined with fixed concentrations of inhibitors, we observed a variety of effects on the choline $K_{M,}$ and V_{MAX}. Analysis of 1PYN inhibitory actions on choline uptake revealed a dramatic increase in the $K_{M,}$ and decrease in the V_{MAX} (Figure 29A) whereas analysis of 1PXN revealed small, possibly insignificant, decrease in K_M and dramatic decrease V_{MAX}. These findings are a brief glimpse to the variety in modes of CHT inhibition is represented by these additional structural classes.

Specificity of Group 2 in Heterologous Preparations.

We tested the specificity of group 2 compounds by monitoring the function of one neurotransmitter transporter in a HEK 293 heterologous cell system. Here, we observed a collection of group 2 compounds lacked inhibitory activity at NET in transfected HEK cells (Figure 30). These results indicate that, as in the case of ML352, it is unlikely that nonspecific effects on membrane integrity or alterations of ion gradients are the basis for CHT inhibition.

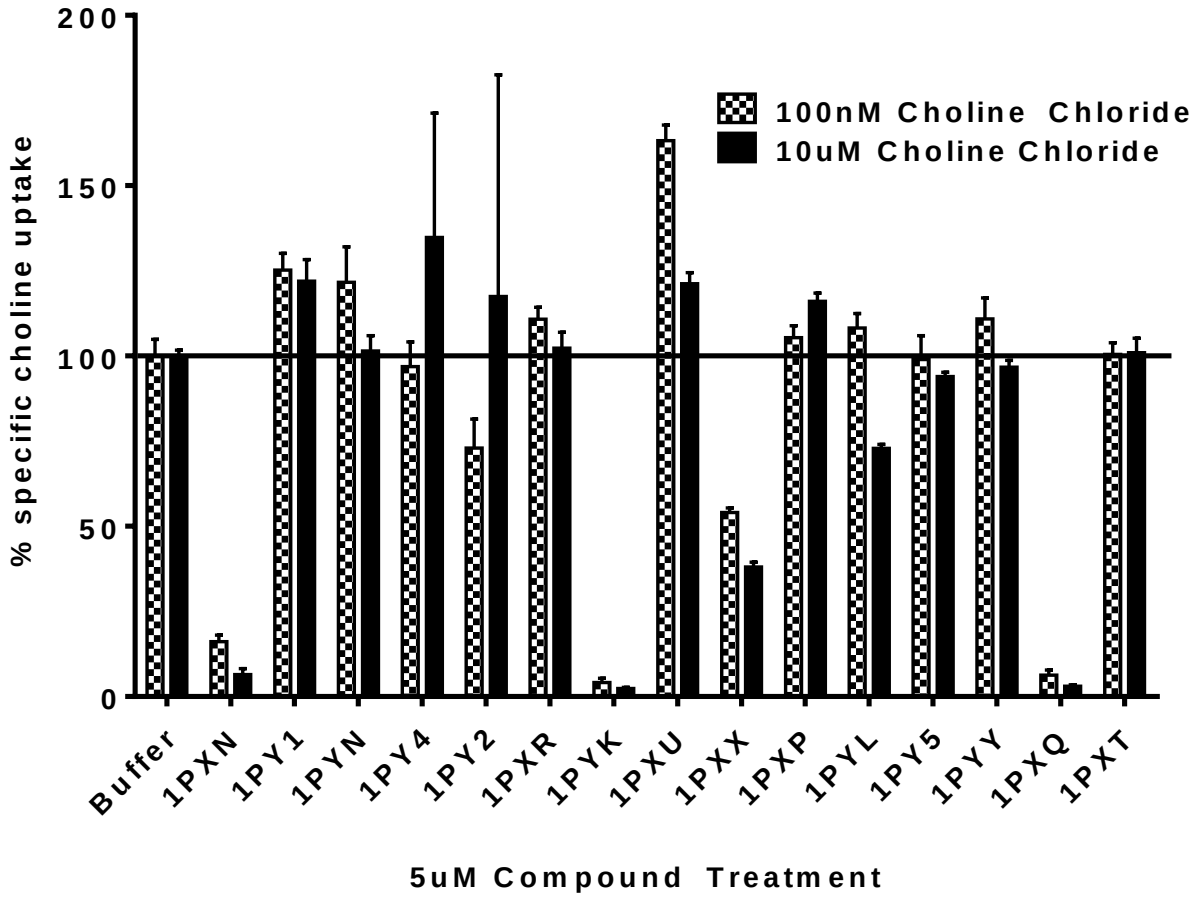

Figure 28. Potency evaluation of group 2 inhibitors from SAR studies. Inhibition of choline transport by compounds in transfected HEK 293 LVAA-CHT cells at two concentrations of choline, 100nm and 10µM, and one concentration of compound, 5µM (n=2).

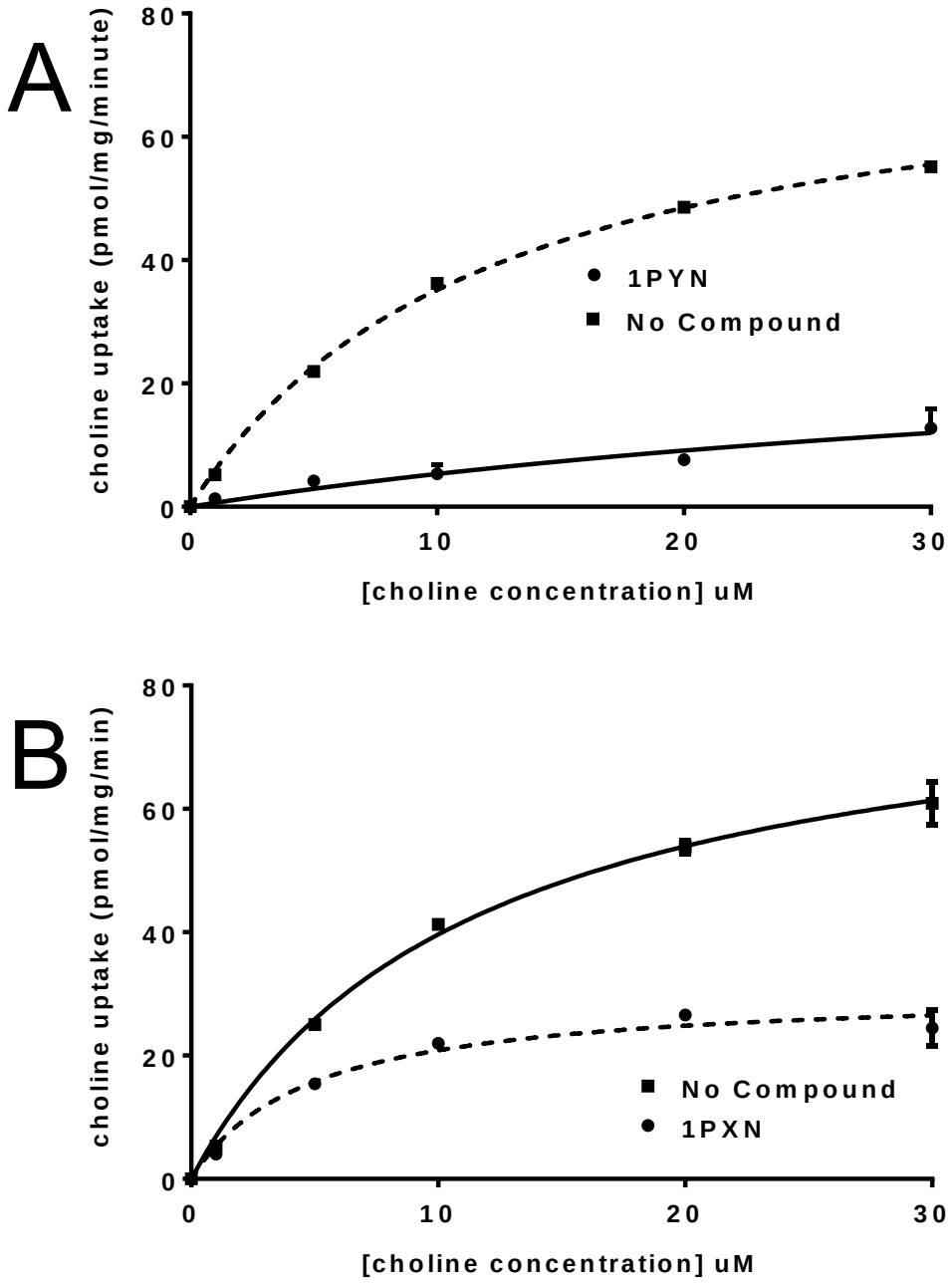

Figure 29. Inhibitory mechanism exhibited by two group 2 compounds, 1PYN and 1PXN. A) 1PYN uncompetitively inhibits choline uptake in HEK 293 LVAA-CHT cells at a concentration of 500nM (n=1) resulting in a V_{MAX}= 31.91 ± 23.37 and a K_M= 50.04 ± 50.04. B) 1PXN uncompetitively inhibits choline uptake in HEK 293 LVAA-CHT cells at a concentration of 500nM (n=1) resulting in a V_{MAX}= 30.71 ± 2.011 and a K_M= 4.74 ± 1.109.

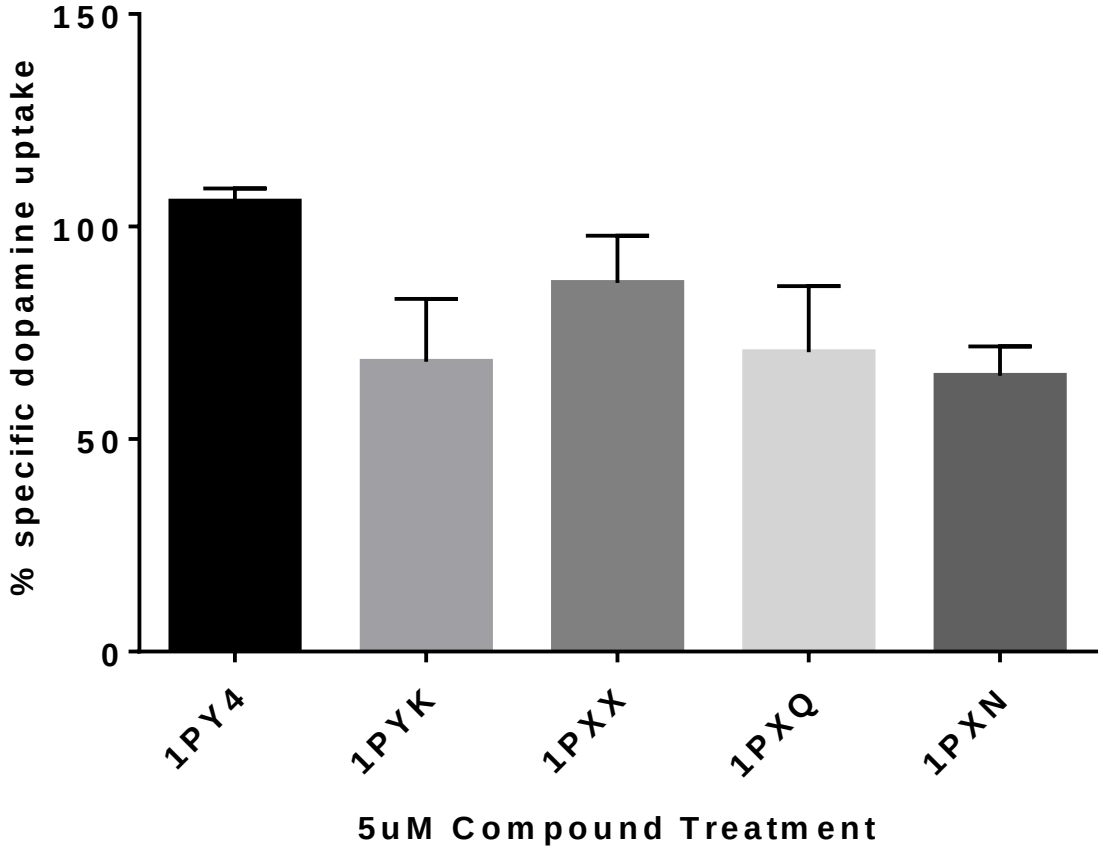

Figure 30. *In vitro* specificity evaluation of group 2 compounds. Group 2 CHT inhibitors exhibited less than fifty percent inhibition of NET in HEK293 cells (n=3). 1PY4 (105.9 ± 1.79 % DA uptake) resulted in an increase in DA uptake by NET while 1PYK, 1PXX, 1PXQ, and 1PXN results in slight inhibition, 71.70 ± 2.69, 86.74 ± 2.36, 70.46 ± 4.67, 64.63 ± 2.07 % DA uptake remaining respectively.

Conclusions

The HTS was extremely fruitful and provided more avenues for the discovery of CHT inhibitors than we had the resources to exploit. During our initial phases of SAR studies, we attempted to keep as many of these avenues of discovery open by studying the potency, mechanism of action, and specificity of compounds from different structure classes. SAR studies based on the core structure of group two provide compounds that retained their ability to inhibit CHT, and possibly a compound that enhanced choline uptake. Pending the replication of this data, a group of compounds that through minor structurally modifications could switch from inhibitors to activators would be a major discovery in CHT pharmacology. Despite our interest in the mode switching in group 2, we did not explore these findings beyond what is documented here.

APPENDIX II

HTS LEAD COMPOUNDS FOR THE DEVELOPMENT OF CHT ACTIVATORS

Introduction

The main chapters of this dissertation focuses on the development of novel CHT inhibitors derived from hits from the HTS conducted in concert with JHICC and the Lindsley lab. The HTS was designed to identify not only CHT inhibitors but also CHT activators. The goal of targeting CHT activators was based to the extensive and somewhat effective use of pro-cholinergics in diseases such as Alzheimer's disease (AD) and Parkinson's disease (PD). In these diseases, procholinergic agents are hypothesized to increase cholinergic signaling in remaining cholinergic neurons that have been depleted by degenerative mechanisms (AD) or offset DA changes (PD).

The HTS from which the CHT inhibitor hits were identified was also analyzed to identify CHT activators. As was discussed in the introduction of Chapter 2, this screen took advantage of the LVAA CHT, the electrogenecity of CHT-mediated choline transport, and the fluorescent-based membrane potential. In this appendix, the details of the HTS activator hits are provided and their preliminary validation are detailed.

Materials and Methods

Choline-Induced Membrane Potential Assay (384-Well HTS Format)

HEK 293 cells stably expressing CHT or CHT LV-AA or control cells were assessed for basal and choline-induced changes in membrane depolarization as previously described (Ruggiero et al., 2012) plated into 384-well, black walled, clear bottom poly- D-lysine coated plates (BioCoat, BD Biosciences, San Jose, CA, USA) at 20,000 cells in 20 µL/well dispensed using a Thermo Electron Multidrop reagent dispenser. Plated cells were grown overnight at 37 °C. The following day, the culture medium was removed and plates washed 3X with an ELX microplate washer (Biotek, Winooski, Vermont, USA), and 20 µL/well of 1.67 µg/mL of the membrane potential dye (Molecular Devices, Sunnyvale, CA, USA, R8042) was added in assay buffer (Hanks Balanced Salt Solution (HBSS), (Gibco) containing 20 mM HEPES, pH 7.3, by a dispenser (Thermo). Cells were incubated for 30 min at 37°C in an atmosphere of 95% air/5% CO_2 prior to addition of compounds at 2.5X their final concentration in HBSS. For control plates, a choline concentration curve +/- HC-3 was prepared in assay buffer at 5X the final concentration to be assayed. Data from these experiments were used to estimate EC_{20} (500 nM) and EC_{80} (60µM) concentrations for choline-induced membrane depolarization later used in inhibitor screening assays. Cell plates and compound plates were loaded into a Hamamatsu FDSS 6000 kinetic imaging plate reader. Baseline fluorescence signals were collected for 9 seconds at 0.5 Hz prior to addition of media, 5uM HC-3 or test compounds at various concentrations, diluted from DMSO stocks. After a subsequent 2 min 16 seconds of recording, choline chloride at EC_{20} was added (time

point 2 min 25 sec), followed 2.5 minutes later by EC_{80} choline was added (time point 6 minutes), with data collected for an additional 2.5 minutes. Fluorescence was captured by Hamamatsu FDSS 6000 imaging software and then data were exported to Microsoft Excel for graphical and statistical analysis.

See Chapter 2 for all other materials and methods.

Results and Discussion

Original HTS Activator Hits

Over 300,000 compounds from the NIH Molecular Library Small Molecule Repository (MLSMR) compound collection at 60 μM, and, based on a cutoff criteria of 3 SD from the mean choline dependent fluorescence. We identified 2,456 preliminary hits for activation of the second signal achieved with choline addition, a 0.80% hit rate, and 395 preliminary hits for activation of the third addition, a 0.12% hit rate. We were interested in only the hits that activated the second addition because we predicted these hits would be more likely to represent a change in the K_M of CHT-mediated choline transport and an allosteric mechanism of action, though it would be reasonable to also consider molecules that increase V_{MAX}. We were able to validate CHT hyperpolarizing activation by 2,222 of the 2,456 compounds available for retesting, a 90% replication rate. 957 of these compounds were tested in 5-point concentration response curves in duplicate in which we found that 62% of these compounds were validated, yielding 594 molecules for further analysis. The validation rate was unexpectedly high, so additional

selection criteria were applied to isolate compounds with greater than 50% activation of choline uptake resulting in 254 hits. We selected 201 of the 254 hits to be tested in a 10 point CRC assay and against un-transfected HEK 293 cells resulting in 68 compounds that had validated CRC responses and no activity in the parental cell line.

Validation of Select HTS Activator Hits

A subset of HTS activator hits were chosen for validation from the 68 activator hits to select for compounds with structures that were appropriate for future SAR studies and drug-like pharmacokinetic properties. These hits were tested in the same fluorescent-based membrane potential assay. CHT inhibition assay using the same cell line they were originally identified in, the HEK 293 cells stably transfected with LVAA-CHT. Initial evaluation of activators using the [^{3}H]choline based CHT assay in the Blakely lab could not validate the activating effects of the HTS hits (data not shown) except for one compound, RBV, that when used at relatively high concentrations, inconsistently showed a limited ability to increase choline uptake (Figure 31). The ability of these compounds to activate the choline-induced membrane depolarization in the fluorescent based membrane potential assay used in the HTS was re-tested in the Blakely lab and, also, failed to validate any of the HTS activator hits as activators of CHT. Again, RBV was validated as a CHT activator and demonstrated some ability to increase the choline-mediated membrane depolarization (Figure 31). The extent to which RBV activated CHT in both assays was much less than criteria, which was greater than 50% activation, from the HTS would have allowed. We end up skeptical of the activation of CHT by RBV though it was the only HTS activator hits that provided some sort of CRC in our hands. A small

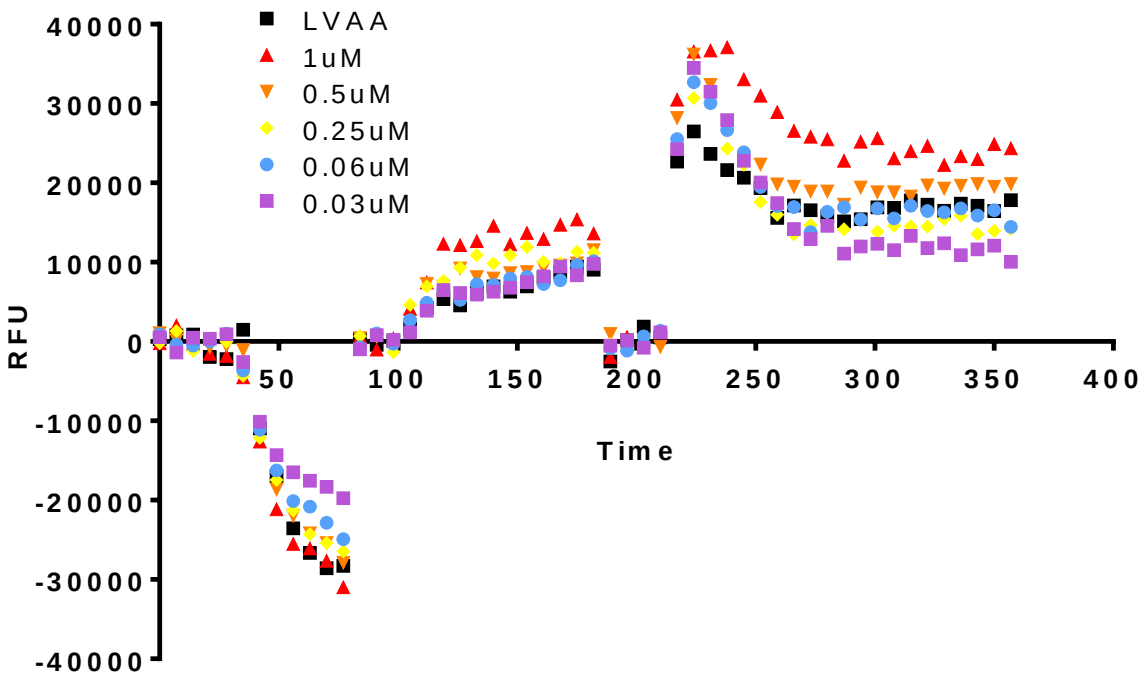

Figure 31. Activating effects of RBV validated by fluorescence based membrane potential assay. RBV was tested in the triple add protocol to validate it as an CHT activator. Various concentrations of RBV were added to HEK 293 cells stablely transfected with LVAA-CHT. Increases in the choline dependent membrane depolarization, represented by the random fluorescence units (RFU) are seen with increasing amounts of RBV when compared to the base line (LVAA).

SAR study was done around RBV in hopes of isolating the active portion of the structure (Figure 32). Unfortunately, none of the compounds from the SAR studies showed a dramatic improvement from the activity of RBV.

Review of the Raw Data from the HTS

After many of the compounds that were deemed CHT activators from the preliminary HTS failed to be validated as CHT activators in the tritium based choline uptake assay, the raw data for 200 compounds that made through the initial selection criteria, no activity on the parental cell line, no inherent fluorescence, and a dose response-like activity, was obtained from JHICC and individually analyzed. The original HTS data was in a format that could only be opened on a Functional Drug Screening System (FDSS) Software program though using this software the files could be saved individually as excel files and replotted using Excel or GraphPad Prism. The raw data obtained for each compound corresponded to the 10 point CRC using the triple add protocol. The graph shown in Figure 33 A. depicts a graph of the unmanipulated data that corresponds to compound A13 on HTS plate CRC4 with the different concentrations of the compound shown in different colors. Figure 33 shows several common characteristics found in the raw data that complicated the data analysis. The first of these is the downward deflection in random fluorescent units (RFU) after the addition of compound. The raw data from other compounds, such as compound A4 as seen in Figure 33 B., show that this deflection is not as sever and the baseline recovers prior to the second addition, the EC_{20} addition of choline. Since this downward deflect was a common characteristic in most of the data, data from the parental cell line was obtained and

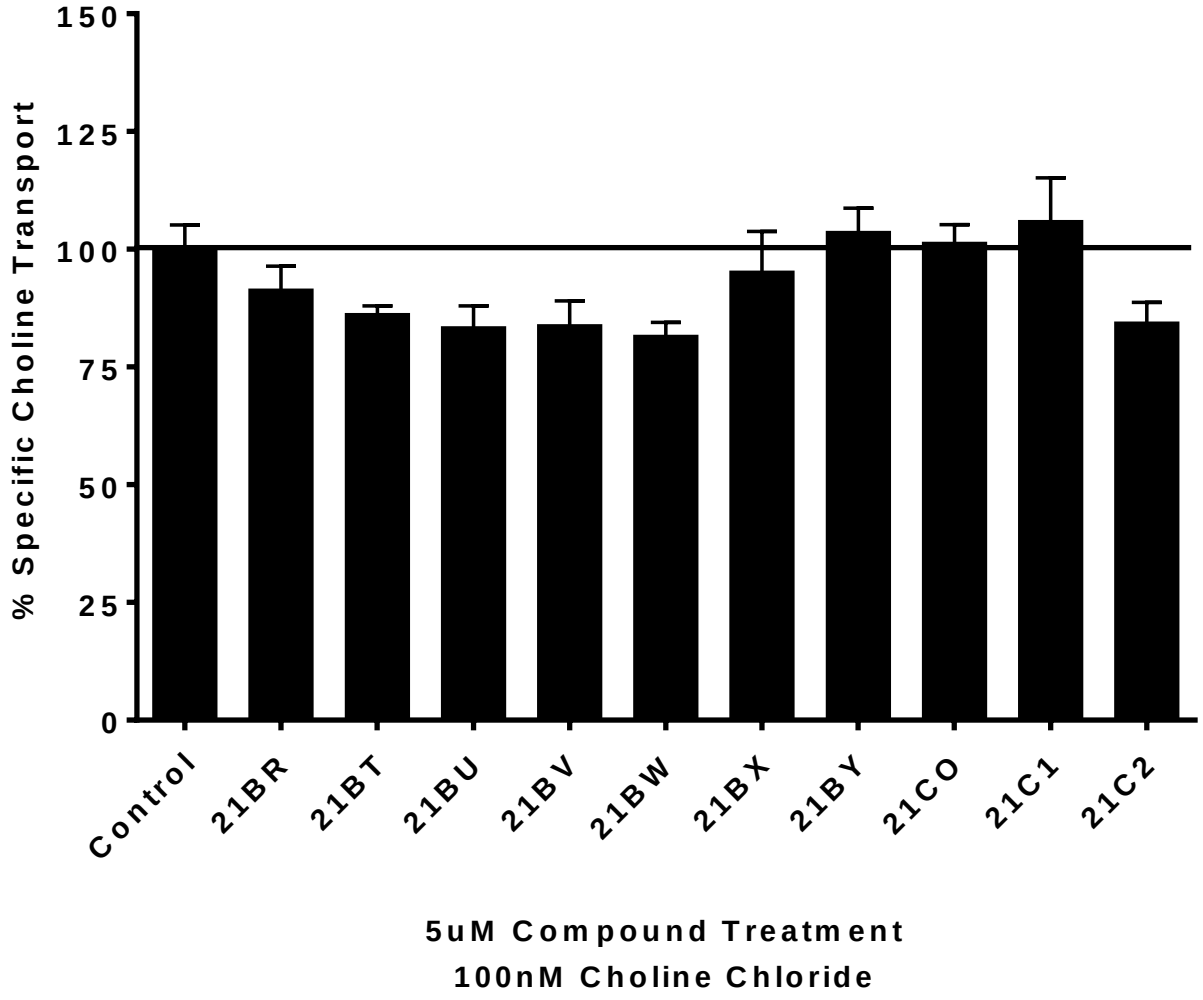

Figure 32. Potency evaluation of a group of activators from SAR studies based on the structure of RBV. Activation of choline transport by compounds in transfected HEK 293 LVAA-CHT cells at one concentrations of choline, 100 nm, and one concentration of compound, 5 µM (n=2).

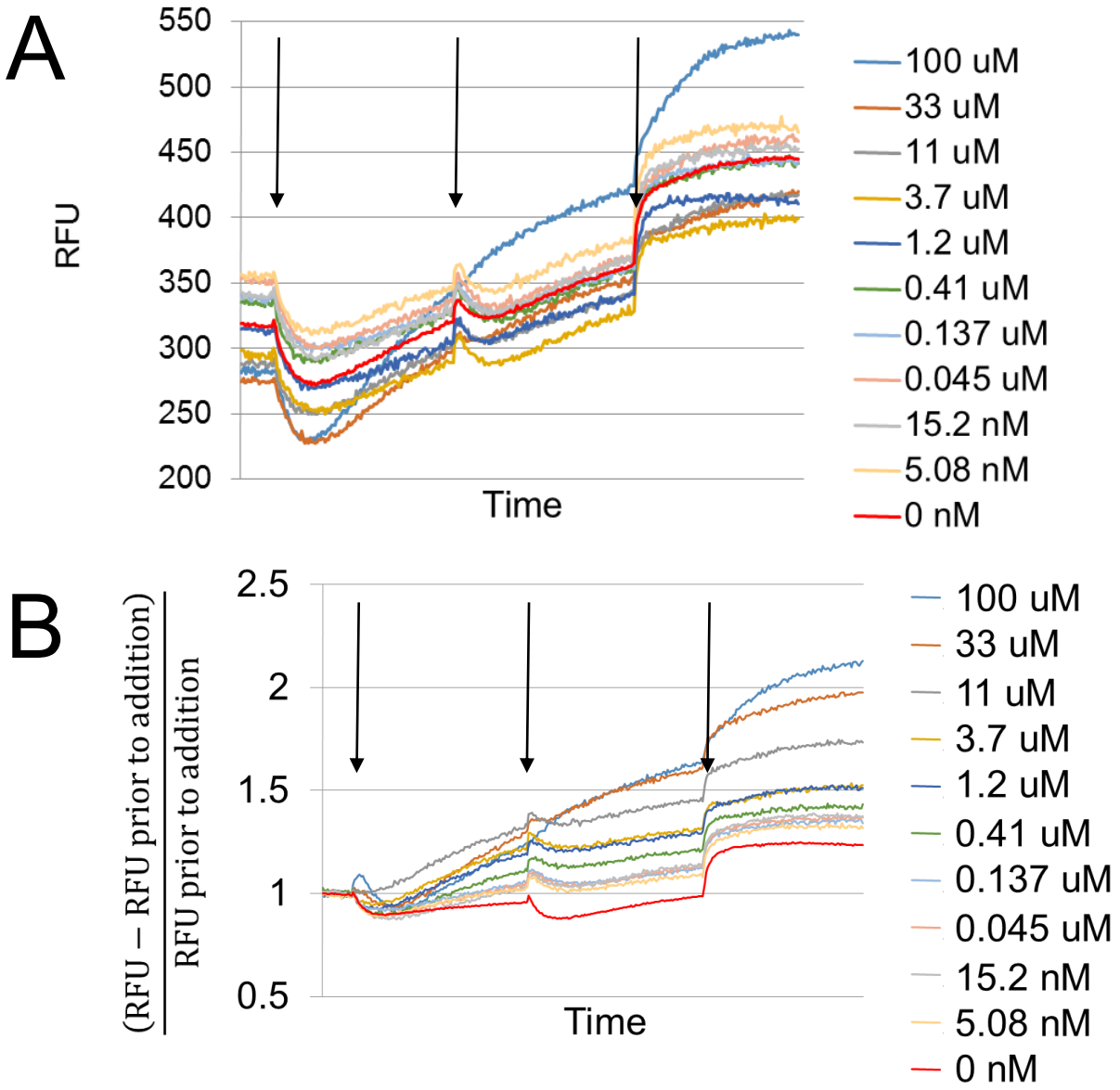

Figure 33. Raw HTS data from Activator screen plotted for reanalysis. A. Triple-add fluorescence data concentration response curve for compound A13 on plate CRC4. The raw data from A13 demonstrates the downward deflection after the first addition, and the drifting base line. The black arrows indicate, moving from left to right, the first, compound addition, second, EC_{20} (100 nM), and third, EC_{80} (10μM), additions of the triple add protocol. A13 was tested at 10 different concentrations and subjected to two choline chloride concentrations. B. Normalized triple-add fluorescence data from compound A13 on plate CRC4. Normalization of the raw data executed by determining the time point immediately prior each addition and subtracting the RFU of that time point from all of the subsequent time point up until the time point immediately prior to the next addition. This allowed each time segment to be normalized to the RFU value immediately prior to the respective addition.

demonstrated a similar downward deflection upon the first addition (data not shown). The second common characteristic found throughout out the data was the drifting base line, as seen in Figure 33 A. The base line from immediately after the first addition until the end of the assay continually increased in RFU meaning that after each addition the RFU did not flat line, or return to a base line equal seen prior to the most recent addition. In attempts to remove the confounding effects of the shifting baseline and more analytically review the data, the raw data was normalized to the RFU value immediately prior to the subsequent addition giving each addition its own baseline. The RFU baseline was subtracted from the subsequent data points and the divided by that baseline to give a ratio. This ratio normalized all of the data to its own starting RFU values.

Conclusions

The activator portion of the HTS proved much more difficult to design with certainty as there is no known activator of CHT, leaving us without a positive control. For this and other reasons, we focused on the hits that effects the second addition in our HTS assay as we would have greater range to see an activation without risking a ceiling effect. According to the HTS and the analysis performed by JHICC, we successfully identified CHT activator hits. Unfortunately, we had a very low success rate for validating those hits in a laboratory setting. We did identify one compound RBV that had some capacity to activate CHT function *in vitro* and may be a starting point for further SAR to create a robust CHT activator.

After the HTS activator hits did not validate, Dr. Blakely and I decided to review the individual traces for 200 of the compounds that were deemed activators. These traces revealed numerous caveats in the fluorescence assay used in the HTS and gained a deeper appreciation for the need of a positive control. The first of these caveats were that the addition of compound frequently caused a decrease in the fluorescence which we concluded was an artifact from fluid movement, but regardless further confounded the data analysis. The conclusion that the decrease in fluorescence was an artifact was later confirmed by observing the phenomena in the parental cell line (data not shown). The second caveat was that a considerable number of the traces showed a shifting base line after the addition of either compound or choline which confounded the interpretation of the effects of the compounds. The increases in the base line could potentially to mask the choline induced increase in RFU after the second and third additions that would indicate a CHT activator. Additionally, the continually increase in base line throughout the assay could be explained by a persistent disruption in the ion flow through CHT regardless of the choline transport status. As CHT is known to be electrogenic, the question to whether the two transport functions of CHT could be isolated, ion flow and choline transport, arose with the analysis of the HTS results. We continued to mine the raw data in attempts to find a starting point for discovery a CHT activator but resources, and time constraints forced us to focus on the inhibitor portion of this research project. The data may still hold potential leads for CHT activators, though I would advise starting with the group 2 inhibitors instead as diversification of that group we revealed a set of compounds that activated HACU to a great extent than RBV, though with similar inconsistencies.

APPENDIX III

INVESTIGATION OF THE UTILITY OF CHT INHIBITORS AS NOVEL THERAPUETICS IN DYSTONIA THROUGH THE USE OF THE DYT1 MOUSE LINE OF DYSTONIA

Introduction

Dystonia is described as a heterogeneous collection of movement disorders characterized by involuntary movements and postures without overt signs of neurodegeneration. The involuntary movement and postures have been described as “prolonged, involuntary twisting movements”(Liang, Tanabe, Jou, Chi, & Dauer, 2014) that are “typically patterned, twisting, and may be tremulous” with “muscle contractions that may be slow or rapid, but are sustained at the peak of movement” that can be exacerbated with voluntary movement and are associated with overflow muscle activation (Camargo, Camargos, Cardoso, & Teive, 2015; Eskow Jaunarajs, Bonsi, Chesselet, Standaert, & Pisani, 2015). Though the general motor deficits presented in dystonias are similar, the etiology, regional presentation throughout the body, the age at which the disorder first presents, and severity are quite diverse (Jinnah, Teller, & Galpern, 2015). Dystonias are broadly divided into two classifications, primary and secondary, for the dystonias that occur in isolation and that occur due to some previous CNS damage, respectively (Camargo et al., 2015). Secondary dystonias have been caused by stroke, trauma, or neurodegeneration and are often accompanied by additional neurological

symptoms (Liang et al., 2014). Unlike secondary dystonias, the cause of primary dystonias is diverse and still not well understood.

A century has passed since Oppenheim described early onset dystonia in 1911(Klein & Fahn, 2013). Unlike other neuroses being described at this time, dystonia only presented with muscular abnormalities and lacked the psychological abnormalities seen in diseases such as Parkinson's disease. Despite the bias towards physical symptoms, dystonia was largely treated as a psychological disorder until the 1950's when surgical treatments demonstrated an influence on symptoms. Since then, a standard of treatment for dystonia has been based around anticholinergic therapeutics the anticholinergics such as trihexylphenidyl, benztropine, and botulinum toxin (Costa et al., 2005). Currently, there is a wide range of options for treatment of dystonia that include anticholinergic drugs, botulinum toxin, antidopaminergic drugs, deep brain stimulation and transcraninal magnetic stimulation and yet complete remediation of the symptoms has yet to be achieved (Adam & Jankovic, 2007; Truong, 2012). Recent research has attempted to create both face valid and construct valid animal models of dystonia, and use these to identify the causes of dystonia and to discover novel mechanisms to cure and treat the disease.

DYT1 Dystonia

Though many of the treatments for dystonia are not specific to the type of the disorder (Jankovic, 2013), we choose to focus on a primary form of dystonia, DYT1 dystonia, due to preliminary data associating it with the cholinergic system though HC-3, and the availability of a mouse model to use in pharmacological studies with ML352.

DYT1 dystonia is a common inherited form of primary dystonia that is defined by a single 3 base pair (bp) in-frame mutation in the TOR1A gene though the presence of this mutation only results in a 30 percent disease penetrance. The 3 bp mutation results in the removal of a single glutamic acid (E) residue in the torsinA protein, a ubiquitously expressed AAA^+ protein shown to play a role in protein folding, and DA signaling (Granata & Warner, 2010). DYT1 is uniquely defined by the E deletion in the TOR1A gene but also two unique clinical characteristics. Patients with DYT1 dystonia have an onset of symptoms before the age of twenty, and an initial onset of symptoms in the limbs (Camargo et al., 2015).

Mouse Models of Dystonia

Creation of construct valid mouse models of dystonia, including the DYT1 knock-in, and DYT1 overexpresser, immediately brought to the forefront to a familiar circuit that has been long implicated in the pathophysiology of dystonia, i.e. the dopaminergic-cholinergic pathways of the striatum (Grundmann et al., 2012). Brain slice recordings from these models measuring long tern depression (LTD) revealed abnormalities in both dopaminergic and cholinergic signaling that are normalized by lessening cholinergic tone through the application of hemicholinium-3 (HC-3), a high affinity choline transporter (CHT) inhibitor, as well as by muscarinic M1 acetylcholine receptor antagonists (Martella et al., 2014; Martella et al., 2009). These mouse models also demonstrate molecular abnormalities in the dopaminergic-cholinergic pathways that may be part of the development of the symptoms seen in dystonia. However, these construct valid models do not have dramatic neuromuscular phenotypes, and thus they lack a relevant readout

to validate drug effects, and invite skepticism as to whether they serve as appropriate models for novel drug development.

Chemical lesion-induced animal models of dystonia or parkinsonian-like neuromuscular phenotypes have been created and equip researchers with a means to measure the therapeutic utility of the compounds (Jackson, Swart, Pearce, & Jenner, 2014; Tillerson, Caudle, Reveron, & Miller, 2002). Models such as the MPTP-treated marmoset have been shown to successfully respond to anticholinergic and pro-dopaminergic therapeutics. However, the current anticholinergic medications exhibit a small window between efficacy and dose-limiting side effects. In summary, treatment of dystonia via the dopaminergic-cholinergic pathway is molecularly validated and somewhat effective for symptom control. Thus, with drugs that modulate the system with a higher degree of finesse, the treatment of dystonia may reach new levels of efficacy and limit adverse consequences.

Recently, a new model of DYT1 dystonia, the N-SKI model, has demonstrated similar phenotypic behaviors as seen in the human form of the disease that were significant enough for them to be quantified and potentially pharmacologically reversed. The DYT1 N-SKI mouse line was produced by Dr. William Dauer's laboratory by crossing a mouse whose *Tor1a* gene was floxed to a mouse heterozygous for the ΔE *Tor1a* mutation that also expressed Cre in CNS specific cells using the nestin promoter (Liang et al., 2014). This cross provides mutant mice whose CNS cells contain only a ΔE mutation copy of the *Tor1a* protein, $Tor1a^{+/\Delta E}$ Cre^{+}. The N-SKI mice did not present with any spontaneous phenotypes seen in previous DYT1 dystonia models, such as squinty eyes or hind paw twisting, but did show phenotypic "hind and forelimb clasping, forepaw

clenching, and twisted truncal postures" while in tail suspension (Liang et al., 2014) that were quantifiable.

Utilizing DTY1 Mouse Model to Obtain Proof-of-concept Data for the use of CHT Inhibitors as Novel Therapeutics

We hope to validate CHT as a target for the development of novel therapeutics for the treatment of dystonia and other movement disorders. Although a reduction in cholinergic tone at first blush might not be considered to have therapeutic benefit, due to the broad influence of cholinergic signaling, the treatment history of dystonia would argue the contrary. The balance of cholinergic tone with other, mainly dopaminergic, inputs may assist in disease management. As CHT is expressed on all known cholinergic terminals, attenuation of cholinergic signaling with CHT inhibitors might reasonably be considered to be too blunt, or "not a novel" pathway to have additional therapeutic benefit compared to its anticholinergic predecessors. However, unlike muscarinic acetylcholine receptor antagonists and botulinum toxin, which influence the overall tone of ACh signaling, CHT supports cholinergic signaling in an activity-dependent manner, established by its high steady-state localization on synaptic vesicles and activity-dependent insertion into the plasma membrane. Thus, targeting CHT may avoid the spectrum of adverse consequences of current anticholinergic therapeutics that act at their targets continually regardless of state of cholinergic activation. It is possible that a CHT antagonist, because of its unique mechanistic actions described above, could provide for a more nuanced modulation of cholinergic signaling for the treatment of dystonia and other movement disorders. This Appendix describes our current efforts to establish a research program

and the future direction necessary to investigate the utility of CHT inhibitors to reverse the physiological symptoms seen in the DYT1 dystonia mouse line.

Materials and Methods

Breeding DYT1 Dystonia Mouse Line

Breeders from the DYT1 dystonia mouse line were graciously given to us by Dr. William Dauer's laboratory. These mice were mated to produce the correct breeding pairs, mouse 1: $Tor1a^{+/\Delta E}$ Cre^{+} with mouse 2: $Tor1a^{flox/+}$. Mouse 1 was heterozygous for flox while Mouse 2 was heterozygous for both the Cre and the ΔE. Mated together these mice produces the genotypes below:

1. $Tor1a^{+/+}$
2. $Tor1a^{flox/+}$ (WILD TYPE)
3. $Tor1a^{+/\Delta E}$ (WILD TYPE/ΔE)
4. $Tor1a^{flox/\Delta E}$
5. Tor1a+/+ Cre^{+}
6. $Tor1a^{flox/+}$ Cre^{+} (Cre ctrl)
7. $Tor1a^{+/\Delta E}$ Cre^{+}
8. $Tor1a^{flox/\Delta E}$ Cre^{+} (SKI)

Genotyping of the DYT1 Dystonia Mouse Line

Mice were tagged with metal ear tags while a 1mM tail clipping was taken for genotyping. The tail clippings were prepped using a REDRxtract-N-Amp™ Tissue PCR Kit (Sigma-aldrich). To the 1.7 mL microcentrifuge tube containing the tail clipping, 40uL of the Extraction Solution and 10uL of the Tissue Preparation Solution were added, vortexed, briefly spun down in a table top centrifuge, and incubated at room temperature for 10 minutes. Upon completion of the 10-minute incubation, the tubes incubated at 95°C

for 3 minutes. Immediately after the 95ºC incubation, 40µL of the Neutralization Solution B was added to each tube. These prepped tails are now ready to provide DNA for use in subsequent polymerase chain reactions (PCR) based genotyping reactions.

There are eight oligonucleotide primers that complete three PCR reactions necessary for the genotyping of the DYT1 mice. These primers are listed as they would be found in the Blakely oligo archive in Table 8. The PCR reactions for the genotyping followed the recipe below.

10µL 2x-Red Taq
1µL 20µM primer stock (2µM final concentration)
1µL DNA from tail
8µL DNA/RNA free water

All stock solutions of primers were kept at 200 mM, and working solutions of the combinations of primers necessary for each of the PCR reaction were made up to be 20uM. Primers RB 5007, 5008, 5009, and 5010 were combined for the Cre PCR primer stock. Primers RB 5011, 5012, and 5013 were combined for the flox PCR primer stock. Primers RB 5014, and RB 5015 were combined for the Tor1a ΔE PCR primer stock.

The PCR program for the ΔE mutation genotyping is as follows,

1. 95ºC for 1 minutes
2. 95ºC for 15 seconds
3. 68ºC for 30 seconds
4. 72ºC for 30 seconds
5. Repeat steps 2-4 37 times
6. 72ºC for 10 minutes
7. 4ºC forever

The PCR program for Cre and flox genotyping is as follows,

1. 94ºC for 3 minutes
2. 94ºC for 30 seconds
3. 55ºC for 30 seconds

4. 72ºC for 30 seconds
5. Repeat steps 2-4 33 times
6. 72ºC for 5 minutes
7. 4ºC forever

Acute Administration of ML352 to DYT1 Mutant and Wild Type

ML352 was formulated as described the Materials and Methods section of Chapter 4. Each mouse was weigh and injected with 1.5 mg/kg of ML352 at 10uL per gram body weight. The mouse rested for 10 minutes prior to being held by its tail for 2 minutes while the behavior was being recorded.

Results and Discussion

Genotyping of the DYT1 dystonia Mouse Line

The genotyping of the DTY1 dystonia mouse line was consistently successful. Though, the PCR reactions did fail when the primers had under gone several freeze thaw cycles and would produce faint bands and bands below the DNA ladder that were interpreted to be primer dimers (data not shown). A successful flox PCR reaction resulted in three bands that corresponded to the sizes of 154 base pairs (bp), 250bp, and 343bp representing the , flox, and KO genotypes respectively. A successful Cre PCR reaction resulted in two bands at 100bp and 324bp representing the Cre transgene and the internal positive control respectively. A successful Tor1a ΔE PCR reaction resulted in two bands at 300bp and 340bp representing the wild type Tor1a gene and the mutant Tor1a gene respectively.

Archive number	Primer use	Direction	Sequence
5007	Cre internal control	sense	GCGGTCTGGCAGTAAAAACTATC
5008	Cre internal control	antisense	GTGAAACAGCATTGCTGTCACTT
5009	Nestin cre forward	sense	CTAGGCCACAGAATTGAAAGATCT
5010	Nestin cre reverse	antisense	GTAGGTGGAAATTCTAGCATCATCC
5011	Tor1a lox gtF	sense	CCTGCCTCAGCCTAACTACG
5012	Tor1a frt gtF	sense	CAACAGAAAGCCCATTTGTCT
5013	Tor1a frt gtR	antisense	AGGCCTTGAATGACAACCAC
5014	mTOR Up	sense	AGTCTGTGGCTGGCTCTCCC
5015	mTOR down	antisense	CCTCAGGCTGCTCACAACCAC

Table 8. Primer sequences for the genontyping of the DYT1 dystonia mouse model.

Preliminary observations from acute administration of ML352 to DYT1 mutant and wild type littermate mice

Only one mutant mouse and one wild type littler mate has been injected with ML352 and recorded in the tail suspension protocol to date. These recordings when compared to the saline injections performed the day before and the day after the ML352 injection, reveal a significant increase in dystonic movements in both the wild type litter mate and the DYT1 mutant following drug injection. These observations were not blinded and made on a very small cohort but the effects of ML352 were quite dramatic.

Conclusions

A reduction in HACU, as with HC-3, should limit the availability of choline for presynaptic ChAT, thereby decreasing the synthesis and release of ACh. Although reducing ACh signaling can be hazardous, disorders such as DYT1 dystonia that present with excess cholinergic signaling may benefit from such a strategy. DYT1 dystonia is a common form of primary dystonia associated with the DYT1 mutation in the torsin1A, and characterized by abnormal involuntary contracting of musculature that causes twisting and turning of a patient's body. Though the specific process by which the disease develops is still unknown, dysfunction in sensory integration controlled by the basal ganglia has been implicated (Breakefield et al., 2008; Eskow Jaunarajs et al., 2015; Sciamanna, Tassone, et al., 2012). We are particularly interested in the use of novel CHT antagonists like ML352 for the treatment of dystonia, as both centrally and peripherally acting anticholinergics are already used in the clinic to relieve its symptoms (Jankovic,

2013; Patel & Martino, 2013), and CHT antagonism using HC-3 has proved effective in restoring alterations in synaptic plasticity in brain slices from a DYT1 dystonia mouse model (Martella et al., 2009; Sciamanna, Tassone, et al., 2012).

We pursed these goals through funding from the Dystonia Medical Research Foundation. Our first goal was to establish a colony of the murine disease model of DYT1 dystonia. With the mice from this colony and the data from the characterization of ML352, we then would able to administer ML352 to DYT1 mutant mice at a sub lethal dose that would reach a therapeutically relevant level in the brain. Unfortunately, the breeding paradigm to create a colony large enough to conduct well controlled experiments to determine the effects of ML352 on the symptoms presented by the DYT1 dystonia line have proved a time consuming process and have yet to provide enough mutant mice for these experiments. The preliminary injections of ML352 into DYT1 mutant mice and their wild type littermates foreshadowed an exacerbation of effects in both genotypes instead of an amelioration. This result suggested unexpected but may be a result of the ability of ML352 to increase the surface expression of CHT, data obtained in a heterologous expression system and possibly thereby a switching in the action of ML352 from inhibitor to activator in an *in vivo* setting. Although, it would be unfortunate if ML352 was unable to reverse the symptoms of DYT1, it would not mean all CHT inhibitors would be subject to this fate. Other CHT inhibitors, that are yet to be characterized within the other structural classes identified by the HTS, and SAR studies, could retain the ability to inhibit CHT without stabilizing CHT in a conformation that increased CHT surface expression.

The DYT1 dystonia research program that we have initiated is still in its infancy and has yet to answer the questions we proposed. Though, with the information provided

here and additional time, the utility of CHT inhibitors in hypercholinergic diseases could be determined. We are grateful to the DMRF for funding of our effort to test the potential therapeutic utility of CHT inhibitors in a preclinical model.

REFERENCES

Adam, O. R., & Jankovic, J. (2007). Treatment of dystonia. *Parkinsonism Relat Disord, 13 Suppl 3*, S362-368. doi:10.1016/S1353-8020(08)70031-2

Alder, J. T., Chessell, I. P., & Bowen, D. M. (1995). A neurochemical approach for studying response to acetylcholine in Alzheimer's disease. *Neurochem Res, 20*(7), 769-771.

Alt, A., Pendri, A., Bertekap, R. L., Li, G., Benitex, Y., Nophsker, M., . . . Macor, J. E. (2015). Evidence for classical cholinergic toxicity associated with selective activation of M1 muscarinic receptors. *J Pharmacol Exp Ther*. doi:10.1124/jpet.115.226910

Amara, S. G. (1992). Neurotransmitter transporters. A tale of two families. *Nature, 360*(6403), 420-421. doi:10.1038/360420d0

Ansell, G. B., & Spanner, S. G. (1974). The inhibition of brain choline kinase by hemicholinium-3. *J Neurochem, 22*(6), 1153-1155.

Apparsundaram, S., Ferguson, S. M., & Blakely, R. D. (2001). Molecular cloning and characterization of a murine hemicholinium-3-sensitive choline transporter. *Biochem Soc Trans, 29*(Pt 6), 711-716.

Apparsundaram, S., Ferguson, S. M., George, A. L., Jr., & Blakely, R. D. (2000). Molecular cloning of a human, hemicholinium-3-sensitive choline transporter. *Biochem Biophys Res Commun, 276*(3), 862-867. doi:10.1006/bbrc.2000.3561

Apparsundaram, S., Martinez, V., Parikh, V., Kozak, R., & Sarter, M. (2005a). Increased capacity and density of choline transporters situated in synaptic membranes of the right medial prefrontal cortex of attentional task-performing rats. *J. Neurosci., 25*(15), 3851-3856. doi:10.1523/JNEUROSCI.0205-05.2005

Apparsundaram, S., Martinez, V., Parikh, V., Kozak, R., & Sarter, M. (2005b). Increased capacity and density of choline transporters situated in synaptic membranes of the right medial prefrontal cortex of attentional task-performing rats. *J Neurosci, 25*(15), 3851-3856. doi:10.1523/JNEUROSCI.0205-05.2005

Bales, K. R., Tzavara, E. T., Wu, S., Wade, M. R., Bymaster, F. P., Paul, S. M., & Nomikos, G. G. (2006). Cholinergic dysfunction in a mouse model of Alzheimer

disease is reversed by an anti-A beta antibody. *J Clin Invest, 116*(3), 825-832. doi:10.1172/JCI27120

Barlow, R. B., & Ing, H. R. (1948). Curare-like action of polymethylene bis-quaternary ammonium salts. *Br J Pharmacol Chemother, 3*(4), 298-304.

Barwick, K. E., Wright, J., Al-Turki, S., McEntagart, M. M., Nair, A., Chioza, B., . . . Crosby, A. H. (2012). Defective presynaptic choline transport underlies hereditary motor neuropathy. *Am J Hum Genet, 91*(6), 1103-1107. doi:10.1016/j.ajhg.2012.09.019

Bazalakova, M. H., & Blakely, R. D. (2006). The high-affinity choline transporter: a critical protein for sustaining cholinergic signaling as revealed in studies of genetically altered mice. *Handb Exp Pharmacol*(175), 525-544.

Bazalakova, M. H., Wright, J., Schneble, E. J., McDonald, M. P., Heilman, C. J., Levey, A. I., & Blakely, R. D. (2007). Deficits in acetylcholine homeostasis, receptors and behaviors in choline transporter heterozygous mice. *Genes Brain Behav, 6*(5), 411-424. doi:10.1111/j.1601-183X.2006.00269.x

Benishin, C. G., & Carroll, P. T. (1983). Multiple forms of choline-O-acetyltransferase in mouse and rat brain: solubilization and characterization. *J Neurochem, 41*(4), 1030-1039.

Berry, A. S., Blakely, R. D., Sarter, M., & Lustig, C. (2015). Cholinergic capacity mediates prefrontal engagement during challenges to attention: evidence from imaging genetics. *Neuroimage, 108*, 386-395. doi:10.1016/j.neuroimage.2014.12.036

Berry, A. S., Demeter, E., Sabhapathy, S., English, B. A., Blakely, R. D., Sarter, M., & Lustig, C. (2014). Disposed to distraction: genetic variation in the cholinergic system influences distractibility but not time-on-task effects. *J Cogn Neurosci, 26*(9), 1981-1991. doi:10.1162/jocn_a_00607

Bessho, T., Takashina, K., Eguchi, J., Komatsu, T., & Saito, K. (2008). MKC-231, a choline-uptake enhancer: (1) long-lasting cognitive improvement after repeated administration in AF64A-treated rats. *J Neural Transm (Vienna), 115*(7), 1019-1025. doi:10.1007/s00702-008-0053-4

Bessho, T., Takashina, K., Tabata, R., Ohshima, C., Chaki, H., Yamabe, H., . . . Saito, K. (1996). Effect of the novel high affinity choline uptake enhancer 2-(2-oxopyrrolidin-1-yl)-N-(2,3-dimethyl-5,6,7,8-tetrahydrofuro[2,3-b] quinolin-4-yl)acetoamide on deficits of water maze learning in rats. *Arzneimittelforschung, 46*(4), 369-373.

Birks, R. I., & Macintosh, F. C. (1957). Acetylcholine metabolism at nerve-endings. *Br Med Bull, 13*(3), 157-161.

Birks, R. I., Macintosh, F. C., & Sastry, P. B. (1956). Pharmacological inhibition of acetylcholine synthesis. *Nature, 178*(4543), 1181.

Black, S. A., Ribeiro, F. M., Ferguson, S. S., & Rylett, R. J. (2010). Rapid, transient effects of the protein kinase C activator phorbol 12-myristate 13-acetate on activity and trafficking of the rat high-affinity choline transporter. *Neurosci., 167*(3), 765-773. doi:10.1016/j.neuroscience.2010.02.026

Bligh, J. (1952). The level of free choline in plasma. *J Physiol, 117*(2), 234-240.

Bollinger, S. R., Engers, D. W., Ennis, E. A., Wright, J., Locuson, C. W., Lindsley, C. W., . . . Hopkins, C. R. (2015). Synthesis and structure-activity relationships of a series of 4-methoxy-3-(piperidin-4-yl)oxy benzamides as novel inhibitors of the presynaptic choline transporter. *Bioorg Med Chem Lett, 25*(8), 1757-1760. doi:10.1016/j.bmcl.2015.02.058

Bonsi, P., Martella, G., Cuomo, D., Platania, P., Sciamanna, G., Bernardi, G., . . . Pisani, A. (2008). Loss of muscarinic autoreceptor function impairs long-term depression but not long-term potentiation in the striatum. *J Neurosci, 28*(24), 6258-6263. doi:10.1523/JNEUROSCI.1678-08.2008

Brandon, E. P., Lin, W., D'Amour, K. A., Pizzo, D. P., Dominguez, B., Sugiura, Y., . . . Lee, K. F. (2003). Aberrant patterning of neuromuscular synapses in choline acetyltransferase-deficient mice. *J Neurosci, 23*(2), 539-549.

Breakefield, X. O., Blood, A. J., Li, Y., Hallett, M., Hanson, P. I., & Standaert, D. G. (2008). The pathophysiological basis of dystonias. *Nat Rev Neurosci, 9*(3), 222-234. doi:10.1038/nrn2337

Breer, H., Knipper, M., & Kahle, C. (1989). High-affinity choline transporter in synaptosmal membranes. *J Protein Chem, 8*(3), 372-374.

Breer, H., Morris, S. J., & Whittaker, V. P. (1977). Adenosine triphosphatase activity associated with purified cholinergic synaptic vesicles of Torpedo marmorata. *Eur J Biochem, 80*(1), 313-318.

Broer, S., & Gether, U. (2012). The solute carrier 6 family of transporters. *Br J Pharmacol, 167*(2), 256-278. doi:10.1111/j.1476-5381.2012.01975.x

Brunello, N., Cheney, D. L., & Costa, E. (1982). Increase in exogenous choline fails to elevate the content or turnover rate of cortical, striatal, or hippocampal acetylcholine. *J Neurochem, 38*(4), 1160-1163.

Camargo, C. H., Camargos, S. T., Cardoso, F. E., & Teive, H. A. (2015). The genetics of the dystonias--a review based on the new classification of the dystonias. *Arq Neuropsiquiatr, 73*(4), 350-358. doi:10.1590/0004-282X20150030

Clark, A. J. (1926a). The antagonism of acetyl choline by atropine. *J Physiol, 61*(4), 547-556.

Clark, A. J. (1926b). The reaction between acetyl choline and muscle cells. *J Physiol, 61*(4), 530-546.

Cohen, E. L., & Wurtman, R. J. (1976). Brain acetylcholine: control by dietary choline. *Science, 191*(4227), 561-562.

Collier, B., & Katz, H. S. (1974). Acetylcholine synthesis from recaptured choline by a sympathetic ganglion. *J Physiol, 238*(3), 639-655.

Conn, P. J., Lindsley, C. W., Meiler, J., & Niswender, C. M. (2014). Opportunities and challenges in the discovery of allosteric modulators of GPCRs for treating CNS disorders. *Nat Rev Drug Discov, 13*(9), 692-708. doi:10.1038/nrd4308

Costa, J., Espirito-Santo, C., Borges, A., Ferreira, J. J., Coelho, M., & Sampaio, C. (2005). Botulinum toxin type A versus anticholinergics for cervical dystonia. *Cochrane Database Syst Rev*(1), CD004312. doi:10.1002/14651858.CD004312.pub2

Crooks, P. A., Ayers, J. T., Xu, R., Sumithran, S. P., Grinevich, V. P., Wilkins, L. H., . . . Dwoskin, L. P. (2004). Development of subtype-selective ligands as antagonists at nicotinic receptors mediating nicotine-evoked dopamine release. *Bioorg Med Chem Lett, 14*(8), 1869-1874. doi:10.1016/j.bmcl.2003.10.074

Cuddy, L. K., Gordon, A. C., Black, S. A., Jaworski, E., Ferguson, S. S., & Rylett, R. J. (2012). Peroxynitrite donor SIN-1 alters high-affinity choline transporter activity by modifying its intracellular trafficking. *J Neurosci, 32*(16), 5573-5584. doi:10.1523/JNEUROSCI.5235-11.2012

Cuddy, L. K., Winick-Ng, W., & Rylett, R. J. (2014). Regulation of the high-affinity choline transporter activity and trafficking by its association with cholesterol-rich lipid rafts. *J Neurochem, 128*(5), 725-740. doi:10.1111/jnc.12490

Dale, H. H. (1906). On some physiological actions of ergot. *J Physiol, 34*(3), 163-206.

Dale, H. H., Laidlaw, P. P., & Symons, C. T. (1910). A reversed action of the vagus on the mammalian heart. *J Physiol, 41*(1-2), 1-18.

Davis, E. (1931). Relations between the actions of adrenaline, acetylcholine, and ions, on the perfused heart. *J Physiol, 71*(4), 431-441.

Diamond, I., & Kennedy, E. P. (1969). Carrier-mediated transport of choline into synaptic nerve endings. *J Biol Chem, 244*(12), 3258-3263.

Diaz-Moran, S., Palencia, M., Mont-Cardona, C., Canete, T., Blazquez, G., Martinez-Membrives, E., . . . Fernandez-Teruel, A. (2013). Gene expression in hippocampus as a function of differential trait anxiety levels in genetically heterogeneous NIH-HS rats. *Behav Brain Res, 257*, 129-139. doi:10.1016/j.bbr.2013.09.041

Dong, Y., Dani, J. A., & Blakely, R. D. (2013). Choline transporter hemizygosity results in diminished basal extracellular dopamine levels in nucleus accumbens and blunts dopamine elevations following cocaine or nicotine. *Biochem Pharmacol, 86*(8), 1084-1088. doi:10.1016/j.bcp.2013.07.019

Doody, R. S. (2003). Current treatments for Alzheimer's disease: cholinesterase inhibitors. *J Clin Psychiatry, 64 Suppl 9*, 11-17.

Drevets, W. C., Zarate, C. A., Jr., & Furey, M. L. (2013). Antidepressant effects of the muscarinic cholinergic receptor antagonist scopolamine: a review. *Biol Psychiatry, 73*(12), 1156-1163. doi:10.1016/j.biopsych.2012.09.031

Dudley, H. W. (1929). Observations on acetylcholine. *Biochem J, 23*(5), 1064-1074.

English, B. A., Appalsamy, M., Diedrich, A., Ruggiero, A. M., Lund, D., Wright, J., . . . Blakely, R. D. (2010). Tachycardia, reduced vagal capacity, and age-dependent ventricular dysfunction arising from diminished expression of the presynaptic choline transporter. *Am J Physiol Heart Circ Physiol, 299*(3), H799-810. doi:10.1152/ajpheart.00170.2010

English, B. A., Hahn, M. K., Gizer, I. R., Mazei-Robison, M., Steele, A., Kurnik, D. M., . . . Blakely, R. D. (2009). Choline transporter gene variation is associated with attention-deficit hyperactivity disorder. *J Neurodev Disord, 1*(4), 252-263. doi:10.1007/s11689-009-9033-8

Ennis, E. A., Wright, J., Retzlaff, C. L., McManus, O. B., Lin, Z., Huang, X., . . . Blakely, R. D. (2015). Identification and characterization of ML352: a novel, noncompetitive inhibitor of the presynaptic choline transporter. *ACS Chem. Neurosci., Just Accepted, Publication Date: January 5, 2015*, 10.1021/cn5001809. doi:cn-2014-001809

Ennis, E. A., Wright, J., Retzlaff, C. L., McManus, O. B., Lin, Z., Huang, X., . . . Blakely, R. D. (2015). Identification and characterization of ML352: a novel, noncompetitive inhibitor of the presynaptic choline transporter. *ACS Chem Neurosci, 6*(3), 417-427. doi:10.1021/cn5001809

Eskow Jaunarajs, K. L., Bonsi, P., Chesselet, M. F., Standaert, D. G., & Pisani, A. (2015). Striatal cholinergic dysfunction as a unifying theme in the pathophysiology of dystonia. *Prog Neurobiol, 127-128*, 91-107. doi:10.1016/j.pneurobio.2015.02.002

Feldberg, W., & Mann, T. (1946). Properties and distribution of the enzyme system which synthesizes acetylcholine in nervous tissue. *J Physiol, 104*(4), 411-425.

Ferguson, S. M., Bazalakova, M., Savchenko, V., Tapia, J. C., Wright, J., & Blakely, R. D. (2004). Lethal impairment of cholinergic neurotransmission in hemicholinium-3-sensitive choline transporter knockout mice. *Proc Natl Acad Sci U S A, 101*(23), 8762-8767. doi:10.1073/pnas.0401667101

Ferguson, S. M., & Blakely, R. D. (2004). The choline transporter resurfaces: new roles for synaptic vesicles? *Mol Interv, 4*(1), 22-37. doi:10.1124/mi.4.1.22

Ferguson, S. M., Savchenko, V., Apparsundaram, S., Zwick, M., Wright, J., Heilman, C. J., . . . Blakely, R. D. (2003a). Vesicular localization and activity-dependent trafficking of presynaptic choline transporters. *J Neurosci, 23*(30), 9697-9709.

Ferguson, S. M., Savchenko, V., Apparsundaram, S., Zwick, M., Wright, J., Heilman, C. J., . . . Blakely, R. D. (2003b). Vesicular localization and activity-dependent trafficking of presynaptic choline transporters. *J. Neurosci., 23*(30), 9697-9709.

Fishwick, K. J., & Rylett, R. J. (2015). Insulin Regulates the Activity of the High-Affinity Choline Transporter CHT. *PLoS One, 10*(7), e0132934. doi:10.1371/journal.pone.0132934

Garguilo, M. G., & Michael, A. C. (1996). Amperometric microsensors for monitoring choline in the extracellular fluid of brain. *J Neurosci Methods, 70*(1), 73-82. doi:10.1016/S0165-0270(96)00105-7

Gates, J., Jr., Ferguson, S. M., Blakely, R. D., & Apparsundaram, S. (2004a). Regulation of choline transporter surface expression and phosphorylation by protein kinase C and protein phosphatase 1/2A. *J Pharmacol Exp Ther, 310*(2), 536-545. doi:10.1124/jpet.104.066795

Gates, J., Jr., Ferguson, S. M., Blakely, R. D., & Apparsundaram, S. (2004b). Regulation of choline transporter surface expression and phosphorylation by protein kinase C and protein phosphatase 1/2A. *J. Pharmacol. Exp. Ther., 310*(2), 536-545. doi:10.1124/jpet.104.066795

Giboureau, N., Som, I. M., Boucher-Arnold, A., Guilloteau, D., & Kassiou, M. (2010). PET radioligands for the vesicular acetylcholine transporter (VAChT). *Curr Top Med Chem, 10*(15), 1569-1583.

Granata, A., & Warner, T. T. (2010). The role of torsinA in dystonia. *Eur J Neurol, 17 Suppl 1*, 81-87. doi:10.1111/j.1468-1331.2010.03057.x

Grundmann, K., Glockle, N., Martella, G., Sciamanna, G., Hauser, T. K., Yu, L., . . . Ott, T. (2012). Generation of a novel rodent model for DYT1 dystonia. *Neurobiol Dis, 47*(1), 61-74. doi:10.1016/j.nbd.2012.03.024

Grutzendler, J., & Morris, J. C. (2001). Cholinesterase inhibitors for Alzheimer's disease. *Drugs, 61*(1), 41-52.

Guastella, J., Nelson, N., Nelson, H., Czyzyk, L., Keynan, S., Miedel, M. C., . . . Kanner, B. I. (1990). Cloning and expression of a rat brain GABA transporter. *Science, 249*(4974), 1303-1306.

Guidry, G., Willison, B. D., Blakely, R. D., Landis, S. C., & Habecker, B. A. (2005). Developmental expression of the high affinity choline transporter in cholinergic sympathetic neurons. *Auton Neurosci, 123*(1-2), 54-61. doi:10.1016/j.autneu.2005.10.001

Guimbal, C., & Kilimann, M. W. (1993). A Na(+)-dependent creatine transporter in rabbit brain, muscle, heart, and kidney. cDNA cloning and functional expression. *J Biol Chem, 268*(12), 8418-8421.

Haga, T. (2014). Molecular properties of the high-affinity choline transporter CHT1. *J Biochem, 156*(4), 181-194. doi:10.1093/jb/mvu047

Haga, T., & Noda, H. (1973). Choline uptake systems of rat brain synaptosomes. *Biochim Biophys Acta, 291*(2), 564-575.

Hahn, M. K., Blackford, J. U., Haman, K., Mazei-Robison, M., English, B. A., Prasad, H. C., . . . Shelton, R. (2008). Multivariate permutation analysis associates multiple polymorphisms with subphenotypes of major depression. *Genes Brain Behav, 7*(4), 487-495. doi:10.1111/j.1601-183X.2007.00384.x

Happe, H. K., & Murrin, L. C. (1992). Development of high-affinity choline transport sites in rat forebrain: a quantitative autoradiography study with [3H]hemicholinium-3. *J Comp Neurol, 321*(4), 591-611. doi:10.1002/cne.903210407

Happe, H. K., & Murrin, L. C. (1993). High-affinity choline transport sites: use of [3H]hemicholinium-3 as a quantitative marker. *J Neurochem, 60*(4), 1191-1201.

Harrington, A. M., Hutson, J. M., & Southwell, B. R. (2007). High affinity choline transporter immunoreactivity in rat ileum myenteric nerves. *Cell Tissue Res, 327*(3), 421-431. doi:10.1007/s00441-006-0332-z

Hasselmo, M. E., & Sarter, M. (2011). Modes and models of forebrain cholinergic neuromodulation of cognition. *Neuropsychopharmacology, 36*(1), 52-73. doi:10.1038/npp.2010.104

Higley, M. J., & Picciotto, M. R. (2014). Neuromodulation by acetylcholine: examples from schizophrenia and depression. *Curr Opin Neurobiol, 29*, 88-95. doi:10.1016/j.conb.2014.06.004

Hodgkin, A. L., & Martin, K. (1965). Choline uptake by giant axons of Loligo. *J Physiol, 179(Suppl)*, 20P-47P.

Holmstrand, E. C., Asafu-Adjei, J., Sampson, A. R., Blakely, R. D., & Sesack, S. R. (2010). Ultrastructural localization of high-affinity choline transporter in the rat anteroventral thalamus and ventral tegmental area: differences in axon

morphology and transporter distribution. *J Comp Neurol, 518*(11), 1908-1924. doi:10.1002/cne.22310

Holmstrand, E. C., Lund, D., Cherian, A. K., Wright, J., Martin, R. F., Ennis, E. A., . . . Blakely, R. D. (2014). Transgenic overexpression of the presynaptic choline transporter elevates acetylcholine levels and augments motor endurance. *Neurochem Int, 73*, 217-228. doi:10.1016/j.neuint.2013.11.008

Hoover, D. B., Ganote, C. E., Ferguson, S. M., Blakely, R. D., & Parsons, R. L. (2004). Localization of cholinergic innervation in guinea pig heart by immunohistochemistry for high-affinity choline transporters. *Cardiovasc Res, 62*(1), 112-121. doi:10.1016/j.cardiores.2004.01.012

Issa, A. M., Gauthier, S., & Collier, B. (1996). Effects of the phosphatase inhibitors calyculin A and okadaic acid on acetylcholine synthesis and content of rat hippocampal formation. *J Neurochem, 66*(5), 1924-1932.

Iwamoto, H., Blakely, R. D., & De Felice, L. J. (2006). Na+, Cl-, and pH dependence of the human choline transporter (hCHT) in Xenopus oocytes: the proton inactivation hypothesis of hCHT in synaptic vesicles. *J Neurosci, 26*(39), 9851-9859. doi:10.1523/JNEUROSCI.1862-06.2006

Jackson, M. J., Swart, T., Pearce, R. K., & Jenner, P. (2014). Cholinergic manipulation of motor disability and L-DOPA-induced dyskinesia in 1-methyl-4-phenyl-1,2,3,6-tetrahydropyridine (MPTP)-treated common marmosets. *J Neural Transm, 121*(2), 163-169. doi:10.1007/s00702-013-1082-1

Jankovic, J. (2013). Medical treatment of dystonia. *Mov Disord, 28*(7), 1001-1012. doi:10.1002/mds.25552

Jinnah, H. A., Teller, J. K., & Galpern, W. R. (2015). Recent developments in dystonia. *Curr Opin Neurol, 28*(4), 400-405. doi:10.1097/WCO.0000000000000213

Jope, R. S., & Jenden, D. J. (1979). Choline and phospholipid metabolism and the synthesis of acetylcholine in rat brain. *J Neurosci Res, 4*(1), 69-82. doi:10.1002/jnr.490040110

Karczmar, A. G. (1993). Brief presentation of the story and present status of studies of the vertebrate cholinergic system. *Neuropsychopharmacology, 9*(3), 181-199. doi:10.1038/npp.1993.81

Karczmar, A. G. (1996). The Otto Loewi Lecture. Loewi's discovery and the XXI century. *Prog Brain Res, 109*, 1-27, xvii. doi:10.1016/S0079-6123(08)62084-1

King, R. G., & Marchbanks, R. M. (1982). The incorporation of solubilized choline-transport activity into liposomes. *Biochem J, 204*(2), 565-576.

Klein, C., & Fahn, S. (2013). Translation of Oppenheim's 1911 paper on dystonia. *Mov Disord, 28*(7), 851-862. doi:10.1002/mds.25546

Knipper, M., Boekhoff, I., & Breer, H. (1989). Isolation and reconstitution of the high-affinity choline carrier. *FEBS Lett, 245*(1-2), 235-237.

Knipper, M., Kahle, C., & Breer, H. (1991). Purification and reconstitution of the high affinity choline transporter. *Biochim Biophys Acta, 1065*(2), 107-113.

Kobayashi, Y., Okuda, T., Fujioka, Y., Matsumura, G., Nishimura, Y., & Haga, T. (2002). Distribution of the high-affinity choline transporter in the human and macaque monkey spinal cord. *Neurosci Lett, 317*(1), 25-28.

Koegelenberg, C. F., Noor, F., Bateman, E. D., van Zyl-Smit, R. N., Bruning, A., O'Brien, J. A., . . . Irusen, E. M. (2014). Efficacy of varenicline combined with nicotine replacement therapy vs varenicline alone for smoking cessation: a randomized clinical trial. *JAMA, 312*(2), 155-161. doi:10.1001/jama.2014.7195

Krishnaswamy, A., & Cooper, E. (2009). An activity-dependent retrograde signal induces the expression of the high-affinity choline transporter in cholinergic neurons. *Neuron, 61*(2), 272-286. doi:10.1016/j.neuron.2008.11.025

Kus, L., Borys, E., Ping Chu, Y., Ferguson, S. M., Blakely, R. D., Emborg, M. E., . . . Mufson, E. J. (2003). Distribution of high affinity choline transporter immunoreactivity in the primate central nervous system. *J Comp Neurol, 463*(3), 341-357. doi:10.1002/cne.10759

Liang, C. C., Tanabe, L. M., Jou, S., Chi, F., & Dauer, W. T. (2014). TorsinA hypofunction causes abnormal twisting movements and sensorimotor circuit neurodegeneration. *J Clin Invest, 124*(7), 3080-3092. doi:10.1172/JCI72830

Lin, W., Dominguez, B., Yang, J., Aryal, P., Brandon, E. P., Gage, F. H., & Lee, K. F. (2005). Neurotransmitter acetylcholine negatively regulates neuromuscular synapse formation by a Cdk5-dependent mechanism. *Neuron, 46*(4), 569-579. doi:10.1016/j.neuron.2005.04.002

Lips, K. S., Pfeil, U., Haberberger, R. V., & Kummer, W. (2002). Localisation of the high-affinity choline transporter-1 in the rat skeletal motor unit. *Cell Tissue Res, 307*(3), 275-280. doi:10.1007/s00441-002-0520-4

Low, D., & Chen, K. S. (2010). Genome-wide gene expression profiling of the Angelman syndrome mice with Ube3a mutation. *Eur J Hum Genet, 18*(11), 1228-1235. doi:10.1038/ejhg.2010.95

Lowenstein, P. R., & Coyle, J. T. (1986). Rapid regulation of [3H]hemicholinium-3 binding sites in the rat brain. *Brain Res, 381*(1), 191-194.

Lund, D., Ruggiero, A. M., Ferguson, S. M., Wright, J., English, B. A., Reisz, P. A., . . . Blakely, R. D. (2010). Motor neuron-specific overexpression of the presynaptic choline transporter: impact on motor endurance and evoked muscle activity. *Neuroscience, 171*(4), 1041-1053. doi:10.1016/j.neuroscience.2010.09.057

Macintosh, F. C., Birks, R. I., & Sastry, P. B. (1958). Mode of action of an inhibitor of acetylcholine synthesis. *Neurology, 8*(Suppl 1), 90-91.

Manaker, S., Wieczorek, C. M., & Rainbow, T. C. (1986). Identification of sodium-dependent, high-affinity choline uptake sites in rat brain with [3H]hemicholinium-3. *J Neurochem, 46*(2), 483-488.

Mandl, P., & Kiss, J. P. (2006). Inhibitory effect of hemicholinium-3 on presynaptic nicotinic acetylcholine receptors located on the terminal region of myenteric motoneurons. *Neurochem Int, 49*(4), 327-333. doi:10.1016/j.neuint.2006.03.001

Manganelli, F., Vitale, C., Santangelo, G., Pisciotta, C., Iodice, R., Cozzolino, A., . . . Santoro, L. (2009). Functional involvement of central cholinergic circuits and visual hallucinations in Parkinson's disease. *Brain, 132*(Pt 9), 2350-2355. doi:10.1093/brain/awp166

Marchbanks, R. M. (1968). The uptake of [14C] choline into synaptosomes in vitro. *Biochem J, 110*(3), 533-541.

Marchbanks, R. M. (1969). The conversion of 14C-choline to 14C-acetylcholine in synaptosomes in vitro. *Biochem Pharmacol, 18*(7), 1763-1766.

Marchbanks, R. M. (1982). The activation of presynaptic choline uptake by acetylcholine release. *J Physiol (Paris), 78*(4), 373-378.

Mark, G. P., Shabani, S., Dobbs, L. K., & Hansen, S. T. (2011). Cholinergic modulation of mesolimbic dopamine function and reward. *Physiol Behav, 104*(1), 76-81. doi:10.1016/j.physbeh.2011.04.052

Martella, G., Maltese, M., Nistico, R., Schirinzi, T., Madeo, G., Sciamanna, G., . . . Pisani, A. (2014). Regional specificity of synaptic plasticity deficits in a knock-in mouse model of DYT1 dystonia. *Neurobiol Dis, 65*, 124-132. doi:10.1016/j.nbd.2014.01.016

Martella, G., Tassone, A., Sciamanna, G., Platania, P., Cuomo, D., Viscomi, M. T., . . . Pisani, A. (2009). Impairment of bidirectional synaptic plasticity in the striatum of a mouse model of DYT1 dystonia: role of endogenous acetylcholine. *Brain, 132*(Pt 9), 2336-2349. doi:10.1093/brain/awp194

Martin, K. (1968). Concentrative accumulation of choline by human erythrocytes. *J Gen Physiol, 51*(4), 497-516.

Matthies, D. S., Fleming, P. A., Wilkes, D. M., & Blakely, R. D. (2006). The Caenorhabditis elegans choline transporter CHO-1 sustains acetylcholine synthesis and motor function in an activity-dependent manner. *J Neurosci, 26*(23), 6200-6212. doi:10.1523/JNEUROSCI.5036-05.2006

Mayser, W., Schloss, P., & Betz, H. (1992). Primary structure and functional expression of a choline transporter expressed in the rat nervous system. *FEBS Lett, 305*(1), 31-36.

Michel, V., Yuan, Z., Ramsubir, S., & Bakovic, M. (2006). Choline transport for phospholipid synthesis. *Exp Biol Med (Maywood), 231*(5), 490-504.

Mineur, Y. S., Obayemi, A., Wigestrand, M. B., Fote, G. M., Calarco, C. A., Li, A. M., & Picciotto, M. R. (2013). Cholinergic signaling in the hippocampus regulates social stress resilience and anxiety- and depression-like behavior. *Proc Natl Acad Sci U S A, 110*(9), 3573-3578. doi:10.1073/pnas.1219731110

Misawa, H., Fujigaya, H., Nishimura, T., Moriwaki, Y., Okuda, T., Kawashima, K., . . . Ohno, H. (2008). Aberrant trafficking of the high-affinity choline transporter in AP-3-deficient mice. *Eur J Neurosci, 27*(12), 3109-3117. doi:10.1111/j.1460-9568.2008.06268.x

Mulder, A. H., Yamamura, H. I., Kuhar, M. J., & Snyder, S. H. (1974). Release of acetylcholine from hippocampal slices by potassium depolarization: dependence on high affinity choline uptake. *Brain Res, 70*(2), 372-376.

Murai, S., Saito, H., Abe, E., Masuda, Y., Odashima, J., & Itoh, T. (1994). MKC-231, a choline uptake enhancer, ameliorates working memory deficits and decreased hippocampal acetylcholine induced by ethylcholine aziridinium ion in mice. *J Neural Transm Gen Sect, 98*(1), 1-13.

Nakata, K., Okuda, T., & Misawa, H. (2004). Ultrastructural localization of high-affinity choline transporter in the rat neuromuscular junction: enrichment on synaptic vesicles. *Synapse, 53*(1), 53-56. doi:10.1002/syn.20029

Neumann, S. A., Lawrence, E. C., Jennings, J. R., Ferrell, R. E., & Manuck, S. B. (2005). Heart rate variability is associated with polymorphic variation in the choline transporter gene. *Psychosom Med, 67*(2), 168-171. doi:10.1097/01.psy.0000155671.90861.c2

Neumann, S. A., Linder, K. J., Muldoon, M. F., Sutton-Tyrrell, K., Kline, C., Shrader, C. J., . . . Manuck, S. B. (2012). Polymorphic variation in choline transporter gene (CHT1) is associated with early, subclinical measures of carotid atherosclerosis in humans. *Int J Cardiovasc Imaging, 28*(2), 243-250. doi:10.1007/s10554-011-9831-4

Nickols, H. H., & Conn, P. J. (2014). Development of allosteric modulators of GPCRs for treatment of CNS disorders. *Neurobiol Dis, 61*, 55-71. doi:10.1016/j.nbd.2013.09.013

Ohno, K., Tsujino, A., Brengman, J. M., Harper, C. M., Bajzer, Z., Udd, B., . . . Engel, A. G. (2001). Choline acetyltransferase mutations cause myasthenic syndrome associated with episodic apnea in humans. *Proc Natl Acad Sci U S A, 98*(4), 2017-2022. doi:10.1073/pnas.98.4.2017

Okuda, T., & Haga, T. (2003). High-affinity choline transporter. *Neurochem Res, 28*(3-4), 483-488.

Okuda, T., Haga, T., Kanai, Y., Endou, H., Ishihara, T., & Katsura, I. (2000). Identification and characterization of the high-affinity choline transporter. *Nat Neurosci, 3*(2), 120-125. doi:10.1038/72059

Okuda, T., Konishi, A., Misawa, H., & Haga, T. (2011). Substrate-induced internalization of the high-affinity choline transporter. *J Neurosci, 31*(42), 14989-14997. doi:10.1523/JNEUROSCI.2983-11.2011

Okuda, T., Okamura, M., Kaitsuka, C., Haga, T., & Gurwitz, D. (2002). Single nucleotide polymorphism of the human high affinity choline transporter alters transport rate. *J Biol Chem, 277*(47), 45315-45322. doi:10.1074/jbc.M207742200

Okuda, T., Osawa, C., Yamada, H., Hayashi, K., Nishikawa, S., Ushio, T., . . . Haga, T. (2012). Transmembrane topology and oligomeric structure of the high-affinity choline transporter. *J Biol Chem, 287*(51), 42826-42834. doi:10.1074/jbc.M112.405027

Olshansky, B., Sabbah, H. N., Hauptman, P. J., & Colucci, W. S. (2008). Parasympathetic nervous system and heart failure: pathophysiology and potential implications for therapy. *Circulation, 118*(8), 863-871. doi:10.1161/CIRCULATIONAHA.107.760405

Pacholczyk, T., Blakely, R. D., & Amara, S. G. (1991). Expression cloning of a cocaine- and antidepressant-sensitive human noradrenaline transporter. *Nature, 350*(6316), 350-354. doi:10.1038/350350a0

Paolone, G., Mallory, C. S., Koshy Cherian, A., Miller, T. R., Blakely, R. D., & Sarter, M. (2013). Monitoring cholinergic activity during attentional performance in mice heterozygous for the choline transporter: a model of cholinergic capacity limits. *Neuropharmacology, 75*, 274-285. doi:10.1016/j.neuropharm.2013.07.032

Parikh, V., St Peters, M., Blakely, R. D., & Sarter, M. (2013). The presynaptic choline transporter imposes limits on sustained cortical acetylcholine release and attention. *J Neurosci, 33*(6), 2326-2337. doi:10.1523/JNEUROSCI.4993-12.2013

Patane, S. (2014). M3 muscarinic acetylcholine receptor in cardiology and oncology. *Int J Cardiol, 177*(2), 646-649. doi:10.1016/j.ijcard.2014.09.178

Patel, S., & Martino, D. (2013). Cervical dystonia: from pathophysiology to pharmacotherapy. *Behav Neurol, 26*(4), 275-282. doi:10.3233/BEN-2012-120270

Perry, W. L. (1953). Acetylcholine release in the cat's superior cervical ganglion. *J Physiol, 119*(4), 439-454.

Pert, C. B., & Snyder, S. H. (1973). Opiate receptor: demonstration in nervous tissue. *Science, 179*(4077), 1011-1014.

Pert, C. B., & Snyder, S. H. (1974). High affinity transport of choline into the myenteric plexus of guinea-pig intestine. *J Pharmacol Exp Ther, 191*(1), 102-108.

Picciotto, M. R., Higley, M. J., & Mineur, Y. S. (2012). Acetylcholine as a neuromodulator: cholinergic signaling shapes nervous system function and behavior. *Neuron, 76*(1), 116-129. doi:10.1016/j.neuron.2012.08.036

Pisani, A., Bernardi, G., Ding, J., & Surmeier, D. J. (2007). Re-emergence of striatal cholinergic interneurons in movement disorders. *Trends Neurosci, 30*(10), 545-553. doi:10.1016/j.tins.2007.07.008

Potter, L. T., Glover, V. A., & Saelens, J. K. (1968). Choline acetyltransferase from rat brain. *J Biol Chem, 243*(14), 3864-3870.

Prado, M. A., Reis, R. A., Prado, V. F., de Mello, M. C., Gomez, M. V., & de Mello, F. G. (2002). Regulation of acetylcholine synthesis and storage. *Neurochem Int, 41*(5), 291-299.

Proskocil, B. J., Sekhon, H. S., Jia, Y., Savchenko, V., Blakely, R. D., Lindstrom, J., & Spindel, E. R. (2004). Acetylcholine is an autocrine or paracrine hormone synthesized and secreted by airway bronchial epithelial cells. *Endocrinology, 145*(5), 2498-2506. doi:10.1210/en.2003-1728

Rainbow, T. C., Parsons, B., & Wieczorek, C. M. (1984). Quantitative autoradiography of [3H]hemicholinium-3 binding sites in rat brain. *Eur J Pharmacol, 102*(1), 195-196.

Ramirez-Castaneda, J., & Jankovic, J. (2013). Long-term efficacy and safety of botulinum toxin injections in dystonia. *Toxins (Basel), 5*(2), 249-266. doi:10.3390/toxins5020249

Ribeiro, F. M., Alves-Silva, J., Volknandt, W., Martins-Silva, C., Mahmud, H., Wilhelm, A., . . . Prado, M. A. (2003). The hemicholinium-3 sensitive high affinity choline transporter is internalized by clathrin-mediated endocytosis and is present in endosomes and synaptic vesicles. *J Neurochem, 87*(1), 136-146.

Ribeiro, F. M., Black, S. A., Cregan, S. P., Prado, V. F., Prado, M. A., Rylett, R. J., & Ferguson, S. S. (2005). Constitutive high-affinity choline transporter endocytosis

is determined by a carboxyl-terminal tail dileucine motif. *J Neurochem, 94*(1), 86-96. doi:10.1111/j.1471-4159.2005.03171.x

Ribeiro, F. M., Black, S. A., Prado, V. F., Rylett, R. J., Ferguson, S. S., & Prado, M. A. (2006). The "ins" and "outs" of the high-affinity choline transporter CHT1. *J Neurochem, 97*(1), 1-12. doi:10.1111/j.1471-4159.2006.03695.x

Ribeiro, F. M., Pinthong, M., Black, S. A., Gordon, A. C., Prado, V. F., Prado, M. A., . . . Ferguson, S. S. (2007). Regulated recycling and plasma membrane recruitment of the high-affinity choline transporter. *Eur J Neurosci, 26*(12), 3437-3448. doi:10.1111/j.1460-9568.2007.05967.x

Ruggiero, A. M., Wright, J., Ferguson, S. M., Lewis, M., Emerson, K. S., Iwamoto, H., . . . Blakely, R. D. (2012). Nonoisotopic assay for the presynaptic choline transporter reveals capacity for allosteric modulation of choline uptake. *ACS Chem Neurosci, 3*(10), 767-781. doi:10.1021/cn3000718

Russ, W. P., & Engelman, D. M. (2000). The GxxxG motif: a framework for transmembrane helix-helix association. *J Mol Biol, 296*(3), 911-919. doi:10.1006/jmbi.1999.3489

Rylett, R. J. (1988). Affinity labelling and identification of the high-affinity choline carrier from synaptic membranes of Torpedo electromotor nerve terminals with [3H]choline mustard. *J Neurochem, 51*(6), 1942-1945.

Rylett, R. J. (1989). Synaptosomal "membrane-bound" choline acetyltransferase is most sensitive to inhibition by choline mustard. *J Neurochem, 52*(3), 869-875.

Saltarelli, M. D., Lopez, J., Lowenstein, P. R., & Coyle, J. T. (1988). The role of calcium in the regulation of [3H]hemicholinium-3 binding sites in rat brain. *Neuropharmacology, 27*(12), 1301-1308.

Saltarelli, M. D., Lowenstein, P. R., & Coyle, J. T. (1987). Rapid in vitro modulation of [3H]hemicholinium-3 binding sites in rat striatal slices. *Eur J Pharmacol, 135*(1), 35-40.

Saltarelli, M. D., Yamada, K., & Coyle, J. T. (1990). Phospholipase A2 and 3H-hemicholinium-3 binding sites in rat brain: a potential second-messenger role for fatty acids in the regulation of high-affinity choline uptake. *J Neurosci, 10*(1), 62-72.

Sandberg, K., & Coyle, J. T. (1985). Characterization of [3H]hemicholinium-3 binding associated with neuronal choline uptake sites in rat brain membranes. *Brain Res, 348*(2), 321-330.

Sarter, M., & Parikh, V. (2005). Choline transporters, cholinergic transmission and cognition. *Nat Rev Neurosci, 6*(1), 48-56. doi:10.1038/nrn1588

Schloss, P., Mayser, W., & Betz, H. (1994). The putative rat choline transporter CHOT1 transports creatine and is highly expressed in neural and muscle-rich tissues. *Biochem Biophys Res Commun, 198*(2), 637-645. doi:10.1006/bbrc.1994.1093

Schueler, F. W. (1955). A new group of respiratory paralyzants. I. The "hemicholiniums". *J Pharmacol Exp Ther, 115*(2), 127-143.

Sciamanna, G., Hollis, R., Ball, C., Martella, G., Tassone, A., Marshall, A., . . . Standaert, D. G. (2012). Cholinergic dysregulation produced by selective inactivation of the dystonia-associated protein torsinA. *Neurobiol Dis, 47*(3), 416-427. doi:10.1016/j.nbd.2012.04.015

Sciamanna, G., Tassone, A., Mandolesi, G., Puglisi, F., Ponterio, G., Martella, G., . . . Pisani, A. (2012). Cholinergic dysfunction alters synaptic integration between thalamostriatal and corticostriatal inputs in DYT1 dystonia. *J Neurosci, 32*(35), 11991-12004. doi:10.1523/JNEUROSCI.0041-12.2012

Sellers, D. J., & Chess-Williams, R. (2012). Muscarinic agonists and antagonists: effects on the urinary bladder. *Handb Exp Pharmacol*(208), 375-400. doi:10.1007/978-3-642-23274-9_16

Shinohara, F., Kihara, Y., Ide, S., Minami, M., & Kaneda, K. (2014). Critical role of cholinergic transmission from the laterodorsal tegmental nucleus to the ventral tegmental area in cocaine-induced place preference. *Neuropharmacology, 79*, 573-579. doi:10.1016/j.neuropharm.2014.01.019

Simon, J. R., & Kuhar, M. J. (1976). High affinity choline uptake: ionic and energy requirements. *J Neurochem, 27*(1), 93-99.

Simpson, J., & Smart, L. (1982). Sodium-dependent choline binding in rat hippocampal synaptosomes. *Eur J Pharmacol, 80*(2-3), 267-270.

Sullivan, L., Fleming, J., Sastry, L., Mehlert, A., Wall, S. J., & Ferguson, M. A. (2014). Identification of sVSG117 as an immunodiagnostic antigen and evaluation of a

dual-antigen lateral flow test for the diagnosis of human African trypanosomiasis. *PLoS Negl Trop Dis, 8*(7), e2976. doi:10.1371/journal.pntd.0002976

Takashina, K., Bessho, T., Mori, R., Eguchi, J., & Saito, K. (2008). MKC-231, a choline uptake enhancer: (2) Effect on synthesis and release of acetylcholine in AF64A-treated rats. *J Neural Transm (Vienna), 115*(7), 1027-1035. doi:10.1007/s00702-008-0048-1

Takashina, K., Bessho, T., Mori, R., Kawai, K., Eguchi, J., & Saito, K. (2008). MKC-231, a choline uptake enhancer: (3) Mode of action of MKC-231 in the enhancement of high-affinity choline uptake. *J Neural Transm (Vienna), 115*(7), 1037-1046. doi:10.1007/s00702-008-0049-0

Tayebati, S. K., & Amenta, F. (2013). Choline-containing phospholipids: relevance to brain functional pathways. *Clin Chem Lab Med, 51*(3), 513-521. doi:10.1515/cclm-2012-0559

Tillerson, J. L., Caudle, W. M., Reveron, M. E., & Miller, G. W. (2002). Detection of behavioral impairments correlated to neurochemical deficits in mice treated with moderate doses of 1-methyl-4-phenyl-1,2,3,6-tetrahydropyridine. *Exp Neurol, 178*(1), 80-90.

Truong, D. (2012). Botulinum toxins in the treatment of primary focal dystonias. *J Neurol Sci, 316*(1-2), 9-14. doi:10.1016/j.jns.2012.01.019

Tucek, S. (1967). Observations on the subcellular distribution of choline acetyltransferase in the brain tissue of mammals and comparisons of acetylcholine synthesis from acetate and citrate in homogenates and nerve-ending fractions. *J Neurochem, 14*(5), 519-529.

Vickroy, T. W., Fibiger, H. C., Roeske, W. R., & Yamamura, H. I. (1984). Reduced density of sodium-dependent [3H]hemicholinium-3 binding sites in the anterior cerebral cortex of rats following chemical destruction of the nucleus basalis magnocellularis. *Eur J Pharmacol, 102*(2), 369-370.

Vickroy, T. W., Roeske, W. R., Gehlert, D. R., Wamsley, J. K., & Yamamura, H. I. (1985). Quantitative light microscopic autoradiography of [3H]hemicholinium-3 binding sites in the rat central nervous system: a novel biochemical marker for mapping the distribution of cholinergic nerve terminals. *Brain Res, 329*(1-2), 368-373.

Vickroy, T. W., Roeske, W. R., & Yamamura, H. I. (1984). Sodium-dependent high-affinity binding of [3H]hemicholinium-3 in the rat brain: a potentially selective marker for presynaptic cholinergic sites. *Life Sci, 35*(23), 2335-2343.

Voleti, B., Navarria, A., Liu, R. J., Banasr, M., Li, N., Terwilliger, R., . . . Duman, R. S. (2013). Scopolamine rapidly increases mammalian target of rapamycin complex 1 signaling, synaptogenesis, and antidepressant behavioral responses. *Biol Psychiatry, 74*(10), 742-749. doi:10.1016/j.biopsych.2013.04.025

Whittaker, V. P. (1965). The application of subcellular fractionation techniques to the study of brain function. *Prog Biophys Mol Biol, 15*, 39-96.

Williams, M. J., & Adinoff, B. (2008). The role of acetylcholine in cocaine addiction. *Neuropsychopharmacology, 33*(8), 1779-1797. doi:10.1038/sj.npp.1301585

Xie, J., & Guo, Q. (2004). Par-4 inhibits choline uptake by interacting with CHT1 and reducing its incorporation on the plasma membrane. *J Biol Chem, 279*(27), 28266-28275. doi:10.1074/jbc.M401495200

Yamada, H., Imajoh-Ohmi, S., & Haga, T. (2012). The high-affinity choline transporter CHT1 is regulated by the ubiquitin ligase Nedd4-2. *Biomed Res, 33*(1), 1-8.

Yamada, K., Saltarelli, M. D., & Coyle, J. T. (1988a). Involvement of phospholipase A2 in the regulation of [3H]hemicholinium-3 binding. *Biochem Pharmacol, 37*(22), 4367-4373.

Yamada, K., Saltarelli, M. D., & Coyle, J. T. (1988b). Solubilization and characterization of a [3H]hemicholinium-3 binding site in rat brain. *J Neurochem, 50*(6), 1759-1764.

Yamada, K., Saltarelli, M. D., & Coyle, J. T. (1989). Specificity of the activation of [3H]hemicholinium-3 binding by phospholipase A2. *J Pharmacol Exp Ther, 249*(3), 836-842.

Yamada, K., Saltarelli, M. D., & Coyle, J. T. (1991a). [3H]hemicholinium-3 binding in rats with status epilepticus induced by lithium chloride and pilocarpine. *Eur J Pharmacol, 195*(3), 395-397.

Yamada, K., Saltarelli, M. D., & Coyle, J. T. (1991b). Effects of calmodulin antagonists on sodium-dependent high-affinity choline uptake. *Brain Res, 542*(1), 132-134.

Yamamura, H. I., & Snyder, S. H. (1972). Choline: high-affinity uptake by rat brain synaptosomes. *Science, 178*(4061), 626-628.

Yamamura, H. I., & Snyder, S. H. (1973). High affinity transport of choline into synaptosomes of rat brain. *J Neurochem, 21*(6), 1355-1374.

Ye, R., Carneiro, A. M., Han, Q., Airey, D., Sanders-Bush, E., Zhang, B., . . . Blakely, R. D. (2014). Quantitative trait loci mapping and gene network analysis implicate protocadherin-15 as a determinant of brain serotonin transporter expression. *Genes Brain Behav, 13*(3), 261-275. doi:10.1111/gbb.12119

Yuan, Z., Wagner, L., Poloumienko, A., & Bakovic, M. (2004). Identification and expression of a mouse muscle-specific CTL1 gene. *Gene, 341*, 305-312. doi:10.1016/j.gene.2004.07.042

Zheng, Q. H., Gao, M., Mock, B. H., Wang, S., Hara, T., Nazih, R., . . . DeGrado, T. R. (2007). Synthesis and biodistribution of new radiolabeled high-affinity choline transporter inhibitors [11C]hemicholinium-3 and [18F]hemicholinium-3. *Bioorg Med Chem Lett, 17*(8), 2220-2224. doi:10.1016/j.bmcl.2007.01.105

Zimmer, H. G. (2006). Otto Loewi and the chemical transmission of vagus stimulation in the heart. *Clin Cardiol, 29*(3), 135-136.

Zurkovsky, L., Bychkov, E., Tsakem, E. L., Siedlecki, C., Blakely, R. D., & Gurevich, E. V. (2013). Cognitive effects of dopamine depletion in the context of diminished acetylcholine signaling capacity in mice. *Dis Model Mech, 6*(1), 171-183. doi:10.1242/dmm.010363